Forces induced by coherent effects

Ariane Soret

université PARIS-SACLAY

NNT: 2019SACLX045

Forces induced by coherent effects

Thèse de doctorat de l'Université Paris-Saclay
préparée à l'École Polytechnique

École doctorale n° 564 Physique en Île-de-France (PIF)
Spécialité de doctorat: Physique

Thèse présentée et soutenue à Palaiseau, le 13 septembre 2019, par

Ariane Soret

Composition du Jury:

M. Gilles Montambaux Professeur — Université Paris Sud, Laboratoire de Physique des Solides (LPS)	Président du Jury
M. David Dean Professeur — Université de Bordeaux, Laboratoire Ondes et Matière d'Aquitaine (LOMA)	Rapporteur
M. Juan José Sáenz Professeur — Donostia International Physics Center (DIPC)	Rapporteur
M. Olivier Arcizet Chargé de Recherche — Institut Néel	Examinateur
M. Sylvain Gigan Professeur — Université Pierre et Marie Curie Laboratoire Kastler Brossel (LKB)	Examinateur
M. Giovanni Jona-Lasinio Professeur Emérite — Sapienza Université de Rome	Examinateur
Mme Karyn Le Hur Professeur — École polytechnique, Centre de Physique Théorique (CPHT)	Directrice de thèse
M. Eric Akkermans Professeur — Technion Israel Institute of Technology, Physics Department	Co-directeur de thèse

Thèse de doctorat

When you don't know where you're going, you have to get there as fast as possible.

Shadock saying

ÉCOLE POLYTECHNIQUE AND TECHNION – ISRAEL INSTITUTE OF TECHNOLOGY

Abstract

Doctor of Philosophy

Forces induced by coherent effects

by Ariane SORET

In this work, we study coherent effects associated to wave propagation in scattering media, in particular electromagnetic waves. In weakly disordered media, light intensity fluctuates spatially over large distances. This phenomenon is the result of complex mesoscopic coherent effects, which occur at a microscopic scale. We show that these mesoscopic coherent fluctuations of light induce radiation forces of a new kind. The strength of these fluctuating forces is determined by a single and easily tunable parameter, the dimensionless conductance, which depends on both the geometry and the scattering properties of the medium. Our findings should therefore have interesting applications such as new probes in soft condensed matter or biophysics. On the methodological viewpoint, we use a hydrodynamic Langevin approach to describe the coherent light fluctuations, where a properly tailored noise accounts for mesoscopic coherent effects. We show how to systematically include the coherent corrections in the noise term, in order to reproduce the intensity fluctuations. This description allows to understand coherent light fluctuations as resulting from a non equilibrium light flow, characterized by two parameters only, the diffusion coefficient and the mobility, otherwise related by an Einstein relation. A clear asset of this method is its dependence upon two parameters only, which provides a compact, numerically accessible, yet accurate description of the rich underlying coherent effects. Moreover, the mapping we present between coherent light and out of equilibrium hydrodynamics is easily generalizable to a large class of quantum or classical wave problems. For future perspectives, this connection between coherent effects in mesoscopics and non equilibrium stochastic processes should be of interest for both the mesoscopics and statistical mechanics communities. For the former, the mapping to non equilibrium hydrodynamics provides a new insight to mesoscopic physics as well as useful tools to study quantities so far difficult to access, such as higher orders intensity correlation functions. For the latter, this work should motivate further study of time independent processes inspired from mesoscopics.

Acknowledgements

First of all, I would like to thank my advisors, Karyn Le Hur and Eric Akkermans, for guiding me through these challenging years while leaving me a fair share of autonomy. It was a pleasure to work on various interesting topics with you both. I also thank you for the opportunities you gave me to meet and interact with other members of the condensed matter community, by sending me to conferences around the globe.

I am also very grateful to the members of the jury, who accepted to evaluate my thesis, Olivier Arcizet, Sylvain Gigan, Giovanni Jona-Lasionio, and especially the referees David Dean and Juan José Sáenz for taking the time to read and review this work. I also thank Gilles Montambaux, for presiding the jury, and for being my tutor during the past three years together with Michel Ferrero.

Thank you also to all the people I who made themselves available to help me or to share their knowledge, Ohad, Slava, Boris, Félix, Thibault, and – in the mathematicians category – my father, and occasionally, my sister. It has also been a pleasure to teach the lab classes, with Yannis, Luca and Alexis, and to have fruitful discussions about our respective research interests.

I also want to thank my office mates from Polytechnique and the Technion, and all the friends who brightened this journey, Nestor, Hannah, Camille, Félix, Tal, Thibault, Marc, Kirill, Louise, Guillaume, Fan, Philipp, Slava, Omri, Eric G., Anton and Monika, Ido and Sivan, Guy, Lluis, and Yacov. I especially thank my partner in crime, Igor, who supported me through the many frustrating periods a PhD is paved with.

An acknowledgement section for a thesis between Polytechnique and the Technion wouldn't be complete without a special thanks to the stairs of Lozère and the hills of the Carmel, who made sure to keep me in shape while I was shaping my mind...

Finally, I thank my parents, who passed on the science virus to me, and gave me the confidence to embrace it.

Contents

List of Figures

List of Tables

List of Symbols

$\langle X \rangle$	Averaged value of X over the disorder $\boldsymbol{\nu}$
$\langle X \rangle_Y$	Averaged value of X w.r.t. the probability law Y
$\widehat{\mathbf{x}}$	A unit vector directed along the vector $\mathbf{x}$
α, β	Space coordinate indices
γ	Radiation source term
γ'	Intensity source term
Γ	Structure factor
l	Elastic mean free path
k	Wave number
v	Group velocity
τ_D	Thouless diffusion time
τ_e	Elastic mean time
g	Dimensionless conductance for a hypercube geometry
$g_{\mathcal{L}}$	Dimensionless conductance for any geometry, of characteristic length $\mathcal{L}$
$c_0 = \frac{2\pi l v^2}{3k^2}$	Prefactor for light intensity correlation functions and noise
I_D	Disordered averaged intensity
P_D	Diffusion probability, or Green's function of the time independent diffusion equation
$\boldsymbol{\nu}$	Noise term of the effective Langevin equation for light
σ	Mobility
D	Diffusion coefficient
χ	Compressibility

$\boldsymbol{f}$	Light fluctuation induced force
C_j	Terms of the dimensionless light intensity correlation function
K_j	Terms of the noise correlation function
$\mathcal{S}$	Action or cost functional in the macroscopic fluctuation theory
$\mathcal{P}[\rho, \mathbf{j}]$	Probability to observe some density ρ and current $\mathbf{j}$ tranjectories
$\mathcal{G}$	Pressure functional
$C(\mathbf{r}, \mathbf{r}')$	Two point correlation function in the macroscopic fluctuation theory language

Chapter 1

Introduction

Casimir forces – or fluctuation induced forces – are forces induced by the confinment of *long ranged* fluctuations of the medium. The existence of such forces was first predicted in 1948, in quantum electrodynamics – an effect famously known as the quantum electrodynamics (QED) Casimir effect [1], where two infinite, parallel plates of a perfectly conducting material, immersed in the quantum electrodynamic vacuum, attract each other due to the confinment of the long ranged fluctuations of the vacuum. This discovery was followed by experimental verifications [2, 3], and the effect – namely, that confining long ranged fluctuations of some medium with external objects induces forces on these objects – has since been observed in a wide variety of systems, discussed at an introductory level in [4]. For example, in 1978, fluctuation induced forces were identified in soft matter physics, using critical binary fluids, in which the chemical potential displays long range fluctuations near a rigid plate [5]. More recent work points at the emergence of fluctuation induced forces in non equilibrium hydrodynamics, due to spatially long ranged fluctuations of the density [6, 7, 8]. To cite a few more examples, these forces have also been found in biophysics [9], condensed matter physics [10] and cold atoms [11], but this list is not exhaustive, and we refer the interested reader to [12] for a more thorough discussion. Although the QED Casimir forces are found to be attractive, and to follow a simple power law, fluctuation induced forces in general can be either attractive, repulsive, and scale differently with respect to the geometry of the system.

In this work, we demonstrate the existence of fluctuation induced forces caused by classical light propagating in a scattering medium – a result which lies at the intersection between mesoscopic physics, Casimir physics, nanomechanics and non equilibrium statistical mechanics.

Wave propagation in random media, either electronic or electromagnetic, gives rise to many rich phenomena in mesoscopic physics and have been widely studied for decades, both theoretically and experimentally [13]. Systems where waves scatter in completely random, disordered media, are fascinating in that significant effects emerge from this apparent chaos. A striking example are fluctuations of light intensity, of the order of its disorder averaged value, which are persistent over large distances. The key word to understand these surprising effects is *coherence*. This thesis is centered around the study of coherent effects associated to waves propagation in scattering media, in particular electromagnetic waves. In weakly disordered media, light intensity fluctuates spatially, leading to characteristic scattering patterns of dark and bright spots – speckle patterns [14, 13, 15, 16, 17, 18, 19]. These intensity fluctuations propagate over large distances, as a result of complex mesoscopic coherent effects, which occur at a microscopic scale. Since these coherent effects lead to spatially long ranged light intensity fluctuations, the question of the emergence of coherent light fluctuation induced forces naturally rises. Mechanical forces caused by light have been widely studied [20, 21, 22] – especially since the introduction

of lasers – and exploited to produce sensors in soft matter physics and biophysics [23, 24]. Here, we show that coherent intensity fluctuations lead to measurable fluctuation induced forces, $\boldsymbol{f} = \mathbf{f} - \langle \mathbf{f} \rangle$, on top of the disorder averaged radiation forces $\langle \mathbf{f} \rangle$. The amplitude of the fluctuating radiation forces is

$$\langle \boldsymbol{f}^2 \rangle = \frac{1}{g_{\mathcal{L}}} \frac{\mathcal{P}^2}{v^2} \left(\mathcal{Q}_2 + \mathcal{Q}_v \right) , \tag{1.1}$$

where $\mathcal{P}$ is the power of the light source and v the group velocity. The dimensionless conductance $g_{\mathcal{L}}$ is a parameter which encapsulates both the geometry and the scattering properties of the random medium; it is the analog of conductance in electronic systems. The two dimensionless numbers $\mathcal{Q}_2$ and $\mathcal{Q}_v$ depend on the shape of the system and on boundary conditions but not on its volume nor on scattering properties. This rather simple expression (1.1) constitutes a central result of this work. It states that the fluctuating forces induced by coherent mesoscopic effects, besides their dependence upon the power of the incoming light beam and the group velocity, are driven by the dimensionless conductance $g_{\mathcal{L}}$, a parameter connected to the strength of disorder and the occurence of coherent effects. $g_{\mathcal{L}}$ is moreover easily tunable, which makes our predictions prone to experimental verification. Our findings should therefore have interesting applications such as new probes in soft condensed matter or biophysics.

On the methodological viewpoint, inspired by [25], we use a hydrodynamic Langevin approach to describe the coherent light fluctuations, where a properly tailored noise accounts for mesoscopic coherent effects. We show how to systematically include the coherent corrections in the noise term in order to reproduce the intensity fluctuations, to higher order than in the original paper by A. Yu. Zyuzin and B. Z. Spivak. This description allows to understand light fluctuations as resulting from a light flow, driven out of equilibrium by coherent effects. The light flow is characterized by two parameters only, the diffusion coefficient and the mobility, otherwise related by an Einstein relation. A clear asset of this method is its dependence upon two parameters only, which provides a compact yet accurate description of the rich underlying coherent effects. Moreover, this effective Langevin description draws a correspondence between the mesoscopic problem of coherent light to a class of non equilibrium stochastic systems, well described in the macroscopic fluctuation theory [26, 27, 28]. This correspondence sheds a new light on our understanding of coherent light. Furthermore, the method here presented is easily generalizable to a large class of quantum or classical wave problems, and should motivate further research on mesoscopic systems using the macroscopic fluctuation theory framework.

Thesis organization

This thesis is organized as follows. In chapter 2, we provide an overview of the properties of classical light propagating in an elastic scattering medium. We re-derive the known result that, on average, the light intensity behaves diffusively, and that it is related to the light current by a Fick's law. We then provide a detailed derivation of the correlation function for the fluctuations of light intensity around its average value, using a diagrammatic approach. In chapter 3, inspired by [25], we derive an effective Langevin equation for the light flow, and we develop a systematic method to properly derive the noise. Chapter 4 contains the main results of this work. Using the chapters 2 and 3, we show that, in random media illuminated by a light beam,

spatially long ranged light intensity fluctuations – which stem from underlying coherent effects – induce fluctuating radiative forces of a new kind. These forces act mechanically on macroscopic objects immersed in the medium. In chapter 5, we study the problem of coherent light from a different angle, inspired by the macroscopic fluctuation theory and the stochastic formalism. We show how to translate the time independent mesoscopics problem of coherent light into a far from equilibrium hydrodynamics framework, which allows us to recover known results from mesoscopics and to obtain other relevant quantities to characterize the system.

Chapter 2

Classical light in scattering media

Light thinks it travels faster than anything but it is wrong. No matter how fast light travels, it finds the darkness has always got there first, and is waiting for it.

Terry Pratchett

This thesis is centered on coherent effects in multiple scattering of light. To appreciate the main results, presented in chapters 3-5, it is useful to understand the physics of classical light in random media, in the multiple scattering regime. This chapter focuses on the properties of monochromatic light propagating through a random dielectric medium. The radiation inside the medium is solution of a Helmholtz equation (2.1) with a random dielectric constant, which is extremely difficult to solve analytically. The properties of the radiation are characterized by two length scales, the wavelength $\lambda = 2\pi/k$, where k is the wavenumber, and the elastic mean free path l between two scattering events. While exact anaytical solutions are cumbersome to obtain, a lot can be said on disorder averaged quantities. In the weak disorder limit $kl \gg 1$, the light intensity behaves diffusively; its propagation through the medium can be represented by brownian like trajectories, see Fig.2.1.a. For one realization of disorder, the light intensity fluctuates spatially around the average diffusive value. These fluctuations lead to characteristic patterns of bright and dark spots – speckle patterns, see Fig.2.1.b – which have been widely studied and measured in weakly disordered electronic and photonic media [14, 13, 15, 16, 17, 18, 19]. It is important to note that a speckle pattern is not a diffraction pattern, where each light beam would scatter only once on a scatterer and exit the system. Instead, a speckle pattern is built out from multiply scattered trajectories of light, which interfere constructively despite the randomness of the medium. Speckle patterns display a complex structure, and carry the fingerprint of the various interference processes which contribute, on a microscopic scale, to the light intensity fluctuations. Quantitatively, the intensity fluctuations can be described by means of their correlation function. The latter is the sum of a spatially short ranged term and a long ranged one; the short ranged term is the strongest in amplitude and gives the bright and dark spots of the speckle patterns, while the long ranged term stems from underlying coherent effects known as *quantum crossings*. These long range fluctuations are weaker in amplitude and hence more difficult to observe, but, suprisingly, lead to measurable forces, which are discussed in chapter 4. Here, we discuss the physical mechanism giving rise to these fluctuations.

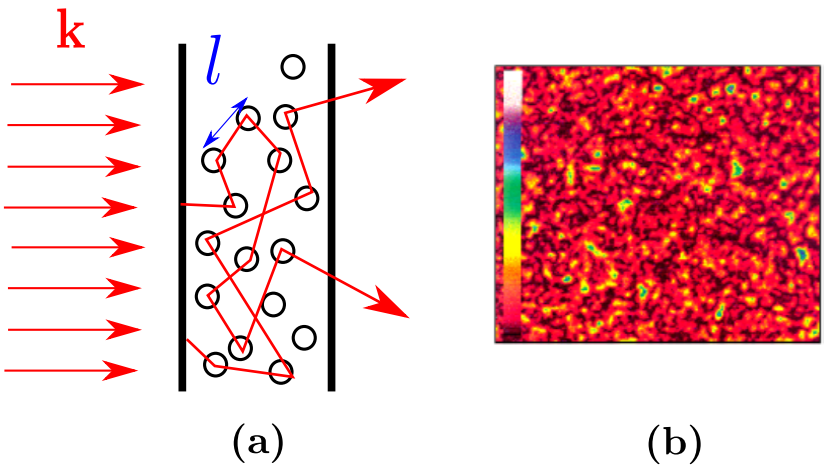

FIGURE 2.1: **(a)** A monochromatic plane wave illumiates a random medium, and undergoes multiple diffusion. On average, the light intensity behaves diffusively. Its propagation is represented by brownian like trajectories, characterized by the elastic mean free path l between two scattering events. For some realization of disorder, the light intensity fluctuates spatially around the average value, giving rise to speckle patterns. **(b)** Experimental observation of speckle patterns [13].

2.1 Classical light in scattering media

Consider a random and d-dimensional dielectric medium of volume $V = L^d$, illuminated by a monochromatic scalar radiation of wave-number k incident along the direction of unit vector $\widehat{\mathbf{k}}$. We do not consider polarization effects, as they can be decoupled from disorder; for more elaborations, see [13]. Inside the medium, the amplitude $E(\mathbf{r})$ of the radiation is solution of the scalar Helmholtz equation,

$$\Delta E(\mathbf{r}) + k^2 \left(1 + \frac{\delta\epsilon(\mathbf{r})}{\langle\epsilon\rangle}\right) E(\mathbf{r}) = s_0(\mathbf{r}) \tag{2.1}$$

where $\delta\epsilon(\mathbf{r})/\langle\epsilon\rangle$ denotes the fluctuation of the dielectric constant $\epsilon(\mathbf{r}) = \langle\epsilon\rangle + \delta\epsilon(\mathbf{r})$, $\langle\cdots\rangle$ is the average over disorder realizations and $s_0(\mathbf{r})$ is the source of the radiation. Besides the wave-number k, the radiation in the medium is characterized by the elastic mean free path l. The intensity is defined by

$$I(\mathbf{r}) = \epsilon(\mathbf{r}) v |E(\mathbf{r})|^2 \tag{2.2}$$

where v is the group velocity. The scalar radiation $E(\mathbf{r})$ is obtained by solving Eq.(2.1), which as mentioned is very difficult to solve analytically. However, exact expressions can be obtained on average over disorder. The behavior of the average intensity and of its fluctuations is then described by the diffusion probability and the structure factor.

2.1.1 Light intensity

Useful information on the monochromatic scalar radiation, of wavenumber k, is provided by the Green's function $G(\mathbf{r}, \mathbf{r}')$ of the Helmholtz equation (2.1),

$$\left[\Delta + k^2 \left(1 + \frac{\delta\epsilon(\mathbf{r})}{\langle\epsilon\rangle}\right)\right] G(\mathbf{r}, \mathbf{r}') = \delta(\mathbf{r} - \mathbf{r}')\,. \tag{2.3}$$

There are two solutions to Eq.(2.3), respectively the retarded and advanced Green's functions $G^R(\mathbf{r},\mathbf{r}')$, $G^A(\mathbf{r},\mathbf{r}')$. In vacuum, when $\delta\epsilon(\mathbf{r}) = 0$, the solutions are

$$G_0^{R,A}(\mathbf{r},\mathbf{r}') = -\frac{e^{\pm ik|\mathbf{r}-\mathbf{r}'|}}{4\pi|\mathbf{r}-\mathbf{r}'|}\,. \tag{2.4}$$

In a random scattering medium, $G^{R,A}(\mathbf{r},\mathbf{r}')$ takes the form

$$G^{R,A}(\mathbf{r},\mathbf{r}') = \sum_{\mathcal{C}_i} |\mathcal{A}(\mathbf{r},\mathbf{r}',\mathcal{C}_i)| e^{\pm ik\mathcal{L}_i}\,, \tag{2.5}$$

where the sum runs over all the possible sets of N scatterers, with N going from 1 to infinity. $\mathcal{A}(\mathbf{r},\mathbf{r}',\mathcal{C}_\mathbf{i})$ is the complex amplitude associated to the sequence of collisions $\mathcal{C}_i$, and $\mathcal{L}_i$ is the length of the corresponding scattering path. The radiation $E(\mathbf{r})$ is related to the Green's function $G^R(\mathbf{r},\mathbf{r}')$ by the Green's identity,

$$\begin{aligned} E(\mathbf{r}) &= \int_V d\mathbf{r}'\, s_0(\mathbf{r}') G^R(\mathbf{r},\mathbf{r}') \\ &= \int_V d\mathbf{r}'\, s_0(\mathbf{r}') \sum_{\mathcal{C}_i} |\mathcal{A}(\mathbf{r},\mathbf{r}',\mathcal{C}_i)| e^{ik\mathcal{L}_i}\,, \end{aligned} \tag{2.6}$$

In the rest of this work, we renormalize the source term $s_0(\mathbf{r})$ so that the intensity $I(\mathbf{r})$ is related to $E(\mathbf{r})$ by $I(\mathbf{r}) = |E(\mathbf{r})|^2$. The intensity is hence built out of a sum of paired scattering trajectories (see Fig.2.2), and can be written in the form

$$I(\mathbf{r}) = \sum_{\mathcal{C}_i} |\tilde{\mathcal{A}}(\mathbf{r})_{\mathcal{C}_i}|^2 + \sum_{\mathcal{C}_i \neq \mathcal{C}_j} \tilde{\mathcal{A}}(\mathbf{r})_{\mathcal{C}_i} \tilde{\mathcal{A}}^*(\mathbf{r})_{\mathcal{C}_j}\,, \tag{2.7}$$

where the phase is contained in the complex amplitudes $\tilde{\mathcal{A}}_i$, $\tilde{\mathcal{A}}_j$, and where $\mathcal{C}_i$, $\mathcal{C}_j$ are the corresponding scattering trajectories. The first term in the right hand side of Eq.(2.7) is phase independent; it is the classical or incoherent contribution to the intensity. Since it is phase independent, this incoherent term survives disorder averaging and constitutes the main contribution to the intensity. In 2.1.3, we will show that, on average, this term satisfies a diffusion equation. The second term is quantum in the sense that it is phase dependent. Most of the terms in the sum cancel out upon disorder averaging. However, it is possible to minimize the dephasing by allowing pairing of trajectories in this second term. This effect is discussed in more details in 2.2. We just note that it gives a negligible correction to the average intensity inside the bulk of the system, and we will neglect it here. However, there exists an electronic analog to this effect, which leads to the phenomenon of weak localization for electrons is disordered metals [13]. In the case of light, the notion of crossings is relevant when it comes to calculating the intensity fluctuations correlation function, which will be discussed in 2.2.

2.1.2 Diffusion probability and structure factor

From the Green's functions in Eq.(2.3), we define the probability $P(\mathbf{r},\mathbf{r}')$ for the radiation to scatter from $\mathbf{r}$ to $\mathbf{r}'$ by

$$P(\mathbf{r},\mathbf{r}') = \frac{4\pi}{v} \langle G^R(\mathbf{r},\mathbf{r}') G^A(\mathbf{r}',\mathbf{r}) \rangle\,, \tag{2.8}$$

where v is a properly defined group velocity. The disorder averaged Green's functions can be calculated using a Dyson development (see section 3.2 in [13]), which gives

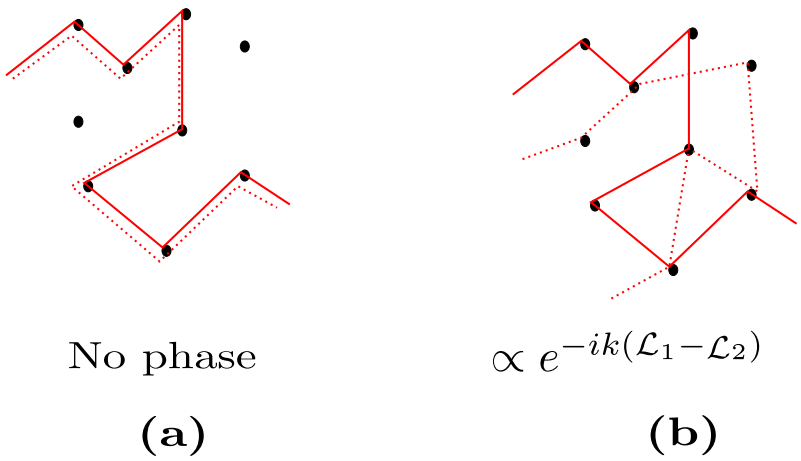

FIGURE 2.2: Paired multiple scattering trajectories of the radiation. **(a)** The paired trajectories with identical scattering sequences contribute to the average intensity, **(b)** while the pairs of trajectories which follow different scattering sequences average to zero.

$$\langle G^{R,A}(\mathbf{r},\mathbf{r}')\rangle = -\frac{1}{4\pi}\frac{e^{\pm ik|\mathbf{r}-\mathbf{r}'|}}{|\mathbf{r}-\mathbf{r}'|}e^{-|\mathbf{r}-\mathbf{r}'|/2l}, \tag{2.9}$$

where the elastic mean free path l is defined by $\frac{4\pi}{l} = \langle V(\mathbf{q})V(\mathbf{q}')\rangle$, and where $V(\mathbf{q}) = \int d\mathbf{r}\, e^{i\mathbf{q}\cdot\mathbf{r}}V(\mathbf{r})$ is the Fourier transform of the disorder potential $V(\mathbf{r}) = k^2\delta\epsilon(\mathbf{r})/\langle\epsilon\rangle$ in Eq.(2.1). To calculate the disorder averaged product in Eq.(2.8), we begin by noting that averaging over disorder cancels out the terms in $G^R(\mathbf{r},\mathbf{r}')G^A(\mathbf{r}',\mathbf{r})$ which are taken over different sets of scatterers $(\mathbf{r_1},...,\mathbf{r_N})$. Hence, we keep only the terms with identical scattering sequences $\mathcal{C}_N$ – which implies identical $\mathcal{L}_N$ and cancels the phase. We note $P_D(\mathbf{r},\mathbf{r}')$ the diffusion probability obtained from Eq.(2.8) with this approximation; $P_D(\mathbf{r},\mathbf{r}')$ satisfies the equation

$$P_D(\mathbf{r},\mathbf{r}') = \frac{4\pi}{v}\int_V d\mathbf{r_1}d\mathbf{r_2}|\langle G^R(\mathbf{r},\mathbf{r_1})\rangle|^2\Gamma(\mathbf{r_1},\mathbf{r_2})|\langle G^A(\mathbf{r}',\mathbf{r_2})\rangle|^2 \tag{2.10}$$

and is represented in Fig.2.3.

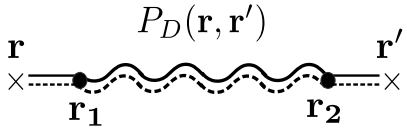

FIGURE 2.3: Schematic representation of the diffusion probability $P_D(\mathbf{r},\mathbf{r}')$. The structure factor $\Gamma(\mathbf{r_1},\mathbf{r_2})$ is represented by the couple of wavelets between $\mathbf{r_1}$ and $\mathbf{r_2}$, while the couples of straight lines stand for the averaged Green's functions $|\langle G^R(\mathbf{r},\mathbf{r_1})\rangle|^2$ and $|\langle G^A(\mathbf{r}',\mathbf{r_2})\rangle|^2$.

The term $\Gamma(\mathbf{r_1},\mathbf{r_2})$ is the so called structure factor, and represents all the possible scattering sequences between $\mathbf{r_1}$ and $\mathbf{r_2}$. The collisions are assumed to be independent and $\Gamma(\mathbf{r_1},\mathbf{r_2})$ is therefore an infinite sum of collision sequences, which translates into an integral equation,

$$\Gamma(\mathbf{r_1},\mathbf{r_2}) = \frac{4\pi}{l}\delta(\mathbf{r_1}-\mathbf{r_2}) + \frac{4\pi}{l}\int_V d\mathbf{r}\,\Gamma(\mathbf{r_1},\mathbf{r})|\langle G^R(\mathbf{r},\mathbf{r_2})\rangle|^2\,. \tag{2.11}$$

In the diffusive approximation, $\Gamma(\mathbf{r_1}, \mathbf{r_2})$ varies slowly in space, and we may use a Taylor expansion of $\Gamma(\mathbf{r_1}, \mathbf{r_2})$ around $\mathbf{r_2}$. Keeping up to the quadratic term and substituting in Eq.(2.11) leads to, after an integration by parts,

$$-D\Delta\Gamma(\mathbf{r_1}, \mathbf{r_2}) = \frac{4\pi v}{l^2}\delta(\mathbf{r_1} - \mathbf{r_2})\,, \tag{2.12}$$

where $D = \frac{vl}{3}$ is the diffusion coefficient. In the diffusive limit, we approximate $\Gamma(\mathbf{r_1}, \mathbf{r_2}) \simeq \Gamma(\mathbf{r}, \mathbf{r}')$, with the notations of Fig.2.3; using this approximation and the Eq.(2.9), the Eq.(2.10) becomes

$$P_D(\mathbf{r}, \mathbf{r}') = \frac{l^2}{4\pi v}\Gamma(\mathbf{r}, \mathbf{r}')\,. \tag{2.13}$$

From Eq.(2.12) we deduce that $P_D(\mathbf{r}, \mathbf{r}')$ satisfies

$$-D\Delta P_D(\mathbf{r}, \mathbf{r}') = \delta(\mathbf{r} - \mathbf{r}')\,. \tag{2.14}$$

The diffusion probability $P_D(\mathbf{r}, \mathbf{r}')$ is hence the Green's function of a time independent diffusion equation, and has the generic form

$$P_D(\mathbf{r}, \mathbf{r}') = \frac{1}{DL}p(\mathbf{r}, \mathbf{r}') \tag{2.15}$$

where $p(\mathbf{r}, \mathbf{r}')$ is a dimensionless function depending on the boundary conditions and where $L \equiv V^{1/3}$ is the characteristic length of the system.

2.1.3 Fick's law and diffusion equation

In the scattering medium, the light intensity is related to the Green's functions in Eq.(2.5) and the radiation source distribution $s_0(\mathbf{r})$ of the Helmholtz equation (2.1) by the Green's identity,

$$I(\mathbf{r}) = \iint_{V\times V} d\mathbf{r_0}d\mathbf{r}'_\mathbf{0}s_0(\mathbf{r_0})s_0(\mathbf{r}'_\mathbf{0})G^R(\mathbf{r_0}, \mathbf{r})G^A(\mathbf{r}, \mathbf{r}'_\mathbf{0})\,. \tag{2.16}$$

Calculating the above integral is a cumbersome task because of the complexity of the solutions $G^R(\mathbf{r}, \mathbf{r}')$, $G^A(\mathbf{r}, \mathbf{r}')$. An equivalent description of the radiation in the scattering medium is given by the specific intensity $I(\widehat{\mathbf{s}}, \mathbf{r})$, also called the irradiance. On a phenomenological viewpoint, the specific intensity is the radiation intensity at point $\mathbf{r}$, propagating along the direction $\widehat{\mathbf{s}}$ [29]. It is rigorously defined [13, 30] from the Green's functions of the Helmholtz equation (2.1), as the Fourier transform of

$$I(\widehat{\mathbf{s}}, \mathbf{k}) = \frac{4\pi}{vV}\sum_{\mathbf{q},\mathbf{q}'}\overline{G^R(q\widehat{\mathbf{s}} + \mathbf{k}/2, q'\widehat{\mathbf{s}}' + \mathbf{k}/2)G^A(q'\widehat{\mathbf{s}}' - \mathbf{k}/2, q\widehat{\mathbf{s}} - \mathbf{k}/2)} \tag{2.17}$$

where $G^{R,A}$ are the Fourier transforms of the Green's functions in Eq.(2.3), and where the average $\overline{\cdots}$ is taken over all directions $\widehat{\mathbf{s}}'$. The specific intensity obeys the radiative transfer equation (see appendix A.5.2 in [13]),

$$\widehat{\mathbf{s}}\cdot\boldsymbol{\nabla}I(\widehat{\mathbf{s}}, \mathbf{r}) = -\frac{1}{l}I(\widehat{\mathbf{s}}, \mathbf{r}) + \frac{1}{l}\overline{I(\widehat{\mathbf{s}}', \mathbf{r})p(\widehat{\mathbf{s}} - \widehat{\mathbf{s}}')} + \frac{1}{l}\gamma(\widehat{\mathbf{s}}, \mathbf{r})\,, \tag{2.18}$$

where the average is taken over all the directions $\hat{\mathbf{s}}'$. The term $\gamma(\hat{\mathbf{s}},\mathbf{r})$ represents a possible source of light intensity placed inside the medium. Note that $\gamma(\hat{\mathbf{s}},\mathbf{r})$ is different from $s_0(\mathbf{r})$, which is the source distribution for the electromagnetic radiation. The term $p(\hat{\mathbf{s}}-\hat{\mathbf{s}}')$ accounts for scattering in other directions than $\hat{\mathbf{s}}$.

The disorder averaged intensity can be written as a sum of two contributions [13, 29],

$$\langle I(\hat{\mathbf{s}},\mathbf{r})\rangle = I_0(\hat{\mathbf{s}},\mathbf{r}) + I_D(\hat{\mathbf{s}},\mathbf{r})\,. \tag{2.19}$$

The first term $I_0(\hat{\mathbf{s}},\mathbf{r})$ is the Drude-Boltzmann term and decreases exponentially due to scattering; it satisfies the equation

$$\hat{\mathbf{s}}\cdot\boldsymbol{\nabla} I_0(\hat{\mathbf{s}},\mathbf{r}) = -\frac{1}{l} I_0(\hat{\mathbf{s}},\mathbf{r})\,. \tag{2.20}$$

The term $I_D(\hat{\mathbf{s}},\mathbf{r})$ is the diffusive part, arising from multiple diffusion inside the disordered medium. We will further on neglect $I_0(\hat{\mathbf{s}},\mathbf{r})$ in the expression of the average intensity: $\langle I(\hat{\mathbf{s}},\mathbf{r})\rangle \simeq I_D(\hat{\mathbf{s}},\mathbf{r})$. However, $I_0(\hat{\mathbf{s}},\mathbf{r})$ does not completely disappear from the description since, as we will see, it behaves as a light source term for $I_D(\hat{\mathbf{s}},\mathbf{r})$. Averaging Eq.(2.18) over disorder and using Eq.(2.20), we obtain, for $I_D(\hat{\mathbf{s}},\mathbf{r})$,

$$\begin{aligned}\hat{\mathbf{s}}\cdot\boldsymbol{\nabla} I_D(\hat{\mathbf{s}},\mathbf{r}) \;&= -\tfrac{1}{l} I_D(\hat{\mathbf{s}},\mathbf{r}) + \tfrac{1}{l}\overline{I_D(\hat{\mathbf{s}}',\mathbf{r})p(\hat{\mathbf{s}}-\hat{\mathbf{s}}')} \\ &\quad + \tfrac{1}{l}\gamma_0(\hat{\mathbf{s}},\mathbf{r}) + \tfrac{1}{l}\gamma(\hat{\mathbf{s}},\mathbf{r})\,,\end{aligned} \tag{2.21}$$

with $\gamma_0(\hat{\mathbf{s}},\mathbf{r}) = \overline{I_0(\hat{\mathbf{s}}',\mathbf{r})p(\hat{\mathbf{s}}-\hat{\mathbf{s}}')}$.

We consider from now on that the scattering is isotropic, which implies that $p(\hat{\mathbf{s}}-\hat{\mathbf{s}}')$ is independent of the angle between $\hat{\mathbf{s}}$ and $\hat{\mathbf{s}}'$. Under the additional assumption that the collisions with the scatterers are elastic (i.e. no absorption), we have $p(\hat{\mathbf{s}}-\hat{\mathbf{s}}')=1$, which implies $\gamma_0(\mathbf{r}) = I_0(\mathbf{r})$, and Eq.(2.21) becomes

$$\hat{\mathbf{s}}\cdot\boldsymbol{\nabla} I_D(\hat{\mathbf{s}},\mathbf{r}) = -\frac{1}{l} I_D(\hat{\mathbf{s}},\mathbf{r}) + \frac{1}{l} I_D(\mathbf{r}) + \frac{1}{l} I_0(\mathbf{r}) + \frac{1}{l}\gamma(\hat{\mathbf{s}},\mathbf{r})\,. \tag{2.22}$$

Similarly to Eq.(2.19), we can write the average of the intensity current $\mathbf{j}(\mathbf{r})$ as a sum of two terms,

$$\langle \mathbf{j}(\mathbf{r})\rangle = \mathbf{j_0}(\mathbf{r}) + \mathbf{j_D}(\mathbf{r})\,, \tag{2.23}$$

where $\mathbf{j_0}(\mathbf{r}) = v\overline{I_0(\hat{s},\mathbf{r})\hat{s}}$ is the current associated to the Drude-Boltzmann term, $\mathbf{j_D}(\mathbf{r}) = v\overline{I_D(\hat{s},\mathbf{r})\hat{s}}$ the current associated to the diffusive contribution, and v the group velocity. Further on, we will neglect $\mathbf{j_0}(\mathbf{r})$ as it exponentially decreases to zero and does not play a role in the derivation of the fluctuation induced forces, discussed in chapter 4. We keep it here for a more complete description. From Eq.(2.20), we obtain

$$\boldsymbol{\nabla}\cdot\mathbf{j_0}(\mathbf{r}) = -\frac{v}{l} I_0(\mathbf{r})\,, \tag{2.24}$$

and, from Eq.(2.22), that the diffusive current satisfies the equation

$$\boldsymbol{\nabla}\cdot\mathbf{j_D}(\mathbf{r}) = \frac{v}{l} I_0(\mathbf{r}) + \frac{v}{l}\gamma(\mathbf{r})\,, \tag{2.25}$$

where $\gamma(\mathbf{r}) = \overline{\gamma(\hat{\mathbf{s}},\mathbf{r})}$ is the light source distribution inside the medium. From Eq.(2.24) and Eq.(2.25), we obtain a continuity equation for the total average current,

$$\boldsymbol{\nabla} \cdot \langle \mathbf{j}(\mathbf{r}) \rangle = \frac{v}{l} \gamma(\mathbf{r}) \,. \tag{2.26}$$

In this thesis, we focus on the cases where the light source is located outside of the random medium, i.e. $\gamma(\mathbf{r}) = 0$ and the light flux is conserved.

In the diffusion approximation, $I_D(\widehat{\mathbf{s}}, \mathbf{r})$ can be written

$$I_D(\widehat{\mathbf{s}}, \mathbf{r}) = I_D(\mathbf{r}) + \frac{3}{v} \mathbf{j_D}(\mathbf{r}) \cdot \widehat{\mathbf{s}} \,. \tag{2.27}$$

Replacing Eq.(2.27) in Eq.(2.22), we obtain

$$\widehat{\mathbf{s}} \cdot \boldsymbol{\nabla} I_D(\mathbf{r}) + \frac{3}{v} \widehat{\mathbf{s}} \cdot \boldsymbol{\nabla} (\mathbf{j_D}(\mathbf{r}) \cdot \widehat{\mathbf{s}}) = -\frac{3}{vl} \mathbf{j_D}(\mathbf{r}) \cdot \widehat{\mathbf{s}} + \frac{1}{l} \gamma(\widehat{\mathbf{s}}, \mathbf{r}) + \frac{1}{l} I_0(\mathbf{r}) \,. \tag{2.28}$$

Projecting Eq.(2.28) on $\widehat{\mathbf{s}}$ and taking the average over all directions $\widehat{\mathbf{s}}$ gives the Fick's law,

$$\mathbf{j_D}(\mathbf{r}) = -D \boldsymbol{\nabla} I_D(\mathbf{r}) + v \overline{\widehat{\mathbf{s}} \gamma(\widehat{\mathbf{s}}, \mathbf{r})} \,. \tag{2.29}$$

In the absence of light sources inside the medium, the Fick's law take the simpler form

$$\mathbf{j_D}(\mathbf{r}) = -D \boldsymbol{\nabla} I_D(\mathbf{r}) \,. \tag{2.30}$$

Finally, combining Eq.(2.25) and Eq.(2.29), we obtain the diffusion equation satisfied by $I_D(\mathbf{r})$,

$$-D \Delta I_D(\mathbf{r}) = \frac{v}{l} I_0(\mathbf{r}) + \frac{v}{l} \gamma(\mathbf{r}) - v \overline{\widehat{\mathbf{s}} \cdot \boldsymbol{\nabla} \gamma(\mathbf{r}, \widehat{\mathbf{s}})} \,. \tag{2.31}$$

Note that $I_0(\mathbf{r})$ plays the role of a source for the diffusive intensity $I_D(\mathbf{r})$; therefore, when the medium is illuminated by an external light source only, i.e. $\gamma = 0$, the right hand side of the diffusion equation Eq.(2.31) is non zero.

Using the Green's identity and the Green's function of the diffusion equation, $P_D(\mathbf{r}, \mathbf{r}')$, introduced in Eq.(2.14), we obtain the expression of $I_D(\mathbf{r})$,

$$I_D(\mathbf{r}) = \int_V d\mathbf{r}' \gamma'(\mathbf{r}') P_D(\mathbf{r}, \mathbf{r}') \,, \tag{2.32}$$

where $\gamma'(\mathbf{r}) = \frac{v}{l} I_0(\mathbf{r}) + \frac{v}{l} \gamma(\mathbf{r}) - v \overline{\widehat{\mathbf{s}} \cdot \boldsymbol{\nabla} \gamma(\mathbf{r}, \widehat{\mathbf{s}})}$ is the source term in the diffusion equation (2.31). We assume from now on that the light source is isotropic, which implies $\overline{\widehat{\mathbf{s}} \cdot \boldsymbol{\nabla} \gamma(\mathbf{r}, \widehat{\mathbf{s}})} = 0$ and

$$-D \Delta I_D(\mathbf{r}) = \frac{v}{l} I_0(\mathbf{r}) + \frac{v}{l} \gamma(\mathbf{r}) \,. \tag{2.33}$$

The average light intensity satisfies a diffusion equation, in which the source term has two origins – the Drude-Boltzmann intensity I_0, and possible extra light sources inside the medium. The diffusive intensity I_D can always be put in the form

$$I_D(\mathbf{r}) = \frac{v\mathcal{P}}{DL} h(\mathbf{u}) \tag{2.34}$$

where $\mathcal{P}$ is the power of the light source, h is a dimensionless function which depends on the shape of the system and of the system and on the boundary conditions, but not on the volume V, and where $L \equiv V^{1/3}$ is the characteristic length of the system. This will be useful for studying the scaling of light fluctuations and light fluctuations induced forces in chapter 4.

The boundary conditions for I_D, necessary to solve Eq.(2.33), are not trivial and deserve to be discussed in detail.

2.1.4 Boundary conditions

The boundary conditions for the disorder averaged intensity $I_D(\mathbf{r})$ are derived from the boundary conditions on $I_D(\hat{\mathbf{s}}, \mathbf{r})$. Since diffusion processes happen inside the disordered medium, any incoming diffusion intensity must vanish on the interface between the medium and the outside,

$$I_D(\hat{\mathbf{s}}, \mathbf{r}) = 0 \text{ for } \mathbf{r} \in \text{interface and for } \hat{\mathbf{s}} \text{ directed inwards} \tag{2.35}$$

However, this condition cannot be satisfied exactly in the diffusive approximation, and has to be replaced instead by a condition on the diffusive light flux (see A5.2 in [13]). We impose that the incoming flux $\mathbf{j_D}$ must vanish at every point of the interface:

$$\mathbf{j_{D,in}}(\mathbf{r}) \cdot \hat{\mathbf{n}} = v\langle \hat{\mathbf{s}} \cdot \hat{\mathbf{n}} I_D(\mathbf{r}, \hat{\mathbf{s}}) \rangle_{\hat{\mathbf{s}},in} = 0 \text{ for any } \mathbf{r} \in \text{the interface} \tag{2.36}$$

with $\hat{\mathbf{n}}$ the normal vector of the interface and the average being done over vectors $\hat{\mathbf{s}}$ directed inwards. More precisely, if we take into account internal reflexions on the inside wall of the interface, the boundary condition becomes:

$$\mathbf{j_{D,in}}(\mathbf{r}) \cdot \hat{\mathbf{n}} = R \;\; \mathbf{j_{D,out}}(\mathbf{r}) \cdot \hat{\mathbf{n}} \tag{2.37}$$

with R the reflexion coefficient.

This leads to the following boundary conditions for $I_D(\mathbf{r})$:

$$\frac{1}{2}(1-R) I_D(\mathbf{r}) = \frac{l}{3}(1+R)\hat{\mathbf{s}} \cdot \nabla I_D(\mathbf{r}) + (1-R)\gamma(\mathbf{r}) \tag{2.38}$$

where $\gamma(\mathbf{r})$ denotes the source terms.

Similarly, the boundary conditions for $P_D(\mathbf{r}, \mathbf{r}')$ are:

$$\frac{1}{2}(1-R) P_D(\mathbf{r}, \mathbf{r}') = \frac{l}{3}(1+R)\hat{\mathbf{s}} \cdot \nabla_{\mathbf{r}} P_D(\mathbf{r}, \mathbf{r}') \tag{2.39}$$

In this work we will consider two limit cases:

- Dirichlet boundary conditions ($R = 0$): $\quad P_D(\mathbf{r}, \mathbf{r}') = \frac{2l}{3}\hat{\mathbf{s}} \cdot \nabla_{\mathbf{r}} P_D(\mathbf{r}, \mathbf{r}')$ (2.40)

- Neumann boundary conditions ($R = 1$): $\quad \hat{\mathbf{s}} \cdot \nabla_{\mathbf{r}} P_D(\mathbf{r}, \mathbf{r}') = 0$ (2.41)

Remark: in this thesis, we mainly consider slab geometries, where P_D varies linearly over distances smaller than l. In this case, we can replace the mixed boundary condition (2.40) by a Dirichlet condition at a distance $\frac{2l}{3}$ from the border, outside of the medium. For example,

the boundary condition at the interface located in the plane $x = 0$ (between the medium and the outside) would be

$$P_D(\mathbf{r}, \mathbf{r}') = 0 \text{ for } \mathbf{r} = \left(-\tfrac{2l}{3}, y, z\right) \tag{2.42}$$

2.2 Light intensity fluctuations

All phase dependent effects have been washed out in the disorder average diffusive limit underlying Eqs.(2.29, 2.31). Indeed, we considered that the only processes contributing to the intensity are the paired trajectories, or diffusons, represented on Fig.2.2.a. However, it is possible for a diffuson to cross with itself or with another diffuson, as illustrated on Fig.2.4. These crossings lead to a phase exchange between the incoming amplitudes and to a new pairing of amplitude. On Fig.2.4.a, a diffuson intersects itself, forming a loop in which the trajectories evolve in opposite directions; such a pairing of time reversed amplitudes is called a cooperon. These processes contribute to the total intensity in the bulk of the system, but the effect is negligible, and we will not take it into account. Let us highlight that the electronic conterpart of this process leads to significant fluctuations of the electronic conductance, and to the phenomenon of weak localization [31]. For light, the pairing of time reversed trajectories becomes important when measuring the outcoming light, and leads to the albedo phenomenon: when illuminating a scattering medium, a part of the coherent light is scattered back due to multiple scattering effects (see chapter 8 in [13]). In the direction opposite to the incidence direction, due to the cooperon contributions, the backscattered coherent light is twice that of the classical value (obtained by neglecting the coherent effects).

The crossings between two paired trajectories, Fig.2.4.b, called quantum crossings, lead to the emergence of spatially long ranged fluctuations of light. For such crossings to remain coherent, the dephasing induced by the unpairing and re-pairing process must be small, which means that the crossing itself has to be localized in space. More precisely, the crossing needs to occur at length scales smaller than the elastic mean free path l. Quantum crossings are conveniently described by Hikami boxes [13, 32, 33] – the square in Fig.2.5.c – an operator which permutes four incoming amplitudes.

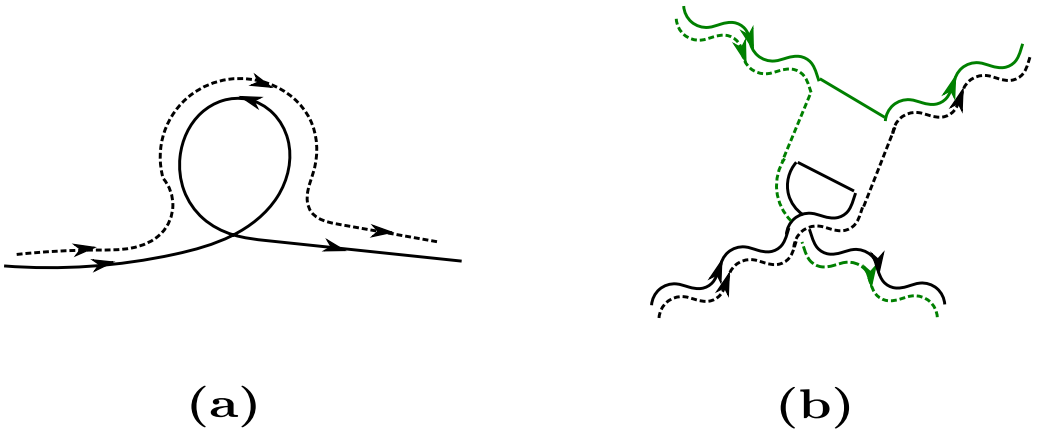

FIGURE 2.4: **(a)** Crossing of a diffuson with itself. Inside the loop, the two scattering trajectories are in opposite directions, forming a cooperon. **(b)** Two incoming diffusons cross and exchange phases so as to form two new outcoming diffusons.

The occurrence of a quantum crossing in a disordered medium of volume L^d is controlled by a single dimensionless parameter, its conductance,

$$g \equiv \frac{k^{d-1}l}{3\pi} L^{d-2} \tag{2.43}$$

which depends on the geometry and on scattering properties of the medium. To see this qualitatively, we may interpret the probability of a quantum crossing to occur as proportional the ratio between the "volume" of a diffuson and the total volume. To estimate a diffuson's volume, we note that the typical length of a diffusive trajectory is $\mathcal{L} = v\tau_D$, where v is the group velocity and $\tau_D = L^2/D$ is the diffusion time or the Thouless time [34, 35] – the typical time required to diffuse from a boundary to another. For a monochromatic radiation of wavelength λ, we may assign a cross section λ^{d-1} to a diffuson [13]. The probability of a quantum crossing to occur is then proportional to

$$\frac{\mathcal{L}\lambda^{d-1}}{L^d} \propto \frac{3\pi}{k^{d-1}l} L^{2-d} = \frac{1}{g}.$$

From now on and without loosing in generality, we consider the three dimensional case, $d = 3$.

In the weak disorder limit $kl \gg 1$, the conductance g is large, $g \ll 1$, and small coherent corrections generated by quantum crossings show up as powers of $1/g$. This scheme allows to expand spatial (connected) correlation function of the fluctuating light intensity $\delta I(\mathbf{r}) \equiv I(\mathbf{r}) - I_D(\mathbf{r})$, defined by

$$\langle \delta I(\mathbf{r}) \delta I(\mathbf{r}') \rangle = \langle I(\mathbf{r}) I(\mathbf{r}') \rangle - I_D(\mathbf{r}) I_D(\mathbf{r}'), \tag{2.44}$$

as

$$\frac{\langle \delta I(\mathbf{r}) \delta I(\mathbf{r}') \rangle}{I_D(\mathbf{r}) I_D(\mathbf{r}')} = C_1(\mathbf{r}, \mathbf{r}') + C_2(\mathbf{r}, \mathbf{r}') + C_3(\mathbf{r}, \mathbf{r}') \ . \tag{2.45}$$

The first contribution C_1 is short ranged and independent of g. The two other contributions are long ranged, and respectively proportional to $1/g$ and $1/g^2$. All three terms contribute to specific features of interference speckle patterns [14], and have been measured in weakly disordered electronic and photonic media [13, 15, 16, 17, 18, 19]. In practice, all three contributions can be derived using a diagrammatic approach, detailed hereafter. For this diagrammatic derivation, it is convenient to consider instead the non normalized correlation function,

$$\langle \delta I(\mathbf{r}) \delta I(\mathbf{r}') \rangle = \langle \delta I(\mathbf{r}) \delta I(\mathbf{r}') \rangle^{(1)} + \langle \delta I(\mathbf{r}) \delta I(\mathbf{r}') \rangle^{(2)} + \langle \delta I(\mathbf{r}) \delta I(\mathbf{r}') \rangle^{(3)} \tag{2.46}$$

where the $\langle \delta I(\mathbf{r}) \delta I(\mathbf{r}') \rangle^{(j)} = I_D(\mathbf{r}) I_D(\mathbf{r}') C_j(\mathbf{r}, \mathbf{r}')$.

2.2.1 Short ranged correlation C_1

The short ranged term $\langle \delta I(\mathbf{r}) \delta I(\mathbf{r}') \rangle^{(1)}$ corresponds to the diagram Fig.2.5.b, where two wave packets propagate by multiple scattering and cross between $\mathbf{r_1}$, $\mathbf{r_2}$ and $\mathbf{r}$, $\mathbf{r}'$. It is equal to

$$\begin{aligned}\langle \delta I(\mathbf{r})\delta I(\mathbf{r}')\rangle^{(1)} &= \left(\tfrac{4\pi}{v}\right)^2 \iint_{V\times V} d\mathbf{r_0} d\mathbf{r}_0' \gamma'(\mathbf{r_0})\gamma'(\mathbf{r}_0') \\ &\int_V d\mathbf{r_1} d\mathbf{r_2} d\mathbf{r_3} d\mathbf{r_4} |\langle G^R(\mathbf{r_0},\mathbf{r_1})\rangle|^2 |\langle G^R(\mathbf{r}_0',\mathbf{r_2})\rangle|^2 \Gamma(\mathbf{r_1},\mathbf{r_3})\Gamma(\mathbf{r_2},\mathbf{r_4}) \\ &\times \langle G^R(\mathbf{r_3},\mathbf{r})\rangle \langle G^A(\mathbf{r}',\mathbf{r_3})\rangle \langle G^R(\mathbf{r_4},\mathbf{r}')\rangle \langle G^A(\mathbf{r},\mathbf{r_4})\rangle\end{aligned} \tag{2.47}$$

with $\gamma'(\mathbf{r})$ the source term for $I_D(\mathbf{r})$ introduced in Eq.(2.32) and $4\pi/v$ a normalization factor. In the diffusive limit, the structure factor Γ varies slowly in space. With the notations of the Fig.2.5, this implies that we can replace $\Gamma(\mathbf{r_1},\mathbf{r_3}) \approx \Gamma(\mathbf{r_0},\mathbf{r})$ and $\Gamma(\mathbf{r_2},\mathbf{r_4}) \approx \Gamma(\mathbf{r}_0',\mathbf{r}')$ in Eq.(2.47). From Eq.(2.13), and using the Green's identity, we obtain

$$\int_V d\mathbf{r_0}\, \gamma'(\mathbf{r_0})\Gamma(\mathbf{r_0},\mathbf{r}) = \frac{4\pi v}{l^2} I_D(\mathbf{r}) \tag{2.48}$$

The squared Green's functions are decoupled; their integral is equal to

$$\int_V d\mathbf{r_1}\, |\langle G^R(\mathbf{r_0},\mathbf{r_1})\rangle|^2 = \frac{l}{4\pi}$$

Using now

$$\int_V d\mathbf{r_3}\, \langle G^R(\mathbf{r_3},\mathbf{r})\rangle \langle G^A(\mathbf{r}',\mathbf{r_3})\rangle = \frac{l}{4\pi}\mathrm{sinc}(k|\mathbf{r}-\mathbf{r}'|)e^{-|\mathbf{r}-\mathbf{r}'|/2l},$$

we obtain finally

$$\begin{aligned}\langle \delta I(\mathbf{r})\delta I(\mathbf{r}')\rangle^{(1)} &= I_D(\mathbf{r})^2 \mathrm{sinc}^2(k|\mathbf{r}-\mathbf{r}'|)e^{-|\mathbf{r}-\mathbf{r}'|/l} \\ &\simeq \tfrac{2\pi l}{k^2} I_D(\mathbf{r})^2 \delta(\mathbf{r}-\mathbf{r}')\end{aligned} \tag{2.49}$$

This short ranged contribution is independent of g, and gives the main contribution to the speckle patterns Fig.2.1.b.

2.2.2 Long ranged term C_2

The notion of quantum crossings (coherent effects) is essential to understand the long ranged contribution to the intensity fluctuations. For the derivation of C_1, we only considered the processes where light intensity propagates diffusively along two trajectories, which unpair at the end of the propagation only, as depicted in Fig.2.5.b. Here, we include quantum crossings, quantitatively described by means of a Hikami box Fig.2.5.c.

The long ranged term C_2 includes processes involving one quantum crossing, illustrated by the diagram on Fig.2.5.c. Reading from the diagram, we obtain

$$\begin{aligned}\langle \delta I(\mathbf{r})\delta I(\mathbf{r}')\rangle^{(2)} &= \left(\tfrac{4\pi}{v}\right)^2 \int_V d\mathbf{r_0} d\mathbf{r}_0' \gamma'(\mathbf{r_0})\gamma'(\mathbf{r}_0') \int_V \prod_{i=1}^{4} d\mathbf{R_i} \prod_{j=1}^{4} d\mathbf{r_j} \\ &|G^R(\mathbf{r_0},\mathbf{r_1})|^2 |G^R(\mathbf{r}_0',\mathbf{r_3})|^2 H(\mathbf{R_i})\Gamma(\mathbf{r_1},\mathbf{R_1})\Gamma(\mathbf{r_3},\mathbf{R_3}) \\ &\times \Gamma(\mathbf{R_2},\mathbf{r_2})\Gamma(\mathbf{R_4},\mathbf{r_4})|G^R(\mathbf{r_2},\mathbf{r}')|^2 |G^R(\mathbf{r_4},\mathbf{r})|^2 ,\end{aligned} \tag{2.50}$$

with $\gamma'(\mathbf{r})$ the source term for $I_D(\mathbf{r})$ introduced in Eq.(2.32), and where $H(\mathbf{R_i})$ is the Hikami box [32]. Its analytical expression is

$$H(\mathbf{R_i}) = 2h_4 \int_V d\mathbf{R} \prod_{i=1}^{4} \delta(\mathbf{R}-\mathbf{R_i}) \boldsymbol{\nabla}_{\mathbf{R_2}} \cdot \boldsymbol{\nabla}_{\mathbf{R_4}} , \tag{2.51}$$

with $h_4 = \frac{l^5}{48\pi k^2}$, as detailed in [13]. In the diffusive limit, $\Gamma(\mathbf{r},\mathbf{r}')$ varies slowly and we can replace $\Gamma(\mathbf{r_1},\mathbf{R_1}) \simeq \Gamma(\mathbf{r_0},\mathbf{R_1})$, $\Gamma(\mathbf{r_3},\mathbf{R_3}) \simeq \Gamma(\mathbf{r}_0',\mathbf{R_3})$, $\Gamma(\mathbf{R_2},\mathbf{r_2}) \simeq \Gamma(\mathbf{R_2},\mathbf{r})$ and $\Gamma(\mathbf{R_4},\mathbf{r_4}) \simeq \Gamma(\mathbf{R_4},\mathbf{r}')$ in Eq.(5.53). The averaged Green's function are then decoupled; their integral is equal to $\frac{l}{4\pi}$. Applying the Hikami box operator on the functions Γ, we obtain,

$$\begin{aligned}\langle \delta I(\mathbf{r})\delta I(\mathbf{r}')\rangle^{(2)} &= 2h_4 \left(\tfrac{4\pi}{v}\right)^2 \left(\tfrac{l}{4\pi}\right)^4 \int_V d\mathbf{r_0} d\mathbf{r}_0' \gamma'(\mathbf{r_0})\gamma'(\mathbf{r}_0') \\ &\int_V d\mathbf{R} \int_V \prod_{i=1}^{4} d\mathbf{R_i} \delta(\mathbf{R}-\mathbf{R_i}) \boldsymbol{\nabla}_{\mathbf{R_2}} \cdot \boldsymbol{\nabla}_{\mathbf{R_4}} \left[\Gamma(\mathbf{r_0},\mathbf{R_1})\Gamma(\mathbf{r}_0',\mathbf{R_3})\Gamma(\mathbf{R_2},\mathbf{r}')\Gamma(\mathbf{R_4},\mathbf{r})\right] \\ &= 2h_4 \left(\tfrac{4\pi}{v}\right)^2 \left(\tfrac{l}{4\pi}\right)^4 \\ &\times \int_V d\mathbf{r_0} d\mathbf{r}_0' \gamma'(\mathbf{r_0})\gamma'(\mathbf{r}_0') \int_V d\mathbf{R}\, \Gamma(\mathbf{r_0},\mathbf{R})\Gamma(\mathbf{r}_0',\mathbf{R}) \boldsymbol{\nabla}_{\mathbf{R}}\Gamma(\mathbf{R},\mathbf{r}') \cdot \boldsymbol{\nabla}_{\mathbf{R}}\Gamma(\mathbf{R},\mathbf{r}) .\end{aligned} \tag{2.52}$$

Using Eq.(2.13) and Eq.(2.32), we obtain finally

$$\langle \delta I(\mathbf{r})\delta I(\mathbf{r}')\rangle^{(2)} = c_0 \int_V d\mathbf{R}\, I_D^2(\mathbf{R}) \boldsymbol{\nabla}_{\mathbf{R}} P_D(\mathbf{R},\mathbf{r}) \cdot \boldsymbol{\nabla}_{\mathbf{R}} P_D(\mathbf{R},\mathbf{r}') , \tag{2.53}$$

with $c_0 = \frac{2\pi l v^2}{3k^2}$. The normalized correlation function is then

$$C_2(\mathbf{r},\mathbf{r}') = \frac{c_0 \int_V d\mathbf{R}\, I_D^2(\mathbf{R}) \boldsymbol{\nabla}_{\mathbf{R}} P_D(\mathbf{R},\mathbf{r}) \cdot \boldsymbol{\nabla}_{\mathbf{R}} P_D(\mathbf{R},\mathbf{r}')}{I_D(\mathbf{r}) I_D(\mathbf{r}')} \tag{2.54}$$

To see that Eq.(2.54) is proportional to $1/g$, it is useful to move to dimensionless variables and functions,

$$\begin{cases} \mathbf{u} = \mathbf{r}/L \\ \\ \tilde{P}_D(\mathbf{u},\mathbf{u}') = DLP_D(\mathbf{r},\mathbf{r}') \end{cases} \tag{2.55}$$

Upon this change of variable, Eq.(2.54) takes the form

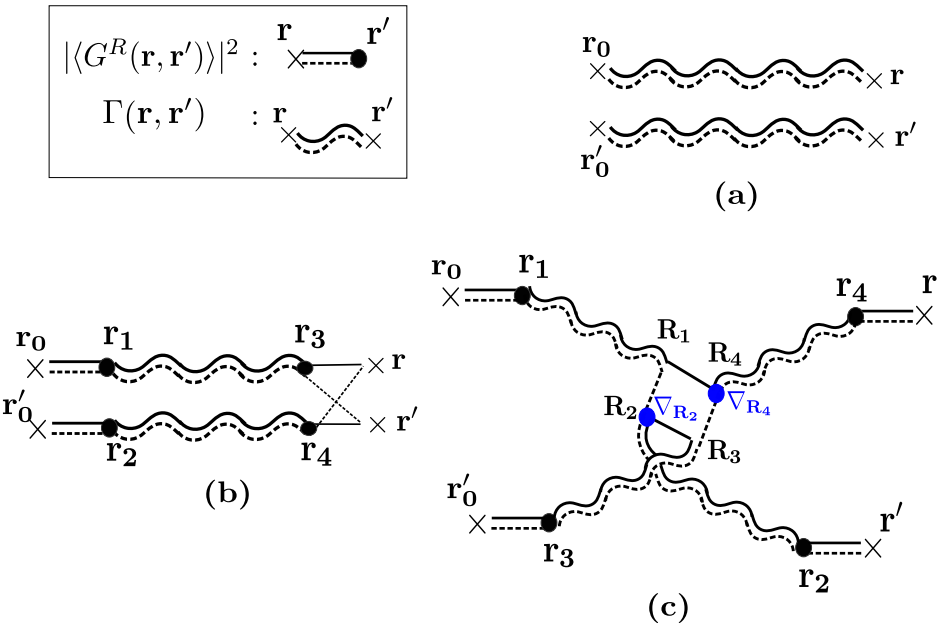

FIGURE 2.5: **(a)** Two diffusion paths propagating without interacting. **(b)** Representation of the short-ranged term in the correlation function of the intensity fluctuations. **(c)** Diagram corresponding to the C_2 term of the intensity correlations. The square represents a Hikami box, describing one quantum crossing between two diffusion paths.

$$\begin{aligned} C_2(\mathbf{r},\mathbf{r}') &= \frac{c_0}{D^2 L}\frac{\int_{\tilde{V}} d\mathbf{U}\, I_D^2(\mathbf{U})\boldsymbol{\nabla}_{\mathbf{U}}\tilde{P}_D(\mathbf{U},\mathbf{u})\cdot\boldsymbol{\nabla}_{\mathbf{U}}\tilde{P}_D(\mathbf{U},\mathbf{u}')}{I_D(\mathbf{r})I_D(\mathbf{r}')} \\ &= \frac{3\pi}{k^2 l L}\mathcal{N}_2 \\ &= \frac{1}{g}\mathcal{N}_2 \end{aligned} \tag{2.56}$$

where $\tilde{V}$ is the renormalized volume and

$$\mathcal{N}_2 = \frac{\int_{\tilde{V}} d\mathbf{U}\, I_D^2(\mathbf{U})\boldsymbol{\nabla}_{\mathbf{U}}\tilde{P}_D(\mathbf{U},\mathbf{u})\cdot\boldsymbol{\nabla}_{\mathbf{U}}\tilde{P}_D(\mathbf{U},\mathbf{u}')}{I_D(\mathbf{r})I_D(\mathbf{r}')}$$

is a dimensionless number, independent of the volume, which depends solely on the boundary conditions, the shape of the system and the nature of the light source.

2.2.3 Long ranged term C_3

The term $C_3(\mathbf{r},\mathbf{r}')$, contains the processes with two diffuson crossings, i.e. two Hikami boxes. It can be shown [13] that all the possible combinations boil down to the diagrams represented in Fig.2.6. Before diving into the diagrammatic calculations, we can convince ourselves that all three diagrams will give a contribution proportional to c_0^2, where c_0 is the prefactor in Eq.(2.53), $c_0 = \frac{2\pi l c^2}{3k^2}$. Indeed, the diagrams in Fig.2.6 are built from four squared Green's functions, six propagators structure factors, and two Hikami boxes. Each of these terms give, respectively, $\left(\frac{l}{4\pi}\right)^4$, $\left(\frac{4\pi v}{l^2}\right)^6$

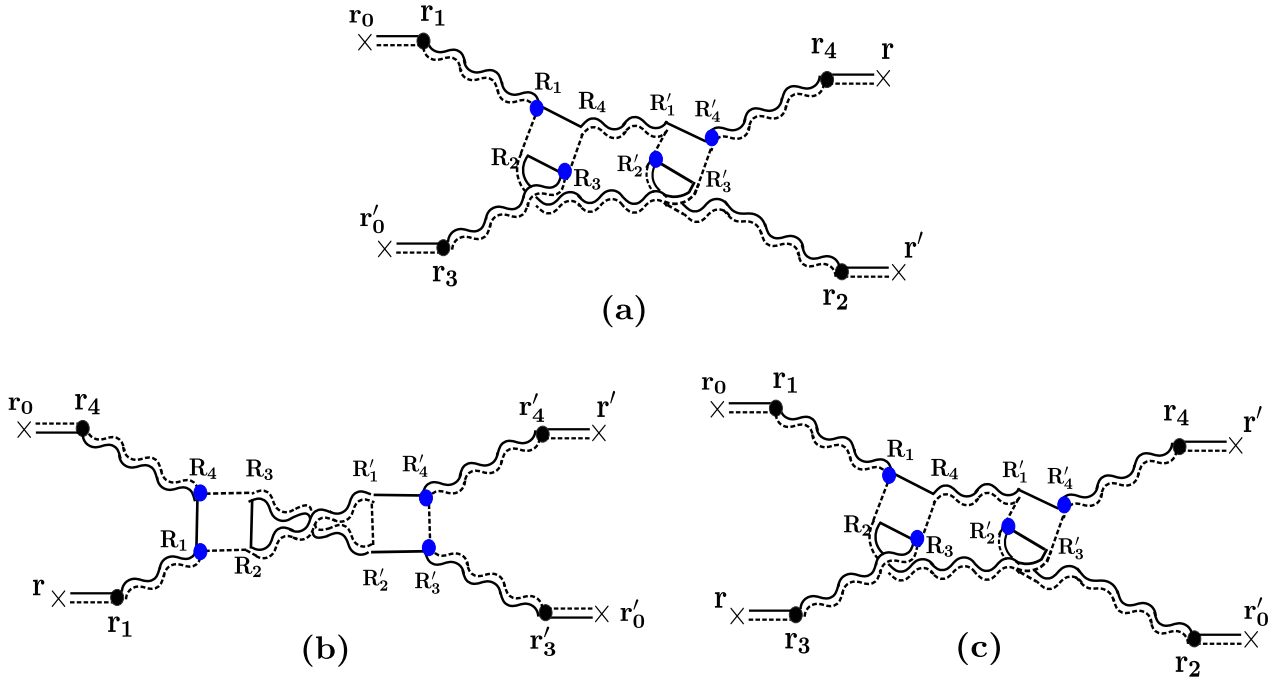

FIGURE 2.6: Diagrammatic representation of the two types of processes contributing to C_3. The blue dots represent the vertices dressed with a ∇ operator.

and $(2h_4)^2 = \left(\frac{l^5}{24\pi k^2}\right)^2$. Taking into account the normalization factor $\left(\frac{4\pi}{v}\right)^2$, we obtain the prefactor for the diagrams,

$$\left(\frac{4\pi}{v}\right)^2 \left(\frac{l}{4\pi}\right)^4 \left(\frac{4\pi v}{l^2}\right)^6 \left(\frac{l^5}{24\pi k^2}\right)^2 = \left(\frac{2\pi l c^2}{3k^2}\right)^2 = c_0^2$$

This prefactor is the fingerprint of the underlying occurrence of quantum crossings.

The correlation function $\langle \delta I(\mathbf{r}) \delta I(\mathbf{r}') \rangle^{(3)}$ is hence the sum of three terms, which we write in the form

$$\langle \delta I(\mathbf{r}) \delta I(\mathbf{r}') \rangle^{(3)} = c_0^2 \sum_{j=1,2,3} D_j(\mathbf{r}, \mathbf{r}') \tag{2.57}$$

where D_1, D_2, D_3 correspond to the diagrams Fig.2.6.a, Fig.2.6.b, Fig.2.6.c respectively.

Following the same method as in the previous section, we obtain for the first diagram D_1,

$$D_1(\mathbf{r}, \mathbf{r}') = c_0^2 \iint_{V \times V} d\mathbf{R}\, d\mathbf{R}' \, |\boldsymbol{\nabla}_{\mathbf{R}} I_D(\mathbf{R})|^2 P_D^2(\mathbf{R}, \mathbf{R}') \boldsymbol{\nabla}_{\mathbf{R}'} P_D(\mathbf{r}, \mathbf{R}') \cdot \boldsymbol{\nabla}_{\mathbf{R}'} P_D(\mathbf{R}', \mathbf{r}') \,. \tag{2.58}$$

The diagrams in Fig.2.6.b and Fig.2.6.c give the same terms, $D_2(\mathbf{r}, \mathbf{r}') = D_3(\mathbf{r}, \mathbf{r}')$, with

$$D_2(\mathbf{r},\mathbf{r}') = c_0^2 \iint_{V\times V} d\mathbf{R}\, d\mathbf{R}'\, \boldsymbol{\nabla}_{\mathbf{R}} I_D(\mathbf{R}) \cdot \boldsymbol{\nabla}_{\mathbf{R}'} I_D(\mathbf{R}') P_D^2(\mathbf{R},\mathbf{R}') \boldsymbol{\nabla}_{\mathbf{R}} P_D(\mathbf{r},\mathbf{R}) \cdot \boldsymbol{\nabla}_{\mathbf{R}'} P_D(\mathbf{R}',\mathbf{r}')\,. \tag{2.59}$$

Using the change of variable in Eqs.(2.55), the dependence of C_3 in $1/g^2$ appears clearly, and we may write

$$C_3(\mathbf{r},\mathbf{r}') = \frac{1}{g^2}\mathcal{N}_3 \tag{2.60}$$

where $\mathcal{N}_3$ is a dimensionless number, independent of the volume, which depends solely on the boundary conditions, the shape of the system and the nature of the light source.

Remark: the diffuson crossings can also be observed by means of the transmission coefficient T, defined as $T = \sum_{a,b} T_{a,b}$, where $T_{a,b}$ corresponds to the intensity transmitted in the direction $\widehat{\mathbf{s}}_\mathbf{b}$ for an incident beam propagating along $\widehat{\mathbf{s}}_\mathbf{a}$. The two diffuson crossings processes, discussed for the term C_3, lead to fluctuations of the transmission coefficient which are expressed simply by (see chapter 12 in [13])

$$\langle \delta T^2 \rangle = \frac{2}{15} \tag{2.61}$$

a number independent of the disorder. These fluctuations are therefore universal, and are referred to in the literature as universal conductance fluctuations [16], similarly to their electronic counterpart [36, 37, 38].

Chapter 3

Langevin approach to mesoscopic fluctuations

Patauger, quelquefois, c'est aussi faire bondir deux ou trois gouttes de lumière.

(While dabbling we sometimes splash up a few drops of light.)

Paul Valéry

In chapter 2, we discussed the properties of light propagating through a random medium, and showed how coherent effects lead to spatially long ranged fluctuations of light. In this chapter, we show that these light fluctuations can be described in a different but equivalent way by noting that quantum crossings occur at lengths of order l. This allows to separate large scale ($\gg l$) incoherent diffusive physics from small scale, coherent and phase preserving quantum crossings. Such scale partition is efficiently described by means of a Langevin equation.

The objective of this chapter is to derive an effective Langevin equation for coherent light, and explain how to systematically incorporate the coherent effects in the noise term. This Langevin approach maps the problem of coherent multiple light scattering onto an effective non equilibrium light flow, characterized by two parameters only, the diffusion coefficient D and the strength of the noise σ – also called the mobility – related by a Einstein relation. The mapping between coherent light and non equilibrium hydrodynamics is intriguing by itself from a fundamental viewpoint. On a practical level, the non equilibrium hydrodynamics framework provides a new insight for the understanding of the light flow's properties, as discussed in chapter 5. The main advantage of the Langevin approach lies in its dependance on two parameters only, D and σ, which greatly simplifies the study of the light fluctuations. The method can be generalized to other diffusive systems, e.g. electronic transport in random metals, which is discussed briefly in the last section.

3.1 Effective Langevin equation for coherent light

The diffusion equation (2.33) and the Fick's law Eq.(2.30), between the diffusive intensity and current, $\mathbf{j_D}(\mathbf{r}) = -D\boldsymbol{\nabla} I_D(\mathbf{r})$, are disorder averaged and do not include the coherent corrections discussed in chapter 2. Since the coherent corrections occur at lengths of order l, we may divide the light intensity and current fluctuations into two groups, the microscopic fluctuations which occur over length scales l, and

diffusive fluctuations propagating over larger distances. In order to quantitatively describe this phenomenon, we generalize the Fick's law, for properly coarse grained functions I and $\mathbf{j}$, averaged over a small volume lk^{-2} but not over disorder. The coherent fluctuations are encapsulated in a zero average noise term $\boldsymbol{\nu}(\boldsymbol{r})$,

$$\mathbf{j}(\mathbf{r}) = -D\boldsymbol{\nabla} I(\mathbf{r}) + \boldsymbol{\nu}(\boldsymbol{r}) \tag{3.1}$$

This effective Langevin equation extends the Fick's law to the fluctuating, not disorder averaged quantities $I(\mathbf{r}) \equiv I_D(\mathbf{r}) + \delta I(\mathbf{r})$ and $\mathbf{j}(\mathbf{r}) \equiv \mathbf{j_D}(\mathbf{r}) + \delta\mathbf{j}(\mathbf{r})$. Removing the averaged quantities from Eq.(3.1) by means of Fick's law Eq.(2.30), we deduce a Langevin equation for the intensity fluctuation $\delta I(\mathbf{r})$, completed with a continuity equation,

$$\begin{cases} \delta\mathbf{j}(\mathbf{r}) = -D\boldsymbol{\nabla}\delta I(\mathbf{r}) + \boldsymbol{\nu}(\boldsymbol{r}) \\ \\ \boldsymbol{\nabla}\cdot\delta\mathbf{j}(\mathbf{r}) = 0 \end{cases} \tag{3.2}$$

We highlight the fact that the noise $\boldsymbol{\nu}(\boldsymbol{r})$ corresponds to coherent effects, and not to the position of scatterers. It is a purely mesoscopic noise, as opposed to the usual scenarios in diffusive systems where the noise is thermal or solely dependent of the scatterers.

The physics contained in Eqs.(3.1,3.2) can be summarized in two important points:
• we can divide light intensity and current fluctuations in two categories, the microscopic fluctuations which occur at length scales l, and diffusive fluctuations propagating over large scales;
• the light intensity and current fluctuations originate from microscopic interference processes which occur at small length scales ($< l$) and which are described by the noise term $\boldsymbol{\nu}$.

We now show that this picture allows to reproduce the $1/g$ expansion of Eq.(2.45), by systematically including quantum crossings contributions in $\boldsymbol{\nu}(\boldsymbol{r})$. The correlation function of the noise is carrefully derived in order to reproduce the quantum crossings effects. This procedure was originally presented in [25] for electronic waves and to the lowest order for electromagnetic waves; we provide here a more modern derivation as well as a computation of higher order terms in $1/g$.

3.1.1 Derivation of the noise term

Before discussing the general method, we present the argument of [25], since it provides an intuitive picture; see also [30]. The idea, to calculate the noise term, is to notice that the local current fluctuations are dominated by the short ranged fluctuations of the intensity Eq.(2.49). Since the light current is related to the intensity by $\mathbf{j}(\mathbf{r}) = v\overline{I(\widehat{\mathbf{s}},\mathbf{r})\widehat{\mathbf{s}}}$, we readily obtain, from Eq.(2.49)[1],

$$\langle \nu_\alpha(\mathbf{r})\nu_\beta(\mathbf{r}')\rangle = \delta_{\alpha\beta}\frac{2\pi l v^2}{3k^2} I_D(\mathbf{r})^2\delta(\mathbf{r}-\mathbf{r}') = \delta_{\alpha\beta}c_0 I_D(\mathbf{r})^2\delta(\mathbf{r}-\mathbf{r}') \tag{3.3}$$

where the factor $1/3$ comes from angular averaging and $c_0 = \frac{2\pi l v^2}{3k^2}$. Using this expression, we recover the long ranged term C_2. Indeed, combining Eqs.(3.2), we obtain

[1] We obtain the same result starting from the quantum mechanics definition of the current $\mathbf{j}(\mathbf{r}) = -\frac{v}{k}\Im\left(\psi(\mathbf{r})\boldsymbol{\nabla}_{\mathbf{r}}\psi^*(\mathbf{r})\right)$, and performing a perturbation development to first order of the product $\langle\psi(\mathbf{r})\boldsymbol{\nabla}_{\mathbf{r}}\psi^*(\mathbf{r})\rangle$, similarly to the derivation of C_1 Eq.(2.49).

$$-D\Delta\delta I(\mathbf{r}) = -\boldsymbol{\nabla}\cdot\boldsymbol{\nu}(\boldsymbol{r}) \tag{3.4}$$

and, using the Green's identity with the Green's function Eq.(2.14),

$$\delta I(\mathbf{r}) = -\int_V d\mathbf{r}'\, P_D(\mathbf{r}',\mathbf{r})\boldsymbol{\nabla}\cdot\boldsymbol{\nu}(\boldsymbol{r}) = \oint_{\partial V} d\mathbf{r}'\, \boldsymbol{\nabla}P_D(\mathbf{r}',\mathbf{r})\cdot\boldsymbol{\nu}(\boldsymbol{r}')\,, \tag{3.5}$$

where we used the boundary condition $\boldsymbol{\nu}(\boldsymbol{r}) = 0$ on the edge ∂V. We deduce the correlation function of the fluctuating intensity,

$$\langle\delta I(\mathbf{r})\delta I(\mathbf{r}')\rangle = c_0\int_V d\mathbf{R}\, I_D^2(\mathbf{R})\boldsymbol{\nabla}_{\mathbf{R}}P_D(\mathbf{R},\mathbf{r})\cdot\boldsymbol{\nabla}_{\mathbf{R}}P_D(\mathbf{R},\mathbf{r}') \tag{3.6}$$

which is exactly Eq.(2.53). Therefore, using the noise term in Eq.(3.3) allows to describe the intensity fluctuations of order $1/g$.

We now show how to include higher order terms, by using a systematic method relying on the diagrammatic description.

The idea, for incorporating the coherent effects in the noise $\boldsymbol{\nu}(\boldsymbol{r})$, is to write an expression of the intensity correlation function Eq.(2.44) using, on the one hand, the Langevin description, and on the other hand, a diagrammatic description. Note that the Eq.(3.5) is an explicit expression of δI only if we assume that the noise $\boldsymbol{\nu}$ is independent of δI. In fact, we now make the assumption that $\boldsymbol{\nu}$ depends solely on the disorder averaged quantities I_D and P_D. More precisely, we assume that any spatial fluctuation of the noise of order δI is negligible for length scales larger than l, which amounts to say that the noise is weak. We check the consistency of this assumption in 3.1.3. With this assumption, we obtain, from Eq.(3.5), the correlation function,

$$\langle\delta I(\mathbf{r})\delta I(\mathbf{r}')\rangle = \iint_{V\times V} d\mathbf{r_1}d\mathbf{r_2}\boldsymbol{\nabla}_{1,\alpha}P_D(\mathbf{r},\mathbf{r_1})\cdot\boldsymbol{\nabla}_{2,\beta}P_D(\mathbf{r}',\mathbf{r_2})\langle\nu_\alpha(\mathbf{r_1})\nu_\beta(\mathbf{r_2})\rangle\,. \tag{3.7}$$

The integral in the right hand side of Eq.(3.7) is long ranged, as are the mesoscopic coherent light fluctuations.

On the other hand, the long ranged correlation function can be derived using the diagrammatic approach presented in chapter 2. It is the sum of two terms,

$$\langle\delta I(\mathbf{r})\delta I(\mathbf{r}')\rangle^{(2)} + \langle\delta I(\mathbf{r})\delta I(\mathbf{r}')\rangle^{(3)}\,, \tag{3.8}$$

where $\langle\delta I(\mathbf{r})\delta I(\mathbf{r}')\rangle^{(2)}$ and $\langle\delta I(\mathbf{r})\delta I(\mathbf{r}')\rangle^{(3)}$ are given in the Eqs.(2.53,2.57).
By identification with Eq.(3.7), we obtain the identity

$$\begin{aligned}\iint_{V\times V} d\mathbf{r_1}d\mathbf{r_2}\boldsymbol{\nabla}_{1,\alpha}P_D(\mathbf{r},\mathbf{r_1})\cdot\boldsymbol{\nabla}_{2,\beta}P_D(\mathbf{r}',\mathbf{r_2}) \quad &\langle\nu_\alpha(\mathbf{r_1})\nu_\beta(\mathbf{r_2})\rangle \\ &= \langle\delta I(\mathbf{r})\delta I(\mathbf{r}')\rangle^{(2)} + \langle\delta I(\mathbf{r})\delta I(\mathbf{r}')\rangle^{(3)}\,.\end{aligned} \tag{3.9}$$

From the identity Eq.(3.9), we predict that $\langle\nu_\alpha(\mathbf{r})\nu_\beta(\mathbf{r}')\rangle$ should be the sum of two terms, corresponding respectively to $\langle\delta I(\mathbf{r})\delta I(\mathbf{r}')\rangle^{(2)}$ and $\langle\delta I(\mathbf{r})\delta I(\mathbf{r}')\rangle^{(3)}$, and therefore proportional to $1/g$ and $1/g^2$ respectively. In the rest of this section, we prove that, indeed, $\langle\nu_\alpha(\mathbf{r})\nu_\beta(\mathbf{r}')\rangle$ is equal to

$$\langle \nu_\alpha(\mathbf{r})\nu_\beta(\mathbf{r}')\rangle = c_0 K_0(\mathbf{r},\mathbf{r}') + c_0^2 \sum_{j=1}^{3} K_j(\mathbf{r},\mathbf{r}') \tag{3.10}$$

where c_0 is the prefactor of the long ranged correlation function Eq.(2.53), and the functions K_j, derived hereafter, depend on the averaged intensity and current $I_D, \mathbf{j_D}$. To recover the dependence in g, notice that c_0 is proportional to the inverse of the conductance,

$$c_0 = \frac{2\pi l v^2}{3k^2} = \frac{D^2}{g} L\,. \tag{3.11}$$

This allows us to identify the term $c_0 K_0$ as the noise term leading to the correlation function $\langle \delta I(\mathbf{r})\delta I(\mathbf{r}')\rangle$, represented by the diagram Fig.(2.5.c), and the terms $c_0^2 \sum_{j=1}^{3} K_j(\mathbf{r},\mathbf{r}')$ as those associated to $\langle \delta I(\mathbf{r})\delta I(\mathbf{r}')\rangle$, in Eq.(2.57). The three functions K_1, K_2, K_3 correspond to the three diagrams of Fig.(2.6).

Let's derive first K_0. Remind that the expression for the long ranged term $\langle \delta I(\mathbf{r})\delta I(\mathbf{r}')\rangle^{(2)}$ obtained from the diagrammatic calculation is equal to

$$\langle \delta I(\mathbf{r})\delta I(\mathbf{r}')\rangle^{(2)} = c_0 \int_V d\mathbf{R}\, I_D^2(\mathbf{R}) \boldsymbol{\nabla}_{\mathbf{R}} P_D(\mathbf{R},\mathbf{r}) \cdot \boldsymbol{\nabla}_{\mathbf{R}} P_D(\mathbf{R},\mathbf{r}')\,, \tag{3.12}$$

with $c_0 = \frac{2\pi l v^2}{3k^2}$.

Comparing Eq.(2.53) with Eq.(3.7) allows to identify the lowest order term in c_0 (or $1/g$ for rescaled correlation functions) of the noise correlation function,

$$c_0 K_0(\mathbf{r},\mathbf{r}') = c_0 I_D^2(\mathbf{r})\delta(\mathbf{r}-\mathbf{r}')\delta_{\alpha\beta}\,, \tag{3.13}$$

and we recover Eq.(3.3). Note that the term $c_0 = \frac{2\pi l v^2}{3k^2}$ in the amplitude of the noise comes directly from the amplitude of the Hikami box and of the value of the other quantities involved in the crossing of two diffusion paths – the structure factor and the average Green's functions $G^{R,A}$. The factor c_0 is the signature of the mesoscopic interference processes which lead to long ranged intensity correlations.

The correlation function $\langle \delta I(\mathbf{r})\delta I(\mathbf{r}')\rangle^{(3)}$ was derived in chapter 2, where we show that it is the sum of three terms,

$$\langle \delta I(\mathbf{r})\delta I(\mathbf{r}')\rangle^{(3)} = c_0^2 \sum_{j=1,2,3} D_j(\mathbf{r},\mathbf{r}') \tag{3.14}$$

where D_1, D_2, D_3 correspond to the diagrams Fig.(2.6.a), Fig.(2.6.b), Fig.(2.6.c) respectively. We remind

$$D_1(\mathbf{r},\mathbf{r}') = c_0^2 \iint_{V\times V} d\mathbf{R}\, d\mathbf{R}'\, |\boldsymbol{\nabla}_{\mathbf{R}} I_D(\mathbf{R})|^2 P_D^2(\mathbf{R},\mathbf{R}') \boldsymbol{\nabla}_{\mathbf{R}'} P_D(\mathbf{r},\mathbf{R}') \cdot \boldsymbol{\nabla}_{\mathbf{R}'} P_D(\mathbf{R}',\mathbf{r}')\,. \tag{3.15}$$

and $D_2(\mathbf{r},\mathbf{r}') = D_3(\mathbf{r},\mathbf{r}')$, with

$$D_2(\mathbf{r},\mathbf{r}') = c_0^2 \iint_{V\times V} d\mathbf{R}\, d\mathbf{R}'\, \boldsymbol{\nabla}_{\mathbf{R}} I_D(\mathbf{R}) \cdot \boldsymbol{\nabla}_{\mathbf{R}'} I_D(\mathbf{R}') P_D^2(\mathbf{R},\mathbf{R}') \boldsymbol{\nabla}_{\mathbf{R}} P_D(\mathbf{r},\mathbf{R}) \cdot \boldsymbol{\nabla}_{\mathbf{R}'} P_D(\mathbf{R}',\mathbf{r}')\,. \tag{3.16}$$

Comparing with Eq.(3.7), we deduce the expressions of the functions K_1, K_2, K_3, which correspond respectively to D_1, D_2, D_3,

$$\begin{cases} K_1(\mathbf{r},\mathbf{r}') = \delta_{\alpha,\beta}\delta(\mathbf{r}-\mathbf{r}')\int d\mathbf{r_1} P_d^2(\mathbf{r_1},\mathbf{r}')\nabla I_D(\mathbf{r_1})\cdot\nabla I_D(\mathbf{r_1}) \\ K_3(\mathbf{r},\mathbf{r}') = K_3(\mathbf{r},\mathbf{r}') = P_D^2(\mathbf{r},\mathbf{r}')\partial_\alpha I_D(\mathbf{r})\partial_\beta I_D(\mathbf{r}') \end{cases} \tag{3.17}$$

To sum, the Langevin equation (3.1) efficiently describes the coherent light flow and its fluctuations to the order $1/g^2$. The Eq.(3.1) is characterized by a constant diffusion coefficient D and a noise term satisfying Eq.(3.10).

3.1.2 Einstein relation

If we keep only the first order term K_0 for the noise correlation function, we may rewrite the noise in the form

$$\boldsymbol{\nu}(\boldsymbol{r}) = \sqrt{\sigma(\mathbf{r})}\boldsymbol{\eta}(\boldsymbol{r}) \tag{3.18}$$

with

$$\sigma = c_0 I_D(\mathbf{r})^2 \tag{3.19}$$

and $\boldsymbol{\eta}(\boldsymbol{r})$ a Gaussian white noise,

$$\begin{cases} \langle \boldsymbol{\eta}(\boldsymbol{r})\rangle = 0 \\ \langle \eta_\alpha(\mathbf{r})\eta_\beta(\mathbf{r}')\rangle = \delta_{\alpha\beta}\delta(\mathbf{r}-\mathbf{r}')\,. \end{cases} \tag{3.20}$$

In this approximation, the Langevin equation (3.1) becomes

$$\mathbf{j}(\mathbf{r}) = -D\boldsymbol{\nabla} I(\mathbf{r}) + \sqrt{\sigma(\mathbf{r})}\boldsymbol{\eta}(\boldsymbol{r})\,. \tag{3.21}$$

This effective Langevin equation provides a description of the light flow and its fluctuations of order $1/g$. The Eq.(3.21) is characterized by the diffusion coefficient D and by the amplitude σ, also called the mobility of the system. However, note that the amplitude of the noise depends on the average value $I_D(\mathbf{r})$, which is different from usual stochastic processes. More precisely, the dependence upon a constant D and a quadratic σ draws a relation with the Kipnis-Marchioro-Presutti (KMP) process – a heat transfer model for boundary driven chains of oscillators [39, 27] – well described by the macroscopic fluctuation theory [40]. A formal correspondence with this process is obtained by identifying the radiation intensity I to the energy density, and $\mathbf{j}$ to the heat flow. However, despite this correspondence, it is important to note that the physical source of non equilibrium is very different in the two cases: in the KMP model, energy density fluctuations result from thermal effects due to the coupling to two reservoirs at distinct temperatures, while intensity fluctuations of the light flow result solely from the coherent effects, induced by the illumination of the random scattering medium. This correspondance is discussed in more details in the chapter 5.

In fluctuating hydrodynamics, an Einstein relation connects the parameters D and σ; it is given by $\sigma = D\chi$, where χ is the compressibility of the system, usually derived from the free energy [41]. For time dependent processes, $\chi(\rho)$ is defined by (see section II.2.1 in [41])

$$\chi(\rho(\mathbf{r})) = \int_V d\mathbf{r}' S(\mathbf{r}-\mathbf{r}',0) = \widehat{S}(0,0) \tag{3.22}$$

where $S(\mathbf{r}-\mathbf{r}', t-t')$ is the (equilibrium) correlation function of the density,

$$S(\mathbf{r}-\mathbf{r}', t-t') = \langle \rho(\mathbf{r},t)\rho(\mathbf{r}',t')\rangle - \langle \rho^2\rangle \,.$$

The Fourier transform $\widehat{S}(\mathbf{k},t) = \int e^{i\mathbf{k}\cdot\mathbf{r}} S(\mathbf{r},t)$ is known as the structure function or intermediate scattering function.

For coherent light, the effective Langevin equation (3.21) is time independent, but there is a subtlety here. Consider a random medium, illuminated by a light beam. The radiation undergoes multiple scattering events, and, as we discussed in chapter 2, it behaves diffusively. However, the Langevin description does not describe the propagation of light between two scattering events, during which light behaves ballistically; the Langevin description is valid only in the diffusion regime. The characteristic time window between two scattering events is given by elastic mean time $\tau_e = l/v$. In the effective Langevin equation (3.21), the ballistic regime has been integrated out; in other words, the Langevin description is equivalent to a time dependent problem, characterized by D and σ, integrated over the elastic mean time $\tau_e = l/v$. This remark allows us to re-introduce a time dependence, in order to derive the compressibility χ, in analogy with fluctuating hydrodynamics. We therefore consider that the intensity and current are time dependent, $I(\mathbf{r},t)$ and $\mathbf{j}(\mathbf{r},t)$, where $I(\mathbf{r},t)$ and $\mathbf{j}(\mathbf{r},t)$ are related by a time dependent Langevin equation

$$\mathbf{j}(\mathbf{r},t) = -D\boldsymbol{\nabla} I(\mathbf{r},t) + \tilde{\boldsymbol{v}}(\mathbf{r},t)\,, \tag{3.23}$$

where the noise term encapsulates the fluctuations created by both the coherent effects and the ballistic trajectories. It is related to the noise term in Eq.(3.21) by

$$\langle \nu_\alpha(\mathbf{r})\nu_\beta(\mathbf{r}')\rangle = \int_0^{\tau_e} dt\, \langle \tilde{v}_\alpha(\mathbf{r},t)\tilde{v}_\beta(\mathbf{r}',0)\rangle \,. \tag{3.24}$$

To derive the compressibility χ, we first note that Eq.(3.24) leads to

$$\langle \tilde{v}_\alpha(\mathbf{r},t)\tilde{v}_\beta(\mathbf{r}',t')\rangle = \sigma\delta_{\alpha\beta}\delta(\mathbf{r}-\mathbf{r}')\delta(t-t') \,. \tag{3.25}$$

The time and space fluctuations are decoupled, hence

$$\langle \delta I(\mathbf{r},t)\delta I(\mathbf{r}',t')\rangle \;\; = \langle \delta I(\mathbf{r})\delta I(\mathbf{r}')\rangle\delta(t-t')\,, \tag{3.26}$$

and

$$\langle \delta I(\mathbf{r})\delta I(\mathbf{r}')\rangle \;\; = \int_0^{\tau_e} dt \langle \delta I(\mathbf{r},t)\delta I(\mathbf{r}',t')\rangle \,. \tag{3.27}$$

From Eqs.(3.22, 3.27), we obtain

$$\begin{aligned}\int_V d\mathbf{r}'\langle\delta I(\mathbf{r})\delta I(\mathbf{r}')\rangle &= \int_V d\mathbf{r}'\int_0^{\tau_e} dt\langle\delta I(\mathbf{r},t)\delta I(\mathbf{r}',t')\rangle \\ &= \int_0^{\tau_e} dt\chi(\mathbf{r}) \\ &= \tau_e\chi(\mathbf{r})\,,\end{aligned} \tag{3.28}$$

and we deduce the compressibility,

$$\begin{aligned}\chi(\mathbf{r}) &= \tfrac{1}{\tau_e}\int_V d\mathbf{r}'\langle\delta I(\mathbf{r})\delta I(\mathbf{r}')\rangle^{(1)} \\ &= \tfrac{1}{\tau_e}\tfrac{2\pi l}{k^2} I_D(\mathbf{r})^2 \\ &= \tfrac{2\pi v}{k^2} I_D(\mathbf{r})^2 \\ &= \tfrac{c_0}{D} I_D(\mathbf{r})^2\,.\end{aligned} \tag{3.29}$$

Using the expression Eq.(3.29), we recover the Einstein relation,

$$\sigma(\mathbf{r})\chi(\mathbf{r})^{-1} = D\,. \tag{3.30}$$

We therefore see that coherent light is well described by an effective Langevin equation, characterized by two parameters D and σ, themselves related by an Einstein equation. This allows to understand the light intensity fluctuations described in chapter 2 as resulting from a hydrodynamic light flow. We explore this connection more thoroughly in chapter 5, where we show that coherent light can in fact be interpreted as an out of equilibrium light flow, well described in the macroscopic fluctuation theory framework [40]. In particular, this allows us to derive a Gallavotti-Cohen relation for coherent light – a fluctuation dissipation theorem for out of equilibrium systems [40, 42].

3.1.3 Validity of the Langevin approach

The Langevin approach is valid for weak noise, i.e. $\lim_{V\to\infty}\sigma = 0$ over diffusive time scales $t \propto L^2$. To check that this requirement is met, we use rescaled variables

$$\begin{cases}\mathbf{x} = \frac{\mathbf{r}}{L} \\ \tau = \frac{t}{L^2}\,.\end{cases} \tag{3.31}$$

In these rescaled units,

$$\begin{cases} I(\mathbf{x},\tau) = I(\mathbf{r},t) \\ \mathbf{j}(\mathbf{x},\tau) = L\mathbf{j}(\mathbf{r},t)\,.\end{cases} \tag{3.32}$$

For the noise, we note that

$$\begin{aligned}\langle \eta(r)\eta(r')\rangle &= \delta(\mathbf{r}-\mathbf{r}')\\ &= \delta(L(\mathbf{x}-\mathbf{x}'))\\ &= \tfrac{1}{L^3}\delta(\mathbf{x}-\mathbf{x}')\\ &= \tfrac{1}{L^3}\langle\tilde{\eta}(\mathbf{x})\tilde{\eta}(\mathbf{x}')\rangle\,,\end{aligned} \tag{3.33}$$

and η is therefore rescaled as $\eta(\mathbf{x}) = \sqrt{L^3}\eta(r)$.
In these units, the Langevin equation (3.1) becomes

$$\begin{aligned}\tfrac{1}{L}\mathbf{j}(\mathbf{x}) &= -D\tfrac{1}{L}\nabla I(\mathbf{x}) + \sqrt{\tfrac{\sigma}{L^3}}\eta(x)\\ \Leftrightarrow\quad \mathbf{j}(\mathbf{x}) &= -D\nabla I(\mathbf{x}) + \sqrt{\tfrac{\sigma}{L}}\eta(x)\end{aligned} \tag{3.34}$$

and the noise term satisfies $\lim_{L\to\infty}\frac{\sigma}{L} = 0$. The Langevin approach is therefore valid.

3.2 Langevin approach for electronic transport

The picture presented in the previous section can be extended to other mesoscopic diffusive systems, e.g. electronic transport in metals, which is thoroughly discussed in [43, 25]. We discuss here the case of diffusive electrons in disordered metals. The propagation of electrons in a mesoscopic sample, of length L and section S, can be described by substituting in Eq.(3.1) the intensity by the electronic density ρ and the light current by the electronic current $\mathbf{J}$,

$$\mathbf{J}(\mathbf{r}) = -D\boldsymbol{\nabla}\rho(\mathbf{r}) + \boldsymbol{\xi}(r) \tag{3.35}$$

with D a constant diffusion coefficient, l_e the elastic mean free path, and where the noise $\boldsymbol{\xi}$ accounts for the mesoscopic fluctuations.

As for diffusive light, the disorder average current $\langle\mathbf{J}(\mathbf{r})\rangle$ is related to the electronic density $\langle n(\mathbf{r})\rangle$ by a Fick's law:

$$\langle\mathbf{J}(\mathbf{r})\rangle = -D\boldsymbol{\nabla}\langle n(\mathbf{r})\rangle \tag{3.36}$$

In the presence of an external applied electric field $\mathbf{E}$, the current is related to the field by Drude's law,

$$\langle\mathbf{J}(\mathbf{r})\rangle = \sigma_D\mathbf{E}(\mathbf{r})\,, \tag{3.37}$$

where σ_D is the Drude conductivity,

$$\sigma_D = e^2 D\rho_0 = \frac{e^2}{h}\left(\frac{k_F}{2\pi}\right)^2 l_e \tag{3.38}$$

with ρ_0 the density of states at the Fermi level. The conductance G of the sample is given by

$$G = \sigma_D\frac{S}{L} \tag{3.39}$$

Similarly to diffusive light, a good parameter to characterize the strength of the disorder is the (electronic) dimensionless conductivity g_e, defined by

$$g_e = \frac{G}{e^2/h} \equiv \frac{k_F^2 l_e S}{L} \tag{3.40}$$

The correlation function $\langle \xi_\alpha(\mathbf{r})\xi_\beta(\mathbf{r}')\rangle$ is derived using a diagrammatic approach by [25]. They found a noise correlation function very similar to the the one for light Eq.(3.10), as expected since the crossings represented in Figs.(2.5,2.6) also hold for electronic waves,

$$\langle \xi_\alpha(\mathbf{r})\xi_\beta(\mathbf{r}')\rangle = X_0(\mathbf{r},\mathbf{r}') + \sum_{j=1}^{3} X_j(\mathbf{r},\mathbf{r}')\,. \tag{3.41}$$

As in Eq.(3.10), the first term, equal to

$$X_0(\mathbf{r},\mathbf{r}') = e^2 \frac{h^2 v_e^2 l_e^2}{6\pi} \langle \rho(\mathbf{r})\rangle^2 \delta_{\alpha\beta}\delta(\mathbf{r}-\mathbf{r}')\,, \tag{3.42}$$

is of order $1/g_e$. The remaining terms $X_1(\mathbf{r},\mathbf{r}')$, $X_2(\mathbf{r},\mathbf{r}')$ and $X_3(\mathbf{r},\mathbf{r}')$ account for fluctuations of order $1/g_e^2$,

$$\begin{aligned}
X_1(\mathbf{r},\mathbf{r}') &= \delta_{\alpha\beta}\delta(\mathbf{r}-\mathbf{r}') \left(\tfrac{4e^2D}{\hbar}\right)^2 \int d\mathbf{r_1} B(\mathbf{r},\mathbf{r_1})\mathbf{E}^2(\mathbf{r_1}) \\
X_2(\mathbf{r},\mathbf{r}') &= \left(\tfrac{4e^2D}{\hbar}\right)^2 E_\alpha(\mathbf{r})E_\beta(\mathbf{r}')B(\mathbf{r},\mathbf{r}') \\
X_3(\mathbf{r},\mathbf{r}') &= \left(\tfrac{4e^2D}{\hbar}\right)^2 2E_\alpha(\mathbf{r})E_\beta(\mathbf{r}') \iint \tfrac{d\epsilon_1 d\epsilon_2}{(2\pi)^2} f'(\epsilon_1)f'(\epsilon_2)\Re(G_{\epsilon_1-\epsilon_2}(\mathbf{r},\mathbf{r}'))
\end{aligned} \tag{3.43}$$

where $f(\epsilon)$ is the Fermi distribution function,

$$B(\mathbf{r},\mathbf{r}') = \iint \frac{d\epsilon_1 d\epsilon_2}{(2\pi)^2} f'(\epsilon_1)f'(\epsilon_2) G_{\epsilon_1-\epsilon_2}(\mathbf{r},\mathbf{r}')G_{\epsilon_2-\epsilon_1}(\mathbf{r}',\mathbf{r})\,,$$

and $G_\epsilon(\mathbf{r},\mathbf{r}')$ the Green's function of the diffusion equation in energy space,

$$(i\epsilon - D\Delta)G_\epsilon(\mathbf{r},\mathbf{r}') = \delta(\mathbf{r}-\mathbf{r}')\,. \tag{3.44}$$

In [25], the authors show that the Langevin approach allows to recover the well known electronic conductance fluctuations. It is obtained from the equations (3.35) and (3.41) by considering a four point setup. To conclude this chapter, we discuss how the mesoscopic fluctuations desribed by the Langevin equation should affect the electronic potential in a simple setup.

3.2.1 Potential fluctuations

Consider a charge distribution $\rho(\mathbf{r}')$. The electric potential at a point $\mathbf{r}$ of the system is given by:

$$V_e(\mathbf{r}) = \frac{1}{4\pi\epsilon_0} \int_V d\mathbf{r}' \frac{\rho(\mathbf{r}')}{|\mathbf{r}-\mathbf{r}'|} \tag{3.45}$$

The electric density fluctuations induce fluctuations of the the potential of amplitude

$$\begin{aligned}\langle \delta V_e(\mathbf{r})\delta V_e(\mathbf{r}')\rangle &= \tfrac{1}{(4\pi\epsilon_0)^2}\iint_{V\times V} d\mathbf{r_1}d\mathbf{r_2}\tfrac{\langle\delta\rho(\mathbf{r_1})\delta\rho(\mathbf{r_2})\rangle}{|\mathbf{r}-\mathbf{r_1}|\cdot|\mathbf{r}'-\mathbf{r_2}|} \\ &= \tfrac{1}{(4\pi\epsilon_0)^2}\iint_{V\times V}\tfrac{d\mathbf{r_1}d\mathbf{r_2}}{|\mathbf{r}-\mathbf{r_1}|\cdot|\mathbf{r}'-\mathbf{r_2}|}\iint_{V\times V} d\mathbf{r_3}d\mathbf{r_4}\nabla P_D(\mathbf{r_1},\mathbf{r_3})\cdot\nabla P_D(\mathbf{r_2},\mathbf{r_4})\langle\xi_\alpha(\mathbf{r_3})\xi_\beta(\mathbf{r_4})\rangle\end{aligned} \tag{3.46}$$

We consider the simple case of an infinite medium $L \to \infty$. In this case, the Green's function is:

$$P_D(\mathbf{r},\mathbf{r}') = \frac{1}{4\pi D|\mathbf{r}-\mathbf{r}'|} \tag{3.47}$$

Re-injecting in Eq.(3.46), we obtain the correlation function for the potential.

Using Eqs.(3.42,3.43), a scaling argument similar to the one used for the light fluctuation induced forces in the chapter 4 4.2, shows that the term X_0 gives a contribution of order $1/g_e$, while the terms X_j give contributions of the order $1/g_e^2$.

To summarize this chapter, we showed that light fluctuations can be described by an effective Langevin equation, where the noise term encapsulates the coherent corrections. The method consisting in systematically including mesoscopic effects in the noise term of an effective Langevin equation can be generalized to a vast class of quantum or classical mesoscopic effects, e.g in electronic transport (briefly illustrated here) and superconductivity [44, 45, 46].

In classical hydrodynamics, the emergence of long ranged density fluctuations is usually the signature of non equilibrium phenomena [40]. The Langevin approach described here therefore maps the problem of coherent light fluctuations to a class of out of equilibrium hydrodynamic systems. For such systems, it has be proven [4, 8, 6] that long ranged density fluctuations lead to characteristic forces, called fluctuation induced forces or Casimir forces. We show in chapter 4 that similar forces are induced by coherent light.

Chapter 4

Fluctuation induced forces

May 4th

In chapter 2, we showed that classical light scattering in a weakly disordered medium fluctuates spatially, and that the fluctuations have a long ranged component of order $1/g$ due to mesoscopic coherent effects. These long ranged fluctuations are weak in amplitude and difficult to observe. However, their long ranged nature raises the question whether or not "confining" them would lead to measurable Casimir like forces. Casimir physics covers a wealth of phenomena where forces between macroscopic objects are induced by long range fluctuations [4] of either classical or quantum origin. The most celebrated example is the so called quantum electrodynamic (QED) Casimir effect [1], but such fluctuation induced forces arise in a wide range of systems [5, 6, 47, 7, 8, 48, 11, 10]. In this chapter, we prove that the coherent and spatially long ranged fluctuations of light induce forces, of a radiative nature. Optical forces generated by fluctuating fields have been widely studied in the recent years [49, 50, 51, 52, 53]. The mechanical forces discussed in this thesis, however, have not yet been identified. These fluctuation induced forces depend on the dimensionless conductance g – an easily tunable parameter – which allows to design setups where these fluctuating forces dominate the other known forces in play [2, 3, 54]. In chapter 3, we showed that light intensity fluctuations can be described by an effective Langevin equation which maps the problem of coherent light fluctuations to a class of out of equilibrium hydrodynamic systems. For such systems, it has been evidenced [4, 8, 6] that long ranged density fluctuations give rise to fluctuation induced forces or Casimir forces. We use this analogy to meet our end goal of deriving light fluctuations induced forces. Before going any further, note the apparent paradox of the effect we wish to demonstrate. Since light waves tend to localize in the presence of disorder, it would seem logical to seek light fluctuation induced forces in situations where there are no scatterers and where light can propagate over large distances. In fact, removing disorder leads to stronger average radiative forces, see 4.1. However, the forces we are interested in are created by the long range light intensity fluctuations, stemming from mesoscopic coherent effects, which only exist in the presence of weak disorder. These forces are nonetheless weaker than the average radiative force, which makes their measurement challenging. This problem can be avoided by playing with the geometry of the setup, in order to cancel out the average component and measure solely the forces of interest. The setup on

Fig.4.2, where a reflective or absorbing membrane is placed exactly in the middle of the box, for example, meets this requirement. We provide a general expression and scaling of the light fluctuation induced forces and show that they have the simple form Eq.(4.18). For analytical and quantitative discussions, we focus mainly on the experimentally relevant slab geometry of Fig.4.2, and compare different boundary conditions in 4.2.

4.1 Radiation forces

The forces under study are of a radiative nature. We therefore begin by providing the expression of radiative forces in terms the light flow $\mathbf{j}$.

Consider the setup in Fig.4.1, where a monochromatic scalar radiation[1] of amplitude $E(\mathbf{r})$, wave number k, incident along the direction of unit vector $\widehat{\mathbf{k}}$, illuminates an absorbing surface S perpendicular to the beam.

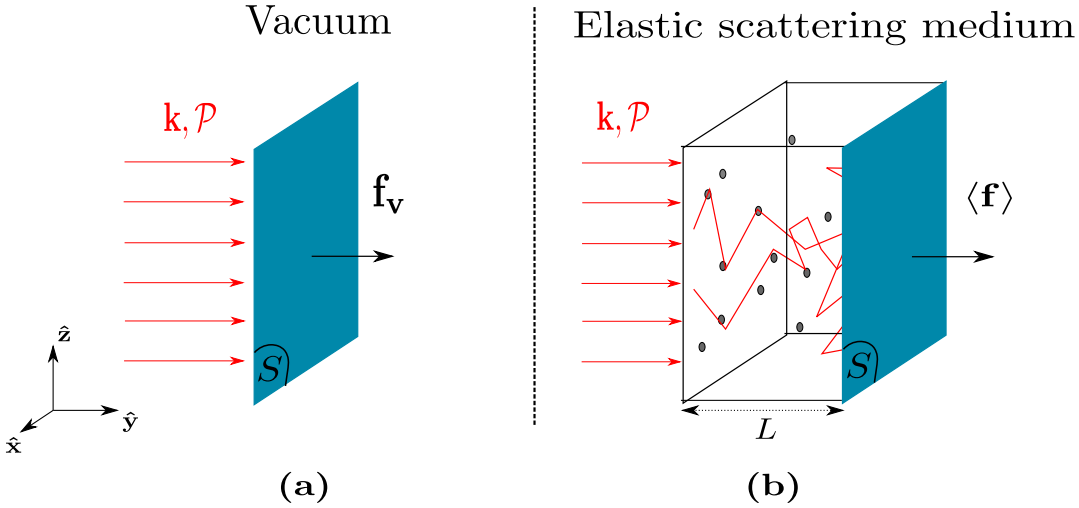

FIGURE 4.1: A monochromatic scalar radiation, of power $\mathcal{P}$ and wave number k, propagates in the direction of the unit vector $\widehat{\mathbf{k}}$. **(a)** The radiation propagates in vacuum until it hits an absorbing plate of surface S, perpendicular to the direction of propagation. **(b)** The light diffuses in an elastic, weakly disordered scattering medium, characterized by the elastic mean free path l, before reaching the plate S.

In the absence of scatterers Fig.4.1.a, the energy current per unit volume inside the medium is described by the Poynting vector $\mathbf{\Pi}(\boldsymbol{r})$, and the light intensity I, in $W.m^{-2}$, is defined as the norm of the Poynting vector,

$$I(\mathbf{r}) = |\mathbf{\Pi}(\mathbf{r})| = \epsilon_0 c |E(\mathbf{r})|^2 , \tag{4.1}$$

where c is the velocity of light in vacuum and ϵ_0 the vacuum permittivity.

In the presence of disorder Fig.4.1.b, and in the weak disorder limit $kl \gg 1$, an equivalent description of the local radiation at a point $\mathbf{r}$ and propagating along a direction $\widehat{\mathbf{s}}$ is provided by the specific intensity $I(\mathbf{r}, \widehat{\mathbf{s}})$, and the light current $\mathbf{j}(\mathbf{r}) = v\overline{I(\mathbf{r}, \widehat{\mathbf{s}})\,\widehat{\mathbf{s}}}$ averaged over all directions $\widehat{\mathbf{s}}$ [13, 29], where v is a conveniently defined group velocity, as discussed in chapter 2. In this approach, the force exerted by

[1] we set aside the effect of polarization (scalar approximation) since the effects of polarization and disorder can be decoupled, see section 2.1 and [13].

light on an absorbing surface S of normal vector $\widehat{\mathbf{n}}$, immersed inside the scattering medium, is

$$\mathbf{f} = \frac{\widehat{\mathbf{n}}}{v^2} \int_S d\mathbf{r}\ \mathbf{j}(\mathbf{r}) \cdot \widehat{\mathbf{n}}\,. \tag{4.2}$$

On average over disorder, the light current is related to the diffusive intensity by a Fick's law, $\mathbf{j_D}(\mathbf{r}) = -D\boldsymbol{\nabla} I_D(\mathbf{r})$. Substituting in Eq.(4.2) gives the average force on the surface S,

$$\langle \mathbf{f} \rangle = \frac{\widehat{\mathbf{n}}}{v^2} \int_S d\mathbf{r}\ \mathbf{j_D}(\mathbf{r}) \cdot \widehat{\mathbf{n}}\,, \tag{4.3}$$

a quantity which depends only on the scattering properties of the medium by means of the transmission coefficient T and of the group velocity v. To see this, let us derive the average force exactly in the simple case of a slab geometry Fig.4.1.b. A monochromatic plane wave of intensity I emitted by an external light source and normally incident on a slab, of thickness L, of an elastic scattering medium. The average force exerted by the scattered light on the opposite wall, of surface S, located at $y = L$, is equal to

$$\langle \mathbf{f} \rangle = \frac{\widehat{\mathbf{y}}}{v^2} \int_S dxdz\, \langle j_y(x, y = L, z) \rangle\,. \tag{4.4}$$

We assume that $L \ll \sqrt{S}$. In this slab geometry, the solution of Eq.(2.31) with absorbing boundary conditions is

$$I_D(\mathbf{r}) = 5I\frac{L + l_0 - y}{L + 2l_0} - 3Ie^{-y/l}\,, \tag{4.5}$$

with $l_0 = \frac{2l}{3}$. From Fick's law, it follows that the diffusive current is equal to

$$\mathbf{j_D}(\mathbf{r}) = 5ID\frac{1}{L + 2l_0} - 3I\frac{D}{l}e^{-y/l}\,. \tag{4.6}$$

The Drude intensity $I_0(\mathbf{r})$ is equal to

$$I_0(\mathbf{r}) = Ie^{-y/l}\,, \tag{4.7}$$

and the associated current, $\mathbf{j_0}(\mathbf{r})$, to

$$\mathbf{j_0}(\mathbf{r}) = 3I\frac{D}{l}e^{-y/l}\,. \tag{4.8}$$

From Eq.(4.6) and Eq.(4.8), we deduce that the total current is constant and equal to

$$\langle \mathbf{j}(\mathbf{r}) \rangle = 5ID\frac{1}{L + 2l_0}\,. \tag{4.9}$$

Reinjecting Eq.(4.9) in Eq.(4.4), we obtain the force on the surface S:

$$\begin{aligned} \langle \mathbf{f} \rangle &= \tfrac{\widehat{\mathbf{y}}}{v^2} S_\perp 5ID\tfrac{1}{L+2l_0} \\ &= \tfrac{\mathcal{P}}{v} T(L)\widehat{\mathbf{y}} \end{aligned} \tag{4.10}$$

where $\mathcal{P} = IS_\perp$ is the incoming light power, and $T(L) = \frac{5l}{3(L+2l_0)}$ the transmission coefficient.

Interestingly, the expression of the total average force on the closed surface ∂V surrounding a light source of power $\mathcal{P}$ has the general expression $\mathcal{P}/v$ regardless of the presence of disorder, with a group velocity v which depends on the nature of the medium. The light source γ inside the medium satisfies

$$\int_V d\mathbf{r}\,\gamma(\mathbf{r}) = l\mathcal{P}\,, \tag{4.11}$$

where $\mathcal{P}$ is the power of the light source. In the absence of scatterers, the energy flux is described by the Poynting vector $\mathbf{\Pi}(\mathbf{r})$. There is no energy dissipation, hence the flux of $\mathbf{\Pi}(\mathbf{r})$ through a closed surface S around the source is independent of the size and shape of the surface. It is equal to the power of the source, $\oint_S d\mathbf{r}\,\mathbf{\Pi}(\mathbf{r})\cdot\widehat{\mathbf{n}}(\mathbf{r}) = \mathcal{P}$, with $\widehat{\mathbf{n}}(\mathbf{r})$ the local unit vector normal to the surface at $\mathbf{r}$. The amplitude of the total normal radiative force in vacuum, f_v, is

$$f_v = \frac{1}{v}\oint_S d\mathbf{r}\,\Pi(\mathbf{r})\cdot\widehat{\mathbf{n}}(\mathbf{r}) = \frac{\mathcal{P}}{c}\,, \tag{4.12}$$

where c is the velocity of light in vacuum.

In an elastic scattering medium, the total average force exerted by the scattered light on the boundary is by definition

$$\langle f\rangle = \frac{1}{v^2}\oint_{\partial V}\langle\mathbf{j}(\mathbf{r})\rangle\cdot\widehat{\mathbf{n}} = \frac{1}{v^2}\int_V \boldsymbol{\nabla}\cdot\langle\mathbf{j}(\mathbf{r})\rangle\,, \tag{4.13}$$

with $\langle\mathbf{j}(\mathbf{r})\rangle = \mathbf{j_0}(\mathbf{r}) + \mathbf{j_D}(\mathbf{r})$. Since $\boldsymbol{\nabla}\cdot\mathbf{j_0}(\mathbf{r}) = -\frac{v}{l}I_0(\mathbf{r})$ and $\boldsymbol{\nabla}\cdot\mathbf{j_D}(\mathbf{r}) = \frac{v}{l}I_0(\mathbf{r}) + \gamma(\mathbf{r})$, we have

$$\begin{aligned}\langle f\rangle &= \tfrac{1}{v^2}\int_V -\tfrac{v}{l}I_0(\mathbf{r}) + \tfrac{v}{l}I_0(\mathbf{r}) + \tfrac{v}{l}\gamma(\mathbf{r})\\ &= \tfrac{1}{vl}\int_V \gamma(\mathbf{r})\\ &= \tfrac{\mathcal{P}}{v}\,,\end{aligned} \tag{4.14}$$

with v the group velocity, which completes the proof.

4.2 Fluctuating forces induced by coherent light flow

We are now in a position to calculate the radiation force $\mathbf{f}$, which includes, on top of its average $\langle\mathbf{f}\rangle$, a fluctuating part

$$\boldsymbol{f} = \mathbf{f} - \langle\mathbf{f}\rangle\,, \tag{4.15}$$

induced by intensity fluctuations. By definition, $\boldsymbol{f}$ averages to zero, but its mean amplitude $\sqrt{\langle\boldsymbol{f}^2\rangle}$ is significant. We begin by deriving the general expression of $\langle\boldsymbol{f}^2\rangle$ and its scaling, Eq.(4.18). We then check the validity of Eq.(4.18) in the simple geometry Fig.4.3. Finally, we consider the experimentally relevant geometry Fig.4.2, where the average diffusive force on the yellow membrane $S = L_\perp \times L_\parallel$ cancels out, which allows to isolate the fluctuating part. We derive $\langle\boldsymbol{f}^2\rangle$ analytically for different boundary conditions.

4.2.1 General expression

Consider an elastic, scattering medium, contained in a volume V and illuminated by an external light beam, such as Fig.4.2. The radiative force on a surface S inside or on the edges of the medium is obtained by substituting Eq.(3.1) into Eq.(4.2). We obtain the fluctuating part by removing the average component using Eq.(2.30), and we find

$$\begin{aligned} \boldsymbol{f} &= \tfrac{1}{v^2} \int_S d\mathbf{r}\, \hat{\mathbf{r}} \cdot [\boldsymbol{\nabla} \delta I(\mathbf{r}) + \boldsymbol{\nu}(\mathbf{r})]\, \hat{\mathbf{r}} \\ &= \tfrac{1}{v^2} \int_S d\mathbf{r}\, [\partial_{\mathbf{r}} \delta I(\mathbf{r}) + \nu_{\hat{\mathbf{r}}}(\mathbf{r})]\, \hat{\mathbf{r}} \end{aligned} \tag{4.16}$$

where $\hat{\mathbf{r}}$ is the local, unit vector normal to the surface S at point $\mathbf{r}$. In the second line, we used the short hand notation

$$\begin{cases} \partial_{\mathbf{r}} = \hat{\mathbf{n}}(\mathbf{r}) \cdot \boldsymbol{\nabla} \\ \\ A_{\hat{\mathbf{r}}}(\mathbf{r}) = \hat{\mathbf{r}} \cdot \mathbf{A}(\mathbf{r}) \end{cases}$$

for any vector field $\mathbf{A}(\mathbf{r})$.

This fluctuation induced force averages to zero over disorder, and its amplitude is given by

$$\begin{aligned} \langle \boldsymbol{f}^2 \rangle &= \frac{1}{v^4} \iint_{S \times S} d\mathbf{r} d\mathbf{r}' [D^2 \partial_{\mathbf{r}} \partial_{\mathbf{r}'} \langle \delta I(\mathbf{r}) \delta I(\mathbf{r}') \rangle + \langle \nu_{\hat{\mathbf{r}}}(\mathbf{r}) \nu_{\hat{\mathbf{r}}}(\mathbf{r}) \rangle] \\ &= \sum_{j=1}^{3} \boldsymbol{f}_j^2 + \sum_{j=0}^{3} \boldsymbol{f}_{\nu,j}^2 \,, \end{aligned} \tag{4.17}$$

where $\boldsymbol{f}_j^2$ is denotes the contribution of the three terms in the intensity correlation function Eq.(2.46), and where $\boldsymbol{f}_{\nu,j}^2$ results from the noise term Eq.(3.10).

4.2.2 Scaling of the fluctuation induced forces

The amplitude of the fluctuation induced force $\boldsymbol{f}$ in Eq.(4.17) is the sum of seven different terms, but a simple scaling argument shows that it is dominated by $\boldsymbol{f}_2^2$ and $\boldsymbol{f}_{\nu,0}^2$, which are both proportional to the inverse of the conductance. It follows that the fluctuating force has the general form

$$\langle \boldsymbol{f}^2 \rangle = \frac{1}{g_{\mathcal{L}}} \frac{\mathcal{P}^2}{v^2} \left(\mathcal{Q}_2 + \mathcal{Q}_\nu \right) . \tag{4.18}$$

This rather simple expression constitutes a central result of this work. It states that the fluctuating forces induced by coherent mesoscopic effects, besides their dependence upon the power $\mathcal{P}$ of the incoming light beam, are driven by the dimensionless conductance $g_{\mathcal{L}}$ of the system. This conductance takes the simple form given in Eq.(2.43) for the geometry of the empty hypercube L^d. For more involved geometries like in Fig.4.2, the conductance takes, in three dimensions $d = 3$, the general form

$$g_{\mathcal{L}} \equiv \frac{k^2 l}{3\pi} \mathcal{L} \tag{4.19}$$

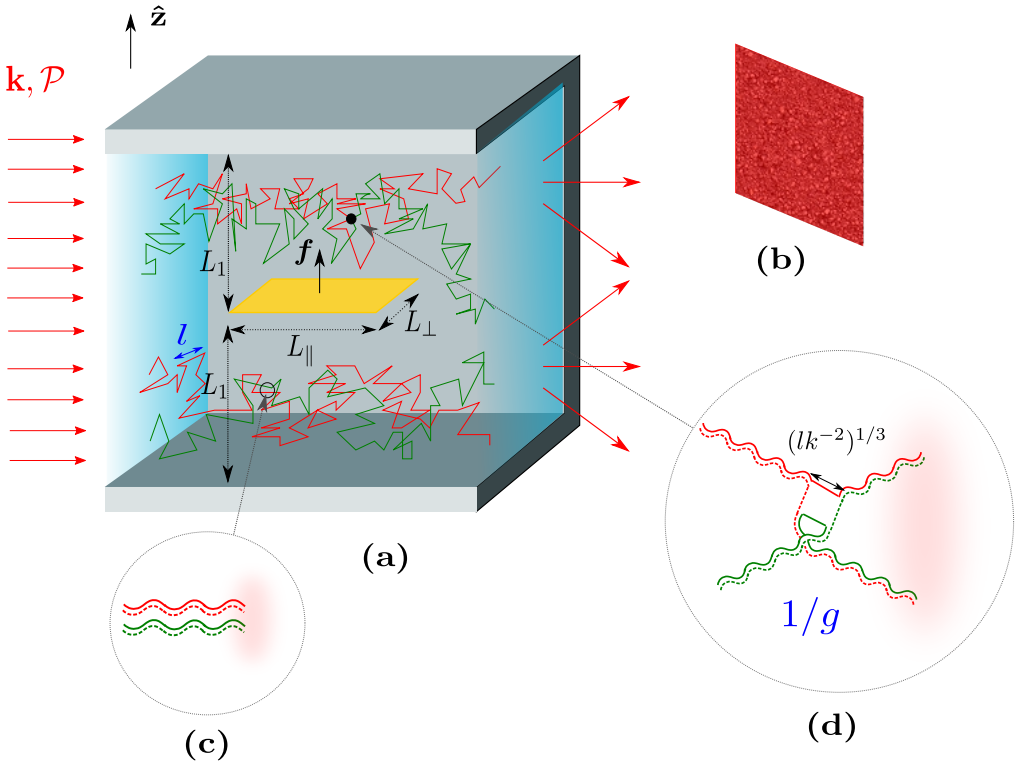

FIGURE 4.2: Schematic visualization of the setup for a plane wave source. **(a)** A monochromatic light beam of wave number k and power $\mathcal{P}$ experiences multiple elastic scattering in a random dielectric medium (e.g. a liquid suspension of elastic scatterers) characterized by the mean free path l. For weak disorder, $kl \gg 1$, the average diffusive light intensity $I_D(\mathbf{r})$ is represented by brownian-like trajectories. **(b)** For each disorder realization, speckle patterns of bright and dark spots evidence spatial fluctuations of light intensity whose correlations are due to interference processes illustrated in **(c)** and **(d)**. **(c)** Two phase-independent diffusive trajectories are built out of paired multiple scattering amplitudes – solution of Eq.(2.1) – having opposite phases and pictured by two coupled (full and dotted) wave-shaped lines. These independent diffusive paths contribute to short range correlations. **(d)** Coherent long ranged correlations result from spatially localized exchanges – quantum crossings – and a new pairing of phase-dependent amplitudes between two diffusive trajectories. The occurrence of a quantum crossing is proportional to the inverse dimensionless conductance $1/g$ (see chapter 2), a small parameter for weak disorder $kl \gg 1$ which depends upon the system geometry. Coherent light fluctuations induce a fluctuating force $\boldsymbol{f}$ on a (suspended) plate immersed inside the scattering medium. When placed at equal distance L_1 from the lower and upper box edges, the average radiation force on both sides of the plate cancels out, leaving only the finite fluctuating part $\boldsymbol{f}$.

where the length $\mathcal{L}$ depends on the geometry of the scattering medium. The two dimensionless numbers $\mathcal{Q}_2$ and $\mathcal{Q}_\nu$ in Eq.(4.18) depend on the shape of the system – but not on its volume – and on boundary conditions.

We provide a proof of Eq.(4.18) for a cubic volume $V = L^3$, in which case

$$g_{\mathcal{L}} = \frac{k^2 l}{3\pi} L \equiv \frac{D^2}{c_0} L\,, \tag{4.20}$$

and with the surface S being on the edge of the system. The reasoning can be adapted for any geometry, e.g. in the experimentally relevant setup of the Fig.4.2 where the surface S is the yellow membrane inside the system. In this case, one must take into account the contributions of the light current from above and underneath the membrane seperatly. There are a few subtleties related to this geometry, which are dealt with in 4.4. More precisely, placing the membrane inside the bulk separates the total volume in two parts – the volumes above and underneath the membrane – which have a priori different conductances. The fuctuating force is hence the sum of two terms of the form Eq.(4.18), with different conductances.

To obtain the scaling of the terms in Eq.(4.17), it is convenient to switch to the rescaled variable $\mathbf{u} = \mathbf{r}/L$, and to use the rescaled functions Eq.(2.55) and Eq.(2.34),

$$\begin{cases} \tilde{P}_D(\mathbf{u},\mathbf{u}') = DLP_D(\mathbf{r},\mathbf{r}') \\ \\ \tilde{\gamma}(\mathbf{u}) = \frac{L^3}{v\mathcal{P}}\gamma'(\mathbf{r}) \\ \\ I_D(\mathbf{r}) = \frac{v\mathcal{P}}{DL}h(\mathbf{u}) \end{cases} \tag{4.21}$$

The functions $\tilde{P}_D(\mathbf{u},\mathbf{u}')$ and $\tilde{\gamma}(\mathbf{u})$ are dimensionless, independent of the size L of the system, and satisfy:

$$\begin{cases} -\Delta_{\mathbf{u}}\tilde{P}_D(\mathbf{u},\mathbf{u}') = \delta(\mathbf{u}-\mathbf{u}') \\ \\ \int\limits_{\tilde{V}} d\mathbf{u}\tilde{\gamma}(\mathbf{u}) = 1 \end{cases} \tag{4.22}$$

Finally, the delta function in three dimensions is rescaled as

$$\delta(\mathbf{r}-\mathbf{r}') = \frac{1}{L^3}\delta(\mathbf{u}-\mathbf{u}')\,. \tag{4.23}$$

Let's now go through the scalings of the different terms in Eq.(4.17).

• First, the contribution f_1^2 is always negligible compared to ${f_{\nu,0}}^2$; more precisely,

$$f_1^2 \sim \frac{1}{L^2}f_{\nu,0}^2\,. \tag{4.24}$$

Indeed, from Eq.(2.49) and Eq.(4.17), we have

$$\begin{aligned} f_1^2 &= \frac{D^2}{v^4}\frac{\tau c_0}{D}\iint\limits_{S\times S} d\mathbf{r}\,d\mathbf{r}'\,(\partial_{\mathbf{r}}I(\mathbf{r}))^2\delta(\mathbf{r}-\mathbf{r}') \\ &= \frac{D^2}{v^4}\frac{\tau c_0}{D}\frac{L^4}{L^7}\frac{v^2\mathcal{P}^2}{D^2}\iint\limits_{\tilde{S}\times\tilde{S}} d\mathbf{u}\,d\mathbf{u}'\,(\partial_{\mathbf{u}}h(\mathbf{u}))^2\delta(\mathbf{u}-\mathbf{u}') \\ &= \frac{1}{L^3}\frac{\mathcal{P}^2}{v^2}\frac{\tau c_0}{D}\iint\limits_{\tilde{S}\times\tilde{S}} d\mathbf{u}\,d\mathbf{u}'\,(\partial_{\mathbf{u}}h(\mathbf{u}))^2\delta(\mathbf{u}-\mathbf{u}')\,, \end{aligned} \tag{4.25}$$

where we used the rescaled variables and functions Eq.(2.55) in the last two lines. The rescaled integral on the right hand side is independent of the volume, and therefore f_1^2 scales like $1/L^3$. On the other hand, from Eq.(3.13) and Eq.(4.17),

$$\begin{aligned} f^2_{\nu,\mathbf{0}} &= \tfrac{c_0}{v^4} \iint_{S\times S} d\mathbf{r}\, d\mathbf{r}'\, I(\mathbf{r})^2 \delta(\mathbf{r}-\mathbf{r}') \\ &= \tfrac{c_0}{v^4} \tfrac{L^4}{L^5} \tfrac{v^2\mathcal{P}^2}{D^2} \iint_{\tilde{S}\times\tilde{S}} d\mathbf{u}\, d\mathbf{u}'\, h(\mathbf{u})^2 \delta(\mathbf{u}-\mathbf{u}') \\ &= \tfrac{1}{L} \tfrac{\mathcal{P}^2}{v^2} \tfrac{c_0}{D^2} \iint_{\tilde{S}\times\tilde{S}} d\mathbf{u}\, d\mathbf{u}'\, h(\mathbf{u})^2 \delta(\mathbf{u}-\mathbf{u}')\,, \end{aligned} \tag{4.26}$$

which shows that $f^2_{\nu,\mathbf{0}}$ scales like $1/L$. Comparing Eq.(4.25) and Eq.(4.26), we obtain the announced result $f^2_{\mathbf{1}} \sim \frac{1}{L^2} f_{\nu,\mathbf{0}}$, and hence $f^2_{\mathbf{1}}$ is negligible compared to $f_{\nu,\mathbf{0}}$.

We rewrite Eq.(4.26) in terms of $1/g_{\mathcal{L}}$ to recover the form Eq.(4.18); using Eq.(4.20), we find

$$f^2_{\nu,\mathbf{0}} = \frac{1}{g_{\mathcal{L}}} \frac{\mathcal{P}^2}{v^2} \mathcal{Q}_\nu\,, \tag{4.27}$$

with

$$\mathcal{Q}_\nu = 2 \iint_{\tilde{S}\times\tilde{S}} d\mathbf{u}\, d\mathbf{u}'\, h(\mathbf{u})^2 \delta(\mathbf{u}-\mathbf{u}')\,.$$

• The term $f^2_{\mathbf{2}}$ is also proportional to $1/g_{\mathcal{L}}$. From Eq.(2.53) and Eq.(4.17),

$$\begin{aligned} f^2_{\mathbf{2}} &= \tfrac{D^2}{v^4} \iint_{S\times S} d\mathbf{r} d\mathbf{r}'\, \partial_{\mathbf{r}}\partial_{\mathbf{r}'} \langle \delta I(\mathbf{r}) \delta I(\mathbf{r}') \rangle^{(2)} \\ &= c_0 \tfrac{D^2}{v^4} \iint_{S\times S} d\mathbf{r} d\mathbf{r}'\, \partial_{\mathbf{r}}\partial_{\mathbf{r}'} \int_V d\mathbf{r}_1 I_D(\mathbf{r}_1)^2 \boldsymbol{\nabla}_{\mathbf{1}} P_D(\mathbf{r}_1,\mathbf{r}) \cdot \boldsymbol{\nabla}_{\mathbf{1}} P_D(\mathbf{r}_1,\mathbf{r}')\,. \end{aligned} \tag{4.28}$$

Using the change of variable $\mathbf{u} = \mathbf{r}/L$ and Eqs.(2.55,2.34), the surface integral in Eq.(4.28) becomes

$$\iint_{S\times S} d\mathbf{r} d\mathbf{r}'\, \partial_{\mathbf{r}}\partial_{\mathbf{r}'} \boldsymbol{\nabla}_{\mathbf{1}} P_D(\mathbf{r}_1,\mathbf{r}) \cdot \boldsymbol{\nabla}_{\mathbf{1}} P_D(\mathbf{r}_1,\mathbf{r}') = \frac{1}{D^2 L^2} s(\mathbf{u}_1)\,, \tag{4.29}$$

where $\mathbf{u}_1 = \mathbf{r}_1/L$, and

$$s(\mathbf{u}_1) = \iint_{\tilde{S}\times\tilde{S}} d\mathbf{u} d\mathbf{u}'\, \partial_{\mathbf{u}}\partial_{\mathbf{u}'} \boldsymbol{\nabla}_{\mathbf{1}} \tilde{P}_D(\mathbf{u}_1,\mathbf{u}) \cdot \boldsymbol{\nabla}_{\mathbf{1}} \tilde{P}_D(\mathbf{u}_1,\mathbf{u}')$$

is a dimensionless function of $\mathbf{r}_1/L$. Using Eq.(2.34), we obtain

$$\begin{aligned} f^2_{\mathbf{2}} &= c_0 \tfrac{D^2}{v^4} \tfrac{v^2\mathcal{P}^2}{D^2L^2} \tfrac{1}{D^2L^2} L^3 \int_{\tilde{V}} d\mathbf{u}_1 h^2(\mathbf{u}_1) s(\mathbf{u}_1) \\ &= \tfrac{\mathcal{P}^2}{v^2} \tfrac{3\pi}{k^2 l L} 2 \int_{\tilde{V}} d\mathbf{u}_1 h^2(\mathbf{u}_1) s(\mathbf{u}_1) \\ &= \tfrac{1}{g_{\mathcal{L}}} \tfrac{\mathcal{P}^2}{v^2} \mathcal{Q}_2\,, \end{aligned} \tag{4.30}$$

where

$$\mathcal{Q}_2 = 2 \int_{\tilde{V}} d\mathbf{u_1} h^2(\mathbf{u_1}) s(\mathbf{u_1})$$

is a dimensionless number, which depends on the shape of the system and of the light source, but which is independent of the size L of the system.

• Using the same change of variable and rescaled functions, and following the same method as for f_2^2, $f_{\nu,0}^2$, it is straightforward to obtain that the terms f_3^2, $f_{\nu,1}^2$, $f_{\nu,2}^2$ and $f_{\nu,3}^2$ all scale like $1/g_{\mathcal{L}}^2$, and are therefore negligible compared to f_2^2 and $f_{\nu,0}^2$. This completes the proof of Eq.(4.18).

We now turn to a quantitative study of the fluctuation induced forces, for different geometries and boundary conditions. To alleviate the notations, we note further on $f_{\nu,0}^2 \equiv f_\nu^2$.

4.3 Point source

We consider first the simple geometry Fig.4.3, where a point source of power $\mathcal{P}$ is placed inside the medium, between the plates. This setup is not as experimentally relevant as the slab geometry Fig.4.4, discussed later in 4.4; however it is interesting from a methodological point of view since the solutions of the diffusion equation (2.31) are simpler. We consider the setup Fig.4.3 with an absorbing membrane. In this geometry,

$$g_{\mathcal{L}} = \frac{k^2 l L_1}{3\pi} \tag{4.31}$$

Let's calculate first the diffusion probability $P_D(\mathbf{r}, \mathbf{r}')$. It is the Green's function of the harmonic Dirichlet problem, with boundary conditions at $z = -L_1/2 - l_0$ and $z = L_1/2 + l_0$ with $l_0 = \frac{2l}{3}$,

$$\begin{cases} -D\Delta_{\mathbf{r}} P_D(\mathbf{r}, \mathbf{r}') = \delta(\mathbf{r} - \mathbf{r}') \\ \\ P_D(\mathbf{r}, \mathbf{r}') = 0 \text{ for } \mathbf{r} = (x, y, -L_1/2 - l_0) \text{ or } \mathbf{r} = (x, y, L_1/2 + l_0) \end{cases} \tag{4.32}$$

$P_D(\mathbf{r}, \mathbf{r}')$ can be obtained in two different ways. One can use a generalized image method [55] (see appendix A), which gives:

$$P_D(\mathbf{r}, \mathbf{r}') = \frac{1}{4\pi D} \left(\frac{1}{|\mathbf{r} - \mathbf{r}'|} + \sum_{m \in \mathbb{Z}^*} \frac{(-1)^m}{|\mathbf{r} - \mathbf{r}'_\mathbf{m}|} \right) \tag{4.33}$$

with $\mathbf{r}'_\mathbf{m}$ the image of $\mathbf{r}'$ w.r.t. the plane $z = sign(m)\frac{l}{2}(2m+1)$. Explicitly: $\mathbf{r}' = (x', y', z'_m)$ with $z'_m = ml + (-1)^{|m|} z'$.

The preferred method to derive $P_D(\mathbf{r}, \mathbf{r}')$ is to start from the Green's function $P(\mathbf{r}, \mathbf{r}', t)$ of the time dependent diffusion equation:

$$(\partial_t - D\Delta) P(\mathbf{r}, \mathbf{r}', t) = \delta(t)\delta(\mathbf{r} - \mathbf{r}')$$

More precisely:

$$P_D(\mathbf{r}, \mathbf{r}') = \left[\int_{-\infty}^{+\infty} dt P(\mathbf{r}, \mathbf{r}') e^{-\gamma t} \right]_{\gamma = 0} \tag{4.34}$$

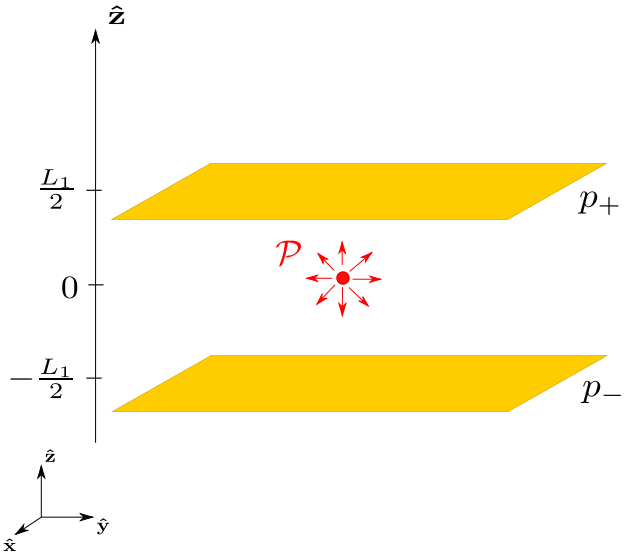

FIGURE 4.3: Two infinite, absorbing or reflecting membranes, located at $z = \pm L_1/2$, are immersed in a scattering medium, contained in an infinite size box ($L \to \infty$). Monochromatic light is emitted by a point source located between the plates, at $z = 0$.

This method has the advantage of being more straightforward since we may use textbook solutions of the diffusion equation, instead of re-deriving the solution from scratch. The details of the derivation for this Green function are given in the appendix A. We obtain

$$P_D(\mathbf{r},\mathbf{r}') = \frac{4}{L_1+2l_0}\sum_{n>0}\int_0^\infty dt \frac{e^{-\rho^2/4Dt}e^{-\pi^2Dn^2t/(L_1+2l_0)^2}}{4\pi Dt}\sin\left(\frac{n\pi(z+L_1/2+l_0)}{L_1+2l_0}\right)\sin\left(\frac{n\pi(z'+L_1/2+l_0)}{L_1+2l_0}\right)$$

$$= \frac{2}{(L_1+2l_0)\pi D}\sum_{n>0} K_0\left(\frac{n\pi|\rho|}{L_1+2l_0}\right)\sin\left(\frac{n\pi(z+L_1/2+l_0)}{L_1+2l_0}\right)\sin\left(\frac{n\pi(z'+L_1/2+l_0)}{L_1+2l_0}\right) \tag{4.35}$$

with $\boldsymbol{\rho} = (x-x', y-y')$. Using the asymptotic behavior of K_0,

$$K_0(x) \sim_{x\to+\infty} \sqrt{\frac{\pi}{2x}}e^{-x},$$

we can obtain an approximate expression for P_D,

$$P_D(\mathbf{r},\mathbf{r}') \sim \frac{1}{\pi D}\sqrt{\frac{2}{(L_1+2y_0)|\rho|}} \times \sum_{n>0}\frac{e^{-n\pi|\rho|/(L_1+2y_0)}}{\sqrt{n}}\sin\left(\frac{n\pi(y+L_1/2+y_0)}{L_1+2y_0}\right)\sin\left(\frac{n\pi(y'+L_1/2+y_0)}{L_1+2y_0}\right) \tag{4.36}$$

We obtain $I_D(\mathbf{r})$ using Green's identity,

$$I_D(\mathbf{r}) = \frac{cP_0}{4\pi D}\sqrt{\frac{1}{(L_1+2y_0)|\rho|}} \sum_{n>0}\frac{e^{-n\pi|\rho|/(L_1+2y_0)}}{\sqrt{n}}\sin\left(\frac{n\pi(y+L_1/2+y_0)}{L_1+2y_0}\right)\sin\left(\frac{n\pi(y_1+L_1/2+y_0)}{L_1+2y_0}\right) \tag{4.37}$$

with $\boldsymbol{\rho} = (x - x_1, y - y_1)$ and $\mathbf{r_1} = (x_1, y_1, z_1)$ the location of the light source.

The average force on the plates $p_\pm$ (see Fig.4.8) is then

$$\mathbf{f}_\pm = \pm \frac{\mathcal{P}}{v} \frac{1}{L_1} \left(y_1 + \frac{L_1}{2} \right) \widehat{\mathbf{z}} \tag{4.38}$$

and, for a light source placed in the middle between the membranes at $z_1 = 0$,

$$\mathbf{f}_\pm = \pm \frac{\mathcal{P}}{2v} \widehat{\mathbf{z}} \tag{4.39}$$

In the case of absorbing membranes, the fluctuation induced force $f_\pm$ is due to the intensity fluctuations. When the source is at $z = 0$, the mean square amplitude of the fluctuating force is equal on each plate, $f_+^2 = f_-^2 \equiv f^2$, with

$$\begin{aligned} f^2 &= \frac{BD^2}{c^4} \iint_{S\times S} d\mathbf{r} d\mathbf{r}' \partial_y \partial_y \int_V d\mathbf{R} |\nabla I_D(\mathbf{R})|^2 P_D(\mathbf{R}, \mathbf{r}) P_D(\mathbf{R}, \mathbf{r}') \\ &= \frac{\mathcal{P}^2}{v^2} \frac{3\pi}{k^2 l L_1} \alpha \\ &= \frac{1}{g_\mathcal{L}} \frac{\mathcal{P}^2}{v^2} \mathcal{Q}_2 \end{aligned} \tag{4.40}$$

where here, $\mathcal{Q}_2 \sim 3.2$ is simply a dimensionless number determined numerically. Therefore, in this simple, idealized setup, all the dependence on the geometry is contained in $g_\mathcal{L}$. No other physical effect, appart from the quantum crossings, intervene in the emergence of the light fluctuation induced forces Eq.(4.18).

4.4 Slab geometry

In this section, we study the fluctuation induced force both analytically and quantitatively in the experimentally relevant slab geometry Fig.4.4. As mentioned in 4.2, the total radiative force is the sum of the disordered average component and of a fluctuating part Eq.(4.18). We can cancel out the average component by taking $L_1 = L_2$, which makes this setup particularly interesting. Besides the geometry, we can also play with the boundary conditions to monitor the fluctuating forces. In the geometry of Fig.4.2, the highest values of the dimensionless $\mathcal{Q}$s are obtained using reflecting cavity edges in the direction of the light beam and absorbing lateral edges. Interestingly, f_2 or f_v can be independently enhanced by an appropriate choice of boundary conditions on the plate: on an absorbing plate where $I_D(\mathbf{r}) = 0$, only f_2 contributes with a maximum for an optimal value of L_1. Alternatively, inserting a reflective plate with $\partial_z I_D(\mathbf{r}) = 0$ selects f_v and leads to fluctuation induced forces with a power law dependence in L_1. This limiting case has an interesting consequence since a measurement of finite fluctuation induced forces on a reflective plate demonstrates the existence of the noise term in the Langevin description of mesoscopic coherent effects.

4.4.1 General setup

In the setup Fig.4.4, a scattering medium is contained in a box $L_\parallel \times L_\perp \times (L_1 + L_2)$. It is illuminated with a monochromatic plane wave propagating in the $\widehat{\mathbf{y}}$ direction and emitted by a light source located outside of the medium, which means that $\gamma = 0$ in the diffusion equation Eq.(2.31). A thin plate or membrane of surface $S = L_\perp \times L_\parallel$

(yellow in Fig.4.2) is placed inside the box, which splits the box into two zones, denoted $j = 1, 2$, respectively above and under the plate (see Fig.4.4). The optimal choice of boundary conditions is found to be Neumann boundary conditions on the slabs at $y = 0, L_\parallel$ and Dirichlet boundary conditions on the slabs at $x = 0, L_\perp$ (see appendix B for details). Those boundary conditions apply to the specific intensity. As discussed in chapter 2, these conditions translate, for $I_D(\mathbf{r})$ and $P_D(\mathbf{r}, \mathbf{r}')$, to Neumann boundary conditions $y = 0, L_\parallel$ and Dirichlet boundary conditions at $x = -l_0, L_\perp + l_0$ with $l_0 = \frac{2l}{3}$,

$$\begin{cases} \text{Dirichlet: } P_D(\mathbf{r}, \mathbf{r}') = 0 \text{ for all } \mathbf{r} = (x, y, z) \text{ s.t. } x = -l_0, L_\perp + l_0 \\ \\ \text{Neumann: } \partial_y P_D(\mathbf{r}, \mathbf{r}') = 0 \text{ for all } \mathbf{r} = (x, y, z) \text{ s.t. } y = 0, L \end{cases} \tag{4.41}$$

We note $S_\perp = L_\perp(L_1 + L_2)$ the illuminated surface, and we introduce the intensity of the light source, assumed to be uniform,

$$I = \frac{\mathcal{P}}{L_\perp(L_1 + L_2)} = \frac{\mathcal{P}}{S_\perp}. \tag{4.42}$$

We consider the cases of a reflective membrane and of an absorbing one. In each case, the boundary conditions on the edges of the box in the direction $\widehat{\mathbf{z}}$ are chosen identical to that of the membrane. We write the fluctuation induced forces in the general form Eq.(4.18), and we give the exact expression of $g_{\mathcal{L}}$. In the geometry under study here, where the volumes delimited by the plates are rectangular boxes, $g_{\mathcal{L}}$ is defined by adapting the Thouless argument or equivalently by using the reasoning in the chapter 12 in [13], namely, in each zone $j = 1, 2$,

$$g_{\mathcal{L}}^{(j)} \equiv \frac{k^2 l V_j}{3\pi(\max(L_j^2, L_\perp^2, L_\parallel^2))}, \tag{4.43}$$

where $V_j = L_j L_\parallel L_\perp$.

We only discuss here these two cases as they are the most relevant experimentally. The order of magnitude of the fluctuation induced forces for other choices of boundary conditions are summarized in the appendix B.

4.4.2 Expression of the fluctuation induced forces

In the slab geometry Fig.4.2, the fluctuating force on the membrane is the sum of the contributions from above and underneath the membrane,

$$\boldsymbol{f} = \boldsymbol{f}_\uparrow + \boldsymbol{f}_\downarrow \tag{4.44}$$

with

$$\begin{cases} \boldsymbol{f}_\uparrow = \frac{1}{v^2} \int\limits_S d\mathbf{r} \left[\partial_z \delta I^{(2)}(\mathbf{r}) + \nu_z^{(2)}(\mathbf{r})\right] \widehat{\mathbf{z}} \\ \\ \boldsymbol{f}_\downarrow = -\frac{1}{v^2} \int\limits_S d\mathbf{r} \left[\partial_z \delta I^{(1)}(\mathbf{r}) + \nu_z^{(1)}(\mathbf{r})\right] \widehat{\mathbf{z}} \end{cases} \tag{4.45}$$

where $I^{(j)}$, $\nu^{(j)}$ are the intensity and noise in the zones $j = 1, 2$, see Fig.4.4. Since the intensity and fluctuating current on opposite sides of the membrane are independent, the mean square value of $\boldsymbol{f}$ is

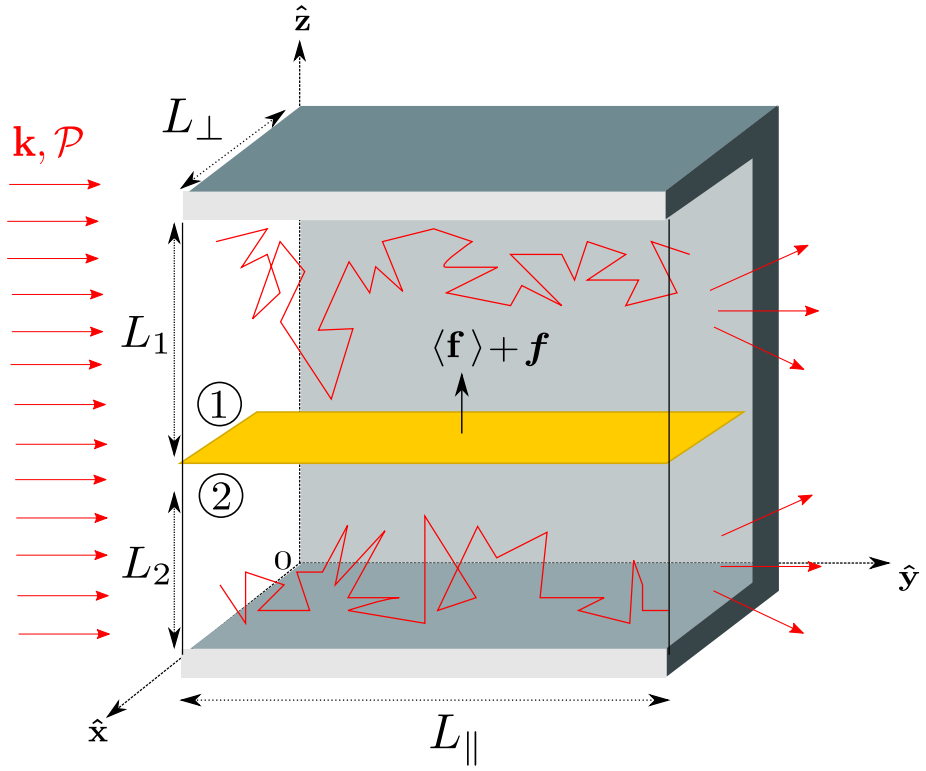

FIGURE 4.4: A scattering medium contained in a box of size $L_\parallel \times L_\perp \times (L_1 + L_2)$ is illuminated by a monochromatic plane wave. A plate (yellow) separates the medium in two zones, labeled by $j = 1, 2$, of thicknesses L_j. The two zones have a priori different conductances. In the particular case $L_1 = L_2$, the average radiative force on the plate vanishes to zero, which is not true a priori in the general case - except for perfectly reflecting plates (see text).

$$\langle f^2 \rangle = \langle f_\uparrow^2 \rangle + \langle f_\downarrow^2 \rangle \tag{4.46}$$

4.4.3 Reflecting membrane

With a reflecting plate or membrane, $\partial_z P_D(\mathbf{r}, \mathbf{r}') = 0$ for all $\mathbf{r}$ on the plates. From Eq.(4.28), we deduce that $f_2^2 = 0$, i.e. that the intensity fluctuations will not contribute to the fluctuation induced forces.
The Green's function $P_D(\mathbf{r}, \mathbf{r}')$ is

$$P_D(\mathbf{r}, \mathbf{r}') = \sum_{n_1>0, n_2, n_3 \geq 0} \frac{\psi_{n_1 n_2 n_3}(\mathbf{r}) \psi_{n_1 n_2 n_3}(\mathbf{r}')}{E_{n_1 n_2 n_3}} , \tag{4.47}$$

where, for $j = 1, 2$,

$$\psi_{n_1 n_2 n_3}(\mathbf{r}) = N \sin\left(\frac{n_1 \pi (x + l_0)}{L_\perp + 2l_0}\right) \cos\left(\frac{n_2 \pi y}{L_\parallel}\right) \cos\left(\frac{n_3 \pi z}{L_j}\right) \tag{4.48}$$

are the eigenfunctions of the diffusion equation with the boundary conditions considered, normalized with $N = \sqrt{\frac{2^3}{L_\parallel L_j L_\perp}}$, and with eigenvalues

$$E_{n_1 n_2 n_3} = D\pi^2 \left(\frac{n_1^2}{L_\perp^2} + \frac{n_2^2}{L_\parallel^2} + \frac{n_3^2}{L_j^2}\right) . \tag{4.49}$$

We deduce $I_D(\mathbf{r})$ using Eq.(2.31) and the Green's identity Eq.(2.32). Since there is no light source inside the medium, the right hand side of the diffusion equation Eq.(2.31) is reduced to $vI_0(\mathbf{r})/l$. We solve Eq.(2.20) to obtain $I_0(\mathbf{r})$,

$$I_0(\mathbf{r}) = Ie^{-y/l} . \tag{4.50}$$

We then obtain for $I_D(\mathbf{r})$,

$$I_D(\mathbf{r}) = \frac{3DI}{l^2} \int_V e^{-y'/l} P_D(\mathbf{r}, \mathbf{r}') d\mathbf{r}' . \tag{4.51}$$

A standard calculation shows that average intensity $I_D(\mathbf{r})$ is independent of z – this results from the fact that the dependence in z of the Green's function Eq.(4.47) is a cosine – which means that the average force on the plate is equal to zero.
As we mentioned at the beginning of the paragraph, with reflecting plates $f_2^2 = 0$ and the main contribution comes from the noise term f_v^2 alone. Re-injecting Eq.(4.47) and Eq.(4.51) in Eq.(4.26), we obtain, after a standard calculation, the fluctuation induced force on the plate,

$$\begin{aligned} \langle f^2 \rangle &= b \frac{I^2}{v^2} \frac{3\pi L_\parallel}{k^2 l L_\perp} \left(\frac{1}{L_1} + \frac{1}{L_2}\right) S_\parallel^2 \beta' \left(\frac{L_\parallel}{L_\perp}\right) \\ &= b \frac{\mathcal{P}^2}{v^2} \frac{3\pi L_\parallel}{k^2 l L_\perp} \left(\frac{1}{L_1} + \frac{1}{L_2}\right) \beta \left(\frac{L_\parallel}{L_\perp}, \frac{S_\parallel}{S_\perp}\right) , \end{aligned} \tag{4.52}$$

where $b \sim 0.13$ is a prefactor, which contains a numerical fit factor and the normalization factor of the eigenfunctions in Eq.(4.48). The term $\beta\left(\frac{L_\parallel}{L_\perp}, \frac{S_\parallel}{S_\perp}\right)$ is a dimensionless function of the aspect ratios $\frac{L_\parallel}{L_\perp}, \frac{S_\parallel}{S_\perp}$, equal to

$$\beta\left(\frac{L_\parallel}{L_\perp},\frac{S_\parallel}{S_\perp}\right)=\frac{S_\parallel^2}{S_\perp^2}\sum_{n_2\geq 0,n_1\text{odd}}\frac{1}{n_1^2\left(n_2^2+n_1^2\frac{L_\parallel^2}{L_\perp^2}\right)^2}. \tag{4.53}$$

The expression in Eq.(4.52) for the fluctuation induced forces holds for any value of the parameters $L_\parallel, L_\perp, Lj$. A plot of this fluctuation induced forces is given on Fig.4.7.b and Fig.4.5.c. To write Eq.(4.52) in the form of the Eq.(4.18), we need to define $g_{\mathcal{L}}^{(j)}$ explicitly and check that $g_{\mathcal{L}}^{(j)}\gg 1$. According to Eq.(4.43), if $L_\parallel\simeq L_\perp$ and $L_\parallel, L_\perp \gg L_j$ then $g_{\mathcal{L}}^{(j)}=\frac{k^2 l L_j L_\perp}{3\pi L_\parallel}$ which leads to

$$\langle f^2\rangle=\frac{\mathcal{P}^2}{v^2}\left(\frac{1}{g_{\mathcal{L}}^{(1)}}+\frac{1}{g_{\mathcal{L}}^{(2)}}\right)\mathcal{Q}_\nu\left(\frac{L_\parallel}{L_\perp},\frac{S_\parallel}{S_\perp}\right), \tag{4.54}$$

with $\mathcal{Q}_\nu\left(\frac{L_\parallel}{L_\perp},\frac{S_\parallel}{S_\perp}\right)=b\beta\left(\frac{L_\parallel}{L_\perp},\frac{S_\parallel}{S_\perp}\right)$.

This expression is valid provided that $g_{\mathcal{L}}^{(j)}\gg 1$, i.e. $\frac{k^2 l L_j L_\perp}{3\pi L_\parallel}\gg 1$. For a scattering medium characterized e.g. by $l=1\,\mu$m and $kl=10$, the requirement becomes $L_j\gg 10^{-7}$m. Further discussion on the orders of magnitude is provided in the next section.

On the other hand, for $L_j\gg L_\parallel, L_\perp$, then $g_{\mathcal{L}}^{(j)}=\frac{k^2 l L_\parallel L_\perp}{3\pi L_j}$ and the fluctuation induced forces can be written in the form

$$\langle f^2\rangle=\frac{\mathcal{P}^2}{v^2}\left(\frac{1}{g_{\mathcal{L}}^{(1)}}\mathcal{Q}_\nu\left(\frac{L_\parallel}{L_1},\frac{L_\parallel}{L_\perp}\right)+\frac{1}{g_{\mathcal{L}}^{(2)}}\mathcal{Q}_\nu\left(\frac{L_\parallel}{L_2},\frac{L_\parallel}{L_\perp}\right)\right), \tag{4.55}$$

with $\mathcal{Q}_\nu\left(\frac{L_\parallel}{L_j},\frac{L_\parallel}{L_\perp},\frac{S_\parallel}{S_\perp}\right)=b\frac{L_\parallel^2}{L_j^2}\beta\left(\frac{L_\parallel}{L_\perp},\frac{S_\parallel}{S_\perp}\right)$. In that case, the requirement $g_{\mathcal{L}}^{(j)}\gg 1$ translates, for $l=1\,\mu$m and $kl=10$, to $L_j\ll 10^7 L_\parallel L_\perp$m.

4.4.4 Absorbing membrane

With an absorbing membrane, $I_D(\mathbf{r})=0$ for all $\mathbf{r}$ on the plates [2]. From Eq.(4.26), we obtain $f_v^2=0$, i.e. contrary to the previous case of a reflecting plate, here the intensity fluctuations are the main contribution to the fluctuation induced forces.

The Green's function is

$$P_D(\mathbf{r},\mathbf{r}')=\sum_{n_1,n_3>0,n_2\geq 0}\frac{\psi_{n_1n_2n_3}(\mathbf{r})\psi_{n_1n_2n_3}(\mathbf{r}')}{E_{n_1n_2n_3}} \tag{4.56}$$

with

$$\psi_{n_1n_2n_3}(\mathbf{r})=N\sin\left(\frac{n_1\pi(x+l_0)}{L_\perp+2l_0}\right)\cos\left(\frac{n_2\pi y}{L_\parallel}\right)\sin\left(\frac{n_3\pi z}{L_j}\right) \tag{4.57}$$

$N=\sqrt{\frac{2^3}{L_\parallel L_j L_\perp}}$, and with $E_{n_1n_2n_3}=D\pi^2\left(\frac{n_1^2}{L_\perp^2}+\frac{n_2^2}{L_\parallel^2}+\frac{n_3^2}{L_j^2}\right)$.

The normal force on the plate is equal to

[2] The Dirichlet boundary condition expressed in Eq.(4.41) is valid at an interface between a scattering and non scattering medium; since the plate is immersed in the medium, the Dirichlet boundary condition is simply formulated as $I_D(\mathbf{r})=0$

$$\langle \mathbf{f} \rangle = \frac{I}{v}\frac{2^6}{\pi^4} L_\perp \left[\sum_{n_1,n_3 \text{ odd}} L_1 \frac{1}{n_1^2\left(n_3^2 + \frac{n_1^2 L_1^2}{L_\perp^2}\right)} - L_2 \frac{1}{n_1^2\left(n_3^2 + \frac{n_1^2 L_2^2}{L_\perp^2}\right)} \right] \widehat{\mathbf{z}} \tag{4.58}$$

and is well approximated by

$$\langle \mathbf{f} \rangle \simeq \frac{I}{v}\frac{2^6}{\pi^4} L_\perp \left(\frac{1}{L_1} \frac{1}{\left(\frac{1}{L_1^2} + \frac{1}{L_\perp^2}\right)} - \frac{1}{L_2} \frac{1}{\left(\frac{1}{L_2^2} + \frac{1}{L_\perp^2}\right)} \right) \widehat{\mathbf{z}}. \tag{4.59}$$

From Eq.(4.59), it is straightforward to obtain that the average force cancels out when $L_1 = L_2$. Re-injecting the expressions of $I_D(\mathbf{r})$, $P_D(\mathbf{r}, \mathbf{r}')$ in Eq.(4.28), we obtain the fluctuation induced force on the membrane,

$$\langle \boldsymbol{f}^2 \rangle = a \frac{I^2}{v^2} \frac{3\pi}{k^2 l} \left[\frac{L_1 L_\perp^5}{L_\parallel^3} \delta\left(\frac{L_1}{L_\parallel}, \frac{L_\perp}{L_\parallel}\right) + \frac{L_2 L_\perp^5}{L_\parallel^3} \delta\left(\frac{L_2}{L_\parallel}, \frac{L_\perp}{L_\parallel}\right) \right], \tag{4.60}$$

with $a \sim 0.3$ a prefactor containing a fit factor and the normalization of the eigenfunctions Eq.(4.57), and $\delta\left(\frac{L_j}{L_\parallel}, \frac{L_\perp}{L_\parallel}\right)$ a dimensionless geometrical correction. The exact expression of $\delta\left(\frac{L_j}{L_\parallel}, \frac{L_\perp}{L_\parallel}\right)$ is quite heavy but can be obtained by a standard calculation using Eq.(4.28). To alleviate the discussion, we do not give its full expression here. After performing the integrals in Eq.(4.28), we can write $\delta\left(\frac{L_j}{L_\parallel}, \frac{L_\perp}{L_\parallel}\right)$ as a product of two sums, which can be well approximated by keeping the first terms,

$$\delta\left(\frac{L_j}{L_\parallel}, \frac{L_\perp}{L_\parallel}\right) \sim \frac{1}{\left(\frac{L_j^2}{L_\parallel^2} + \frac{L_\perp^2}{L_\parallel^2}\right)^2} \left[\frac{1}{\left(1 + \frac{L_\parallel^2}{L_j^2} + \frac{L_\parallel^2}{L_\perp^2}\right)^2} + \frac{1}{\frac{L_\parallel^2}{L_j^2} + \frac{L_\parallel^2}{L_\perp^2}} \right]. \tag{4.61}$$

Note that the light fluctuation induced forces in this case tends to zero in both limits $L_1 \to 0$ and $L_1 \to \infty$; a plot of these two limits is given on Fig.4.5.a and Fig.4.5.b. A maximum is reached when $L_1 \simeq L_\perp$, see Fig.4.7.a. Note also that the fluctuation induced forces increase as $L_\parallel$ decreases. In the configuration where $L_j = L_\perp \gg L_\parallel$, Eq.(4.43) becomes $g_{\mathcal{L}}^{(j)} = \frac{k^2 l L_\parallel L_\perp}{3\pi L_j}$ and the fluctuation induced forces can be written in the form

$$\langle \boldsymbol{f}^2 \rangle = \frac{\mathcal{P}^2}{v^2} \left(\frac{1}{g_{\mathcal{L}}^{(1)}} \mathcal{Q}_2\left(\frac{L_1}{L_\parallel}, \frac{L_\perp}{L_\parallel}, \frac{S_\perp}{S_\parallel}\right) + \frac{1}{g_{\mathcal{L}}^{(2)}} \mathcal{Q}_2\left(\frac{L_2}{L_\parallel}, \frac{L_\perp}{L_\parallel}, \frac{S_\perp}{S_\parallel}\right) \right) \tag{4.62}$$

with $\mathcal{Q}_2\left(\frac{L_j}{L_\parallel}, \frac{L_\perp}{L_\parallel}, \frac{S_\perp}{S_\parallel}\right) = a \frac{L_\perp^4}{L_\parallel^2} \frac{S_\parallel^2}{S_\perp^2} \delta\left(\frac{L_j}{L_\parallel}, \frac{L_\perp}{L_\parallel}\right)$.

4.4.5 Orders of magnitude

Numerous efforts have been recently made to develop high sensitivity cantilevers able to measure forces of weak amplitude [56]. We propose to observe the present fluctuation induced forces using an atomic force microscope, in a setup similar to the one used [54], where Casimir-Lifshitz forces of a few piconewtons have been measured between a gold plate and a sphere coated with gold in a liquid, Fig.4.6.

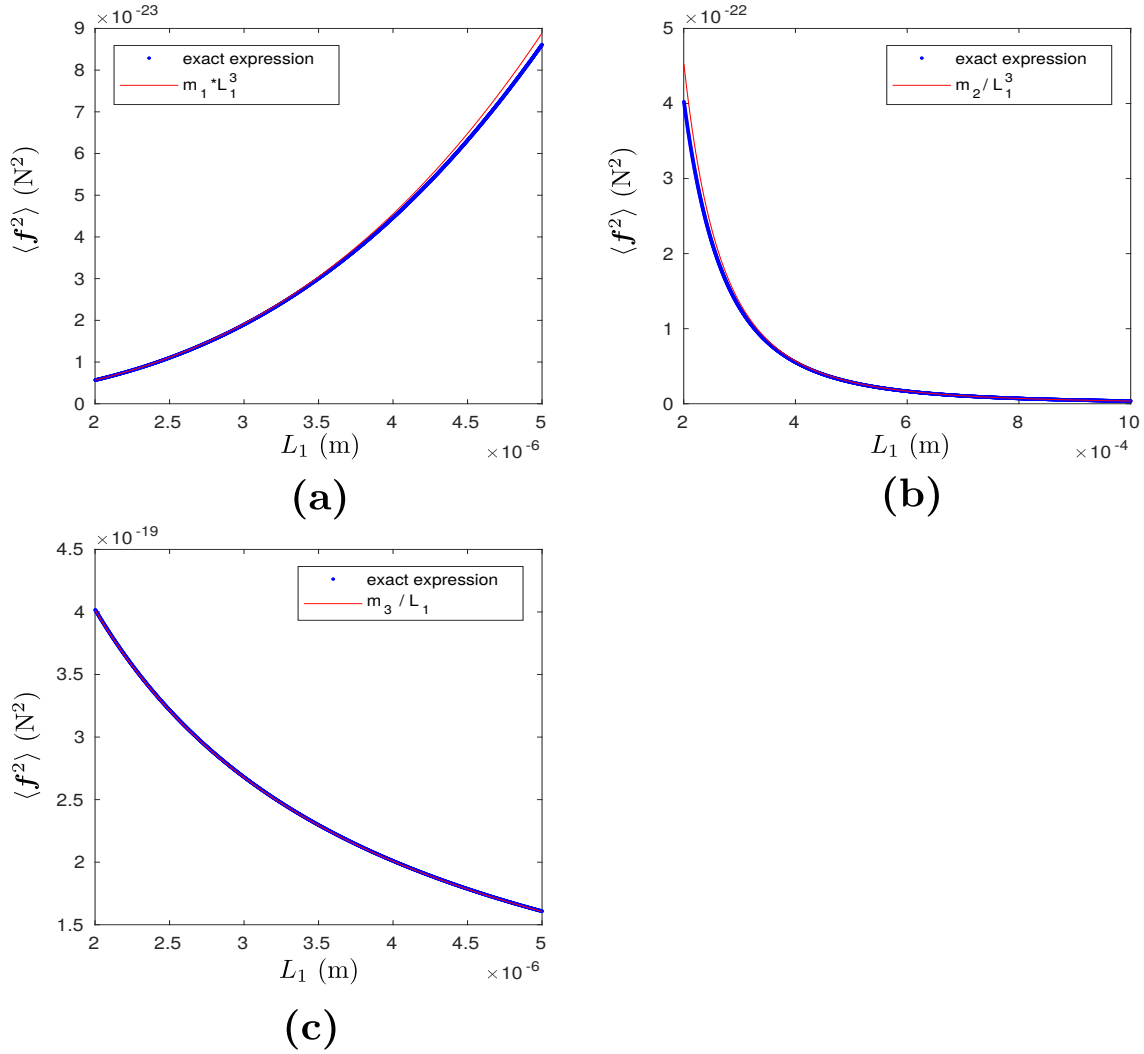

FIGURE 4.5: Asymptotic behavior and fitted functions of $\langle f^2 \rangle$ with Neumann boundary conditions in the direction of the illuminating light beam and Dirichlet boundary conditions in the direction $\widehat{\mathbf{x}}$, for an absorbing plate **(a)**, **(b)** and a reflecting plate **(c)**. We assume $L_2 \gg L_1$ for simplicity; we therefore neglect the fluctuation induced forces from the zone 2 in Fig.4.4. We fix $L_\parallel = L_\perp = 40\,\mu$m, as in Table 4.1. **(a)** For $L_1 \ll L_\parallel, L_\perp$, we have $g_{\mathcal{L}}^{(1)} = \frac{k^2 l L_1 L_\perp}{3\pi L_\parallel}$, and $\langle f^2 \rangle$ scales like L_1^3. The fit parameter m_1 numerically matches the value obtained by taking $L_1 \ll L_\parallel, L_\perp$ in Eq.(4.60).**(b)** For $L_1 \gg L_\parallel, L_\perp$, $g_{\mathcal{L}}^{(1)} = \frac{k^2 l L_\parallel L_\perp}{3\pi L_1}$ and the fluctuating force scales like $1/L_1^3$, with a fit factor m_2 also matching the theoretical value expected in the limit $L_1 \gg L_\parallel, L_\perp$. **(c)** In the case of reflecting plates, the force scales like $1/L_1$ at all length scales, with m_3 matching the value expected from Eq.(4.52).

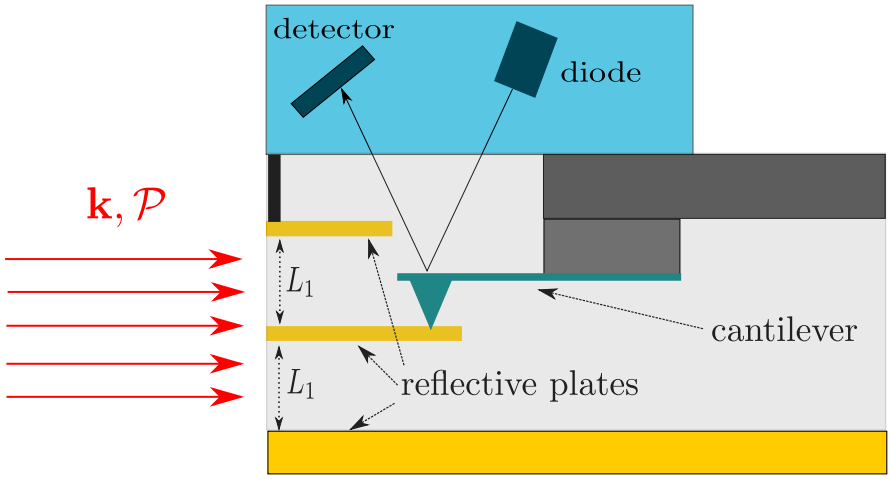

FIGURE 4.6: Setup proposal for the observation of light fluctuations induced forces, inspired by [54] (see text).

Replacing the liquid by a weakly scattering medium $kl \sim 10$ and using square plates of size $40\,\mu\text{m}\times 40\,\mu\text{m}$ – the typical size of the sphere used in [54] – and illuminating the medium with a light beam of intensity $I \sim 10^9\,\text{W}\cdot m^{-2}$, we expect light fluctuation induced forces of amplitude up to a few hundreds of piconewtons, i.e. strong enough to be detected and stronger than the Casimir-Lifshitz forces. In this setup, the light fluctuation induced forces are also significantly enhanced compared to the other forces in play, namely the Van der Waals forces and the QED Casimir forces [1, 57, 2, 3]. Indeed, the Van der Waals forces between solids are relevant for length scales smaller or equal to a nm, which is a few orders of magnitude smaller than separation L_1 and L_2 between the membrane and the edges. The QED Casimir pressure between reflecting plates is given by

$$P_{QED} = \frac{1.3\cdot 10^{-7}}{d_\mu^4} N/cm^2 \tag{4.63}$$

where d_μ is the distance between the plates in μm. In the setup Fig.4.4, the Casimir forces cancel out for $L_1 = L_2$. For $L_2 \gg L_1$, the Casimir force and the membrane of surface $40\,\mu\text{m}\times 40\,\mu\text{m}$ is

$$\mathbf{f}_{QED} = -\frac{1.3\cdot 10^{-7}}{L_{1\mu}^4} S_{cm}\,\hat{\mathbf{z}} \tag{4.64}$$

where $L_{1\mu} = L_1\cdot 10^6$ is L_1 in μm, and $S_{cm} = S\cdot 10^4$ is S in cm^2.

The comparison between the QED forces and the mesoscopic Casimir forces (in the case of reflecting plates) is summarized in the Table 4.1.

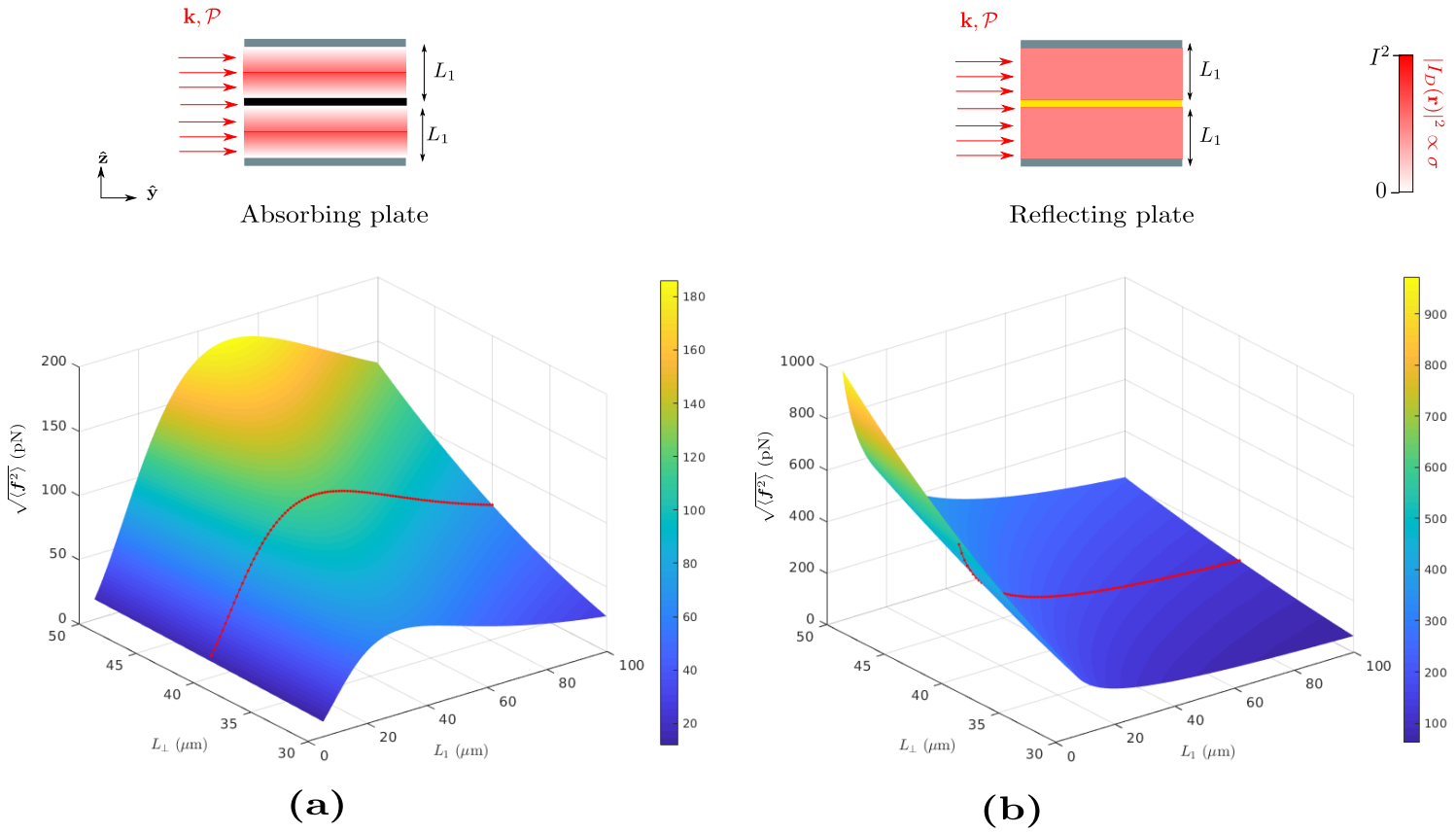

FIGURE 4.7: Amplitude of $\sqrt{\langle f^2 \rangle}$ on the plate in Fig.4.4 as a function of L_1 and $L_\perp$ with fixed $L_\parallel = 40\,\mu$m and $l = 1\,\mu$m. **(a)** Absorbing plate with $I_D(\mathbf{r}) = 0$, so that $\langle f^2 \rangle = f_2^2$. It vanishes in both limits $L_1 \to 0$ and $L_1 \to +\infty$, which results from the form of $I_D(\mathbf{r}) I_D(\mathbf{r}') C_2(\mathbf{r}, \mathbf{r}')$. **(b)** Reflecting plate where $\partial_z I_D(\mathbf{r}) = 0$, hence $f_2 = 0$ and $\langle f^2 \rangle = f_v^2$. From Eq.(4.55), we see that $\sqrt{f_v^2}$ scales like $1/\sqrt{L_1}$. The red lines correspond to $L_\perp = 40\,\mu$m as in Table 4.1.

TABLE 4.1: **Typical strength of light fluctuation induced forces in the setup of Fig.4.4 obtained for visible light, $k \sim 10^7$ m^{-1} and an elastic mean free path $l \simeq 1\,\mu$m i.e in a weakly disordered medium ($kl \sim 10$) and $v = 2.10^8$ m$\cdot$ s^{-1}. We consider the optimal case of reflecting cavity edges along $\hat{\mathbf{x}}$ and absorbing edges along $\hat{\mathbf{y}}$ (see text) and compare the cases of an absorbing and reflecting plate (Fig.4.7). We derive $g_{\mathcal{L}} = \frac{k^2 l}{3\pi} \frac{L_1 L_\perp L_\parallel}{\max(L_1^2, L_\perp^2, L_\parallel^2)}$ hence identifying the length $\mathcal{L}$ (see SM section 5.2). The amplitude of $\langle f^2 \rangle$ is calculated for different values of L_1 ranging from $5\,\mu$m to $100\,\mu$m, with $L_\perp = L_\parallel = 40\,\mu$m, so that $L_1 > l$ and $g_{\mathcal{L}} \gg 1$ in all cases. We choose $I = 10^9$ W$\cdot$ m^{-2}, an intensity strong enough to obtain measurable forces without altering the medium.**

	$L_1(\mu\text{m})$	$\sqrt{\langle f^2 \rangle}$(pN)	$\mathcal{Q}_2 + \mathcal{Q}_\nu$	$g_{\mathcal{L}}$	f_{QED} (pN)
Absorbing plate $\mathcal{Q}_\nu = 0$	5	13	$1.0 \cdot 10^{-3}$	53	
	40	118	$1.0 \cdot 10^{-2}$	424	
	100	68	$2.2 \cdot 10^{-4}$	170	
Reflecting plate $\mathcal{Q}_2 = 0$	5	567	1.9	53	$3 \cdot 10^{-3}$
	40	201	$2.3 \cdot 10^{-2}$	424	$8 \cdot 10^{-7}$
	100	127	$7.6 \cdot 10^{-4}$	170	$2 \cdot 10^{-8}$

4.4.6 Interaction force

The intensity fluctuations being long ranged, it is tempting to see whether they induce and interacting force between two membranes, as illustrated on Fig.4.8. In this configuration, two membranes attached by a spring are suspended in a scattering medium. The fluctuation of the tension on the spring gives the fluctuating interaction force between the plates,

$$\boldsymbol{f}_{12} = \boldsymbol{f}_{p_+} - \boldsymbol{f}_{p_-} \tag{4.65}$$

where $\boldsymbol{f}_{p_\pm}$ is the fluctuation induced force on the plates $p_\pm$. The mean square displacement is

$$\langle \boldsymbol{f}_{12}^2 \rangle = \langle \boldsymbol{f}_{p_+}^2 \rangle + \langle \boldsymbol{f}_{p_-}^2 \rangle - \frac{1}{v^4} \int_{p_+} d\mathbf{r} \int_{p_-} d\mathbf{r}'\, D^2 \partial_z \partial_{z'} \langle \delta I^{(1)}(\mathbf{r}) \delta I^{(1)}(\mathbf{r}') \rangle + \langle \nu_z^{(1)}(\mathbf{r}) \nu_z^{(1)}(\mathbf{r}') \rangle \tag{4.66}$$

where the integral on the right hand side is due to crossed correlation functions. Since the noise is delta correlated, the term $\langle \nu_z^{(1)}(\mathbf{r}) \nu_z^{(1)}(\mathbf{r}') \rangle$ does not contribute to the integral. However, the intensity crossed correlation function $\langle \delta I^{(1)}(\mathbf{r}) \delta I^{(1)}(\mathbf{r}') \rangle$ contribute provided that we impose absorbing boundary conditions on the membranes, Fig.4.8. This setup is therefore relevant for measuring the fluctuation induced forces stemming from the intensity fluctuations alone. Quantitatively, the crossed correlation term is comparable to the fluctuation induced forces studied in 4.4.3 and 4.4.4.

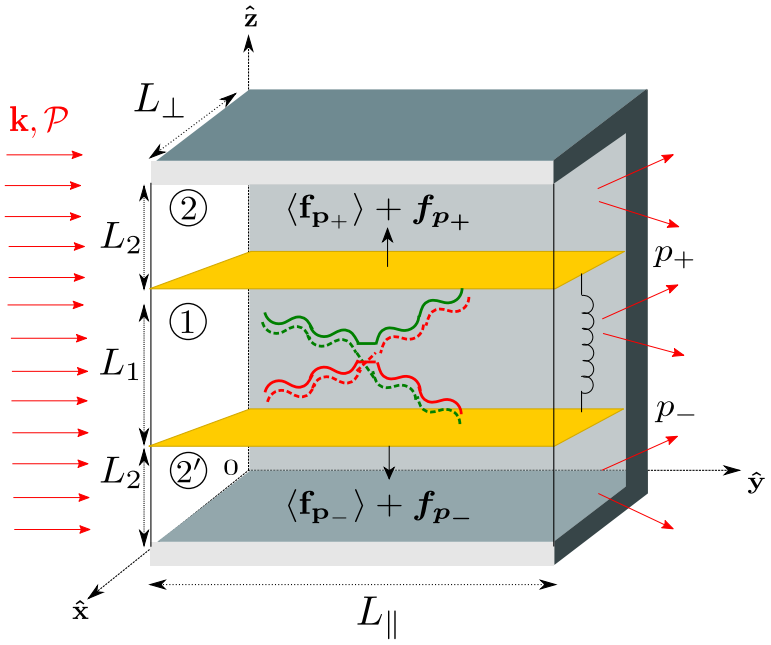

FIGURE 4.8: Two membranes (yellow) attached by a spring are suspended in a scattering medium, illuminated by a monochromatic scalar radiation. The spring allows to measure the interaction force between the plates, mediated by the crossed correlation function of the intensity fluctuations, which englobes processes where a quantum crossing leads to long ranged fluctuations between two points on opposite membranes, as illustrated by the crossing in the figure.

To conclude this chapter, we showed that coherent light fluctuations induce measurable forces, which are monitored by the easily tunable parameter $g_{\mathcal{L}}$. The propagation of diffusive light through random media have broadly been studied in the literature, mostly through transmission properties and long range correlations, either spatial or spectral. However, mechanical effects resulting from coherent mesoscopic effects, presented here, have never been considered, and open a new approach to the field. For example, in addition to transmission measurements [58], the present coherent mechanical forces could be used as a new type of mechanical sensors at submicronic scale, relevant in soft condensed matter, biophysics [24], nanoelectromechanical (NEMS) and quantum technologies [59, 60].

Chapter 5

Macroscopic fluctuation theory for coherent light

It's not because things are difficult that we do not dare, it's because we do not dare that they are difficult.

Seneca

Idiots dare everything. In fact, that's how you recognize them.

Michel Audiard

In the chapter 3, we showed that coherent light can be accurately described by means of an effective Langevin equation 3.1. Keeping only the main contribution of the noise term leads to an effective Langevin equation (3.21), which describes coherent light fluctuations to first order in $1/g$. The specific dependence of the effective Langevin equation (3.21) in a constant diffusion coefficient D and a quadratic mobility σ reminds the Kipnis-Marchioro-Presutti (KMP) model – a heat transfer model for boundary driven one dimensional chains of mechanically uncoupled oscillators strongly out of equilibrium [39, 27]. The latter process belongs to a class of non equilibrium stochastic model, well described by the macroscopic fluctuation theory [26, 27, 28]. In this chapter, we apply methods inspired by the macroscopic fluctuation theory and the stochastic formalism to the study of coherent light – an approach easily generalizable to other wave problems in mesoscopics. A first important point to notice is that coherent light is described by a time independent Langevin equation, while the macroscopic fluctuation theory and fluctuating hydrodynamics have been developed for and applied to time dependent processes, in which time is an essential parameter to define the entropy or even the notion of "non equilibrium" – the breaking of time reversal symmetry. Hence, the mesoscopic time independent problem of a coherent light flow displays a crucial difference with the systems considered so far in the macroscopic fluctuation theory. We show that despite this difference, the stochastic formalism allows to recover known results obtained from mesoscopics such as the correlation function. Moreover, inspired by the macroscopic fluctuation theory and stochastic formalism, we extend the notion of time reversal symmetry and entropy production to mesoscopic systems, and obtain a Gallavotti-Cohen relation for a time independent process. The results presented here should be of interest for both the mesoscopics and statistical mechanics communities. For the former, the mapping to non equilibrium hydrodynamics provides a new insight to mesoscopic physics as well as useful tools to study quantities so far difficult to access, such as higher orders intensity correlation functions. For the latter, this work should motivate further study of time independent processes inspired from mesoscopics, hence

providing new models which might so far have been overlooked.
We begin by an introduction to the macroscopic fluctuation theory framework and the stochastic formalism, then we apply these tools to the study of a coherent light flow.

5.1 The macroscopic fluctuation theory

Far from equilibrium phenomena are ubiquitous, and underlie most of the energy flow processes which play crucial roles in various fields ranging from biology, soft matter physics, geophysics and astrophysics. Such out of equilibrium systems are out of the range of classical thermodynamics and near equilibrium fluctuation theories [61, 62]. Given the importance of these phenomena, a new theory has been developed in the past two decades to describe them – the macroscopic fluctuation theory [26, 27, 28, 40], inspired by thermodynamics formalism and stochastic models.

5.1.1 General framework

Consider a system of volume V, in contact with boundary reservoirs at the boundary ∂V, such as, for example, the setup on Fig.5.1. We denote by $\mathbf{r}, t$ respectively the position and time variables. At the macroscopic scale, the system is characterized by a density $\rho(\mathbf{r}, t)$ and a current $\mathbf{j}(\mathbf{r}, t)$, whose behavior depends on two parameters, a diffusion coefficient $D(\rho)$ and a mobility $\sigma(\rho)$, which a priori depend on the density ρ. Common situations in which D depends on ρ, for example, are those where interaction between particles are included [63]. To alleviate the notations, we will sometimes omit to write the dependence of D and σ on the density or on the variables. Unless explicitly stated otherwise, these coefficients will always be assumed to depend on ρ – and consequently on $\mathbf{r}$ and t. For convenience, we use rescaled variables $\mathbf{x} = \mathbf{r}/L$ and $\tau = t/L^2$ (see section 3.1.3). The macroscopic dynamics is determined by a Langevin equation together with a continuity equation,

$$\begin{cases} j_\alpha(\mathbf{x}, \tau) = -D_{\alpha\beta}\partial_\beta \rho(\mathbf{x}, \tau) + \sigma_{\alpha\beta} E_\beta(\mathbf{r}) + \sqrt{\sigma_{\alpha\beta}}\eta_\beta(\mathbf{x}, \tau) \\ \\ \partial_\tau \rho(\mathbf{x}, \tau) + \boldsymbol{\nabla} \cdot \mathbf{j}(\mathbf{x}, \tau) = 0. \end{cases} \tag{5.1}$$

where $\mathbf{E}$ is an external field (supposed to be time independent for simplicity) and η is a Gaussian white noise,

$$\begin{cases} \langle \boldsymbol{\eta}(\mathbf{x}, \tau) \rangle = 0 \\ \\ \langle \eta_\alpha(\mathbf{x}, \tau)\eta_\beta(\mathbf{x}', \tau') \rangle = \delta_{\alpha\beta}\delta(\mathbf{x} - \mathbf{x}')\delta(\tau - \tau') \end{cases} \tag{5.2}$$

The parameters $D(\rho)$ and $\sigma(\rho)$ are related by the Einstein relation,

$$\sigma(\rho) D(\rho)^{-1} = f_0''(\rho)\,. \tag{5.3}$$

where f_0 is the free energy of the system at equilibrium. The relation (5.3) is remarkable, since it connects the two parameters describing the non equilibrium dynamics, D and σ, to an equilibrium quantity, f_0. This relation implies the Gallavotti-Cohen relation – a fluctuation dissipation relation for non equilibrium systems – as discussed in the section 5.1.5. The boundary conditions are then given by

$$f_0'(\rho(\mathbf{x}, \tau)) = \mu(\mathbf{x}, \tau) \text{ for all } \mathbf{x} \in \partial V \tag{5.4}$$

where μ is the chemical potential.

In classical thermodynamics, the second derivative of the free energy defines the compressibility χ of the system; we can therefore re-write the Einstein relation (5.3) as

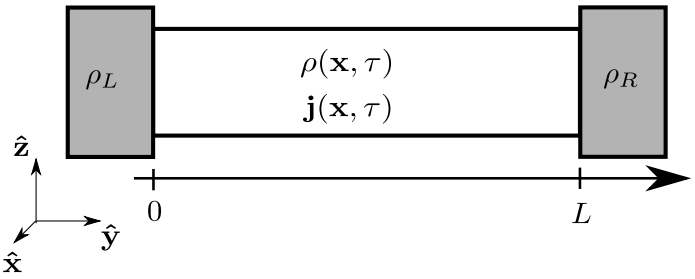

FIGURE 5.1: Standard example of a boundary driven diffusive system. The system is connected to two thermal baths at $x = 0, L$, at which the density is determined by the boundary conditions, $\rho(x, y = 0, z) = \rho_L, \rho(x, y = L, z) = \rho_R$. The bulk dynamics obeys Eq.(5.1).

$$\sigma(\rho)D(\rho)^{-1} = \chi(\rho)\,. \tag{5.5}$$

The system is *at equilibrium* when $\mathbf{j}(\mathbf{x},\tau) = 0$, and in a *steady state* when $\nabla \cdot \mathbf{j}(\mathbf{x},\tau) = 0$. We note $\overline{\rho}$ the steady state solution, supposed to be unique [40].

Finally, we introduce the time reversal operator, Θ. By definition, Θ acts on density and current in the following way,

$$\begin{cases} \Theta(\rho(\mathbf{r},t)) = \rho(\mathbf{r},-t) \\ \\ \Theta(\mathbf{j}(\mathbf{r},t)) = -\mathbf{j}(\mathbf{r},-t) \end{cases} \tag{5.6}$$

We develop the notion of time reversal and its consequences in the following sections. In 5.2, we adapt this notion to the case of coherent light.

5.1.2 Fundamental formula and quasi potential

As in thermodynamics [64], a crucial step in the macroscopic fluctuation theory description is the definition of the appropriate thermodynamical potential to characterize the system. The macroscopic fluctuation theory framework introduces the notion of quasi potential – the analog of the free energy for an out of equilibrium system [65] – as an appropriate thermodynamical functional describing the system. The quasi potential is obtained from a path integral formulation of the Langevin equation Eq.(5.1), which is derived using the Martin-Siggia-Rose procedure [66]. This procedure consists in expressing the noise as a functional of ρ and $\mathbf{j}$, and to translate the noise probability distribution in a probability functional for the profile $\{\rho, \mathbf{j}\}$. There are alternative ways to derive Eq.(5.7), see e.g. [40, 67] but we choose here the Langevin method since it makes a more direct connection with chapter 3. From Eqs.(5.1,5.2), we deduce that the probability to observe a profile $\{\rho, \mathbf{j}\}$ over a time window $[T_1, T_2]$,

$$\mathcal{P}_{[T_1,T_2]}[\{\rho,\mathbf{j}\}] \sim \exp\left(-\frac{1}{2}L^d \int_{T_1}^{T_2} d\tau \int_{\tilde{V}} d\mathbf{x}\,(j_\alpha + D_{\alpha\beta}\nabla_\beta \rho)\sigma^{-1}_{\alpha\gamma}(j_\gamma + D_{\gamma\delta}\nabla_\delta \rho)\right), \tag{5.7}$$

where the space integral is performed over the rescaled volume $\tilde{V}$, the $d-$dimensional hypercube, and where the continuity equation $\partial_\tau \rho(\mathbf{x},\tau) + \boldsymbol{\nabla} \cdot \mathbf{j}(\mathbf{x},\tau) = 0$ is implicitly assumed. The equation (5.7) is called the *fundamental formula* in the literature, and constitutes the first building block of the macroscopic fluctuation theory.

The time reversal operator Θ, when applied to $\mathcal{P}_{[T_1,T_2]}[\{\rho,\mathbf{j}\}]$, defines the probability associated to the *adjoint process* $\{\Theta\rho,\Theta\mathbf{j}\}$. By definition,

$$\mathcal{P}_{[T_1,T_2]}[\{\rho,\mathbf{j}\}] = \Theta\mathcal{P}_{[-T_2,-T_1]}[\{\Theta\rho,\Theta\mathbf{j}\}]\,. \tag{5.8}$$

We use this notion to obtain the Gallavotti-Cohen relation in 5.1.5.

The integral

$$L^d \int_{T_1}^{T_2} d\tau \int_{\tilde{V}} d\mathbf{x}\,(j_\alpha + D_{\alpha\beta}\nabla_\beta\rho)\sigma^{-1}_{\alpha\gamma}(j_\gamma + D_{\gamma\delta}\nabla_\delta\rho)$$

corresponds to the energy, or cost, necessary to produce the extra current $\mathbf{j} + D\boldsymbol{\nabla}\rho$. Minimizing Eq.(5.7) over all the currents which satisfy the continuity equation defines the *cost functional* for the profile ρ,

$$\mathcal{I}_{[T_1,T_2]}[\rho] = \inf_{\mathbf{j}:\partial_\tau\rho(\mathbf{x},\tau)=-\boldsymbol{\nabla}\cdot\mathbf{j}(\mathbf{x},\tau)} \int_{T_1}^{T_2} d\tau \int_{\tilde{V}} d^d\mathbf{r}\,(j_\alpha + D_{\alpha\beta}\nabla_\beta\rho)\sigma^{-1}_{\alpha\gamma}(j_\gamma + D_{\gamma\delta}\nabla_\delta\rho) \tag{5.9}$$

In the context of stochastic processes, $\exp[-\mathcal{I}_{[T_1,T_2]}[\rho]]$ gives the probability of observing the trajectory ρ during the time window $[T_1,T_2]$. Here, the term "trajectory ρ" means the profile $\rho(\mathbf{r},t)$ taken over the time window $[T_1,T_2]$. We can now define the quasi potential. For a system characterized by a density profile ρ at the time τ, the quasi potential is given by

$$\mathcal{V}[\rho] = \inf_{\tilde{\rho}\,:\,\substack{\tilde{\rho}(t=-\infty)=\overline{\rho},\\ \tilde{\rho}(t=0)=\rho}} \mathcal{I}_{[-\infty,\tau]}[\tilde{\rho}] \tag{5.10}$$

Namely, the quasi potential is related to the energy required to obtain the density profile ρ at the time τ, starting from the stationary profile $\overline{\rho}$ at time $-\infty$. It is the analog of free energy for non equilibrium systems [65]. The quantity

$$\mathcal{P}[\rho] = \exp[-\mathcal{V}[\rho]] \tag{5.11}$$

gives the probability to observe a variation ρ around the steady state solution $\overline{\rho}$.

The quasi potential is in general very difficult to calculate analytically or even numerically. However, we can obtain useful information from perturbation developments of $\mathcal{V}$ around its minimum, which corresponds to the most likely solutions, and can be obtained by the saddle point principle. For example, we can deduce the density correlation functions using a perturbation development of the Legendre transform of $\mathcal{V}$. This is the object of the section 5.1.4. A convenient way to perform the correlation functions derivation is to use the Hamilton-Jacobi equation, which is discussed in the next section.

5.1.3 Hamiltonian formulation

It is useful to translate the fundamental formula (5.7) in the Hamiltonian language. From the Hamiltonian of the system, we can derive the Hamilton-Jacobi equation (see chapter 7 in [68]), which constitutes a self-contained equation of the quasi potential [26], from which useful physical quantities can be derived, see 5.1.4.

Notice that the exponent in the right hand side of Eq.(5.7) has the structure of an action, associated to the Langrangian

$$\mathcal{L}[\{\rho,\mathbf{j}\}] = \frac{1}{2}\int_{\tilde{V}} d\mathbf{x}\,(j_\alpha + D_{\alpha\beta}\partial_\beta\rho)\sigma^{-1}_{\alpha\gamma}(j_\gamma + D_{\gamma\delta}\partial_\delta\rho) \tag{5.12}$$

For simplicity, we further on consider the case of a diagonal D and σ, but the result Eq.(5.17) is valid in the general case [26]. The Lagrangian becomes

$$\mathcal{L}[\{\rho,\mathbf{j}\}] = \int_{\tilde{V}} d\mathbf{x}\,\frac{(\mathbf{j}+D\boldsymbol{\nabla}\rho)^2}{2\sigma} \tag{5.13}$$

Since our end goal is the study of the density fluctuations (we could adapt the reasoning for current fluctuations [40]), we use the fundamental formula (5.7) to obtain the probability distribution of the density ρ. Namely, we integrate over all the possible currents satisfying the continuity equation,

$$\mathcal{P}[\rho] = \int \mathcal{D}\mathbf{j}\,\delta\left(\partial_\tau\rho(\mathbf{x},\tau) + \boldsymbol{\nabla}\cdot\mathbf{j}(\mathbf{x},\tau)\right)\exp\left[-\int_{\tilde{V}} d\mathbf{x}\,\frac{(\mathbf{j}+D\boldsymbol{\nabla}\rho)^2}{2\sigma}\right] \tag{5.14}$$

To take into account the delta function, we introduce the Lagrange multiplier π,

$$\mathcal{P}[\rho] = \int \mathcal{D}\mathbf{j}\,\exp\left[-\int_{\tilde{V}} d\mathbf{x}\,\left(\pi\left(\partial_\tau\rho(\mathbf{x},\tau) + \boldsymbol{\nabla}\cdot\mathbf{j}(\mathbf{x},\tau)\right) + \frac{(\mathbf{j}+D\boldsymbol{\nabla}\rho)^2}{2\sigma}\right)\right].$$

Using an integration by parts for the term $\pi\boldsymbol{\nabla}\cdot\mathbf{j}(\mathbf{x},\tau)$ with boundary conditions $\pi = 0$ at the boundaries, we obtain

$$\mathcal{P}[\rho] = \int \mathcal{D}\mathbf{j}\,\exp\left[-\int_{\tilde{V}} d\mathbf{x}\,\pi\partial_\tau\rho(\mathbf{x},\tau) - \mathbf{j}(\mathbf{x},\tau)\cdot\boldsymbol{\nabla}\pi + \frac{(\mathbf{j}+D\boldsymbol{\nabla}\rho)^2}{2\sigma}\right]. \tag{5.15}$$

We now regroup the currents $\mathbf{j}$ to form a Gaussian square, and integrate it out to obtain finally

$$\mathcal{P}[\rho] = \int \mathcal{D}\mathbf{j}\,\exp\left[-\int_{\tilde{V}} d\mathbf{x}\,\pi\partial_\tau\rho(\mathbf{x},\tau) - \mathcal{H}[\rho,\pi]\right], \tag{5.16}$$

where $\mathcal{H}[\rho,\pi]$ is the Hamiltonian,

$$\mathcal{H}[\rho,\pi] = \int_{\tilde{V}} d\mathbf{x}\,\left(\boldsymbol{\nabla}\pi\cdot\sigma(\rho)\boldsymbol{\nabla}p - \pi\boldsymbol{\nabla}\cdot\mathbf{J}\right) \tag{5.17}$$

and where $\mathbf{J} = -D(\rho)\boldsymbol{\nabla}\rho$.

The Hamilton-Jacobi equation is a general result of analytical mechanics, see chapter 7 in [68], which is simply expressed by

$$\mathcal{H}\left[\rho, \frac{\delta\mathcal{V}}{\delta\rho}\right] = 0\,. \tag{5.18}$$

In the present case, using Eq.(5.17), the Hamilton-Jacobi equation is

$$\int_{\tilde{V}} d\mathbf{x} \left(\boldsymbol{\nabla} \frac{\delta \mathcal{V}}{\delta \rho} \cdot \sigma(\rho) \boldsymbol{\nabla} p - \frac{\delta \mathcal{V}}{\delta \rho} \boldsymbol{\nabla} \cdot \mathbf{J} \right) = 0 \tag{5.19}$$

We can now obtain the density correlation function, from a perturbation development of the Hamilton-Jacobi equation.

5.1.4 Density correlations

The macroscopic fluctuation theory provides a general method for calculating the correlation function of the density at all orders. The idea is to define a generating function for the correlation functions [40, 28, 69]. By definition, the correlation functions are given by

$$C_n(\mathbf{r_1}, ..., \mathbf{r_n}) = \langle \rho(\mathbf{r_1}) ... \rho(\mathbf{r_n}) \rangle_{\mathcal{P}} \tag{5.20}$$

where the average $\langle ... \rangle_{\mathcal{P}}$ is taken over the stationary ensemble, described by the probability distribution Eq.(5.11). We introduce a generating functional $\mathcal{G}[h]$, for the correlation functions, defined by

$$\begin{aligned} \exp[L^d \mathcal{G}[h]] &= \langle \exp[L^d \int_V d\mathbf{r}\, h(\mathbf{r}) \rho(\mathbf{r})] \rangle_P \\ &= \int \mathcal{D}(\rho) e^{-L^d \mathcal{V}(\rho) + L^d \int_V d\mathbf{r}\, h(\mathbf{r}) \rho(\mathbf{r})} \\ &\sim \exp \left[\sup_\rho \left(-L^d \mathcal{V}(\rho) + L^d \int_V d\mathbf{r}\, h(\mathbf{r}) \rho(\mathbf{r}) \right) \right] \end{aligned} \tag{5.21}$$

which gives for $\mathcal{G}$,

$$\mathcal{G}[h] = \sup_\rho \left[\mathcal{V}[\rho] + \int_V d\mathbf{r}\, h(\mathbf{r}) \rho(\mathbf{r}) \right] . \tag{5.22}$$

The functional $\mathcal{G}$ is called the pressure functional; it is the Legendre transform of $\mathcal{V}$, and a generating functional for the C_n functions,

$$C_n(\mathbf{r_1}, ..., \mathbf{r_n}) = \left. \frac{\delta^n \mathcal{G}[h]}{\delta h(\mathbf{r_1}) ... \delta h(\mathbf{r_n})} \right|_{h=0} \tag{5.23}$$

In what follows, we focus on the two point correlation function; to alleviate the notations, and to avoid any confusion with the C_2 term in the light correlation function Eq.(2.54), we note it $C(\mathbf{r}, \mathbf{r}')$,

$$C(\mathbf{r}, \mathbf{r}') = \left. \frac{\delta^2 \mathcal{G}[h]}{\delta h(\mathbf{r}) \delta h(\mathbf{r}')} \right|_{h=0} . \tag{5.24}$$

The Hamilton-Jacobi Eq.(5.19) can then be re-written as

$$\int_V d\mathbf{r}\, \nabla h(\mathbf{r}) \cdot \sigma \left(\frac{\delta \mathcal{G}}{\delta h} \right) \nabla h(\mathbf{r}) + \nabla h(\mathbf{r}) \cdot \mathbf{J} \left(\frac{\delta \mathcal{G}}{\delta h} \right) = 0 . \tag{5.25}$$

From now on we assume, for simplicity, that there are no external fields, $\mathbf{E} = 0$. Expanding Eq.(5.25) around the minimum at $h = 0$, we obtain an integral equation for C,

$$\int_V d\mathbf{r}\, \nabla h(\mathbf{r}) \cdot \left(\sigma(\bar{\rho}) \nabla h(\mathbf{r}) - \nabla \int_V D(\bar{\rho}) C(\mathbf{r}, \mathbf{r}') h(\mathbf{r}') \right) = 0 \,. \tag{5.26}$$

We expect the correlation function to have a short range component, describing fluctuations around the equilibrium state. We therefore write C in the form

$$C(\mathbf{r}, \mathbf{r}') = C_{eq}(\mathbf{r}) \delta(\mathbf{r} - \mathbf{r}') + B(\mathbf{r}, \mathbf{r}') \,. \tag{5.27}$$

Replacing in Eq.(5.26), we find

$$C_{eq}(\mathbf{r}) = \frac{\sigma(\bar{\rho})}{D(\bar{\rho})} \tag{5.28}$$

and

$$D(\bar{\rho})(\Delta_{\mathbf{r}} + \Delta_{\mathbf{r}'}) B(\mathbf{r}, \mathbf{r}') = \alpha(\mathbf{r}) \delta(\mathbf{r} - \mathbf{r}') \tag{5.29}$$

with $\alpha(\mathbf{r}) = \nabla \cdot (\sigma'(\bar{\rho}) D^{-1} \mathbf{J}(\bar{\rho}))$.

The Eqs.(5.27,5.28,5.29) are valid for any D and σ. For example, D constant and $\sigma = a\bar{\rho} + b\bar{\rho}^2$ correspond to well known models,

$$\begin{cases} b = 0,\ a = 1 \text{ random walk} \\ b = 1,\ a = 0 \text{ Kipnis–Marchioro-Presutti (KMP)} \\ b = -1,\ a = 1 \text{ symmetric simple exclusion process (SSEP)} \\ b = 1,\ a = 1 \text{ symmetric simple inclusion process (SSIP)} \end{cases}$$

In the case where D is constant and $\sigma \propto \rho^2$ (KMP model), we find

$$B(\mathbf{r}, \mathbf{r}') = -\frac{\sigma''(\bar{\rho})}{2D} |\nabla \bar{\rho}|^2 G(\mathbf{r}, \mathbf{r}') \tag{5.30}$$

with $G(\mathbf{r}, \mathbf{r}')$ the Green's function of the Dirichlet Laplacian,

$$\Delta_{\mathbf{r}} G(\mathbf{r}, \mathbf{r}') = \delta(\mathbf{r} - \mathbf{r}') \tag{5.31}$$

Note the similarity with $\langle \delta I(\mathbf{r}) \delta I(\mathbf{r}') \rangle^{(2)}$ in Eq.(5.53); these two functions are identical up to an integral over $\int_V P_D(\mathbf{r}, \mathbf{r}')$.

5.1.5 Gallavotti-Cohen relation

The macroscopic fluctuation theory provides a universal fluctuation relation for boundary driven far from equilibrium systems, known as the Gallavotti-Cohen relation [42]. This relation states that the ratio between the probability to observe a certain density trajectory, and the probability to observe its time reversed, is related to the energy transferred from the reservoirs.

Consider a trajectory $\mathbf{j}(t)$ such that its time average is equal to a given vector field $\mathbf{J}$,

$$\int_{-\infty}^{+\infty} dt\, \mathbf{j}(t) = \mathbf{J}\,. \tag{5.32}$$

Let $\Phi(\mathbf{J})$ be the associated time averaged cost function, for $T \to +\infty$,

$$\Phi(\mathbf{J}) = \lim_{T\to+\infty} \frac{1}{2T} \inf_{(\rho,\mathbf{j})\in A_T} \mathcal{I}_{[-T,T]}(\rho, j) \tag{5.33}$$

where $A_T = \left\{ (\rho, \mathbf{j}) : \frac{1}{T}\int_0^T dt\, \mathbf{j}(t) = \mathbf{J}; \partial_t \rho = -\nabla\cdot\mathbf{j}, \rho(0) = \rho_0 \right\}$.

Remark: it can be shown that the singularities of the functional Φ correspond to dynamical phase transitions [27, 40]. These aspects are beyond the scope of this work, but we refer to [70, 71] for elaborations on the relation between the Φ, dynamical phase transitions, and the breaking of time translation invariance.

It is straightforward to show that, that if $(\tilde{\rho}, \tilde{\mathbf{j}})$ is optimal to observe $\Phi(\mathbf{J})$, then the time reversed trajectories $(\Theta\tilde{\rho}, \Theta\tilde{\mathbf{j}})$ are optimal for $\Phi(-\mathbf{J})$ [40]. A standard calculation then leads to

$$\Phi(\mathbf{J}) - \Phi(-\mathbf{J}) = -\int_V d\mathbf{r}\, \frac{D\boldsymbol{\nabla}\rho\cdot\mathbf{J}}{\sigma}\,. \tag{5.34}$$

Using the Einstein relation (5.3), we have that

$$\boldsymbol{\nabla} f_0'(\rho) = f_0''(\rho)\boldsymbol{\nabla}\rho = \frac{D}{\sigma}\boldsymbol{\nabla}\rho\,,$$

which we substitute in Eq.(5.34) and, performing an integration by parts, we obtain the Gallavotti-Cohen relation,

$$\Phi(\mathbf{J}) - \Phi(-\mathbf{J}) = \int_{\partial V} d\mathbf{s}\, \mu\, \mathbf{J}\cdot\hat{\mathbf{n}} \tag{5.35}$$

where $\mu = f_0'(\rho)$ is the chemical potential at the boundaries. The Gallavotti-Cohen relation states that the ratio between the probabilities to observe the average current $\mathbf{J}$ and its time reversed counterpart $-\mathbf{J}$ only depends on the boundary conditions, and not on the specific fluctuations inside the bulk. The difference on the left hand side on Eq.(5.35) is also called the entropy production rate; the Eq.(5.35) is then interpreted as a fluctuation theorem, relating the entropy production to the dissipation on the right hand side [26, 40, 72]. We discuss this last point in more detail in 5.2.4.

Remark: in the presence of an external field $\mathbf{E}$, the Gallavotti-Cohen relation becomes

$$\Phi(\mathbf{J}) - \Phi(-\mathbf{J}) = -\int_V d\mathbf{r}\, \mathbf{J}(\mathbf{r})\cdot\mathbf{E}(\mathbf{r}) + \int_{\partial V} d\mathbf{s}\, \mu\, \mathbf{J}\cdot\hat{\mathbf{n}}\,. \tag{5.36}$$

5.2 Macroscopic fluctuation theory approach for coherent light

In this section, we apply the methods from the macroscopic fluctuation theory to the mesoscopic problem of coherent light. Consider a volume $V = L^d$ of elastic scatterers, illuminated by a light beam (not necessarily monochromatic), Fig.5.2. There are

two important points to address in order to properly adapt the macroscopic fluctuation theory to a time independent mesoscopic system. First, we need to specify the boundary conditions. There is no chemical potential for coherent light, as opposed to the stochastic processes dealt with in 5.1. Second, we have to define an equivalent notion for time reversal. This will allow us to obtain the mesoscopic counterpart of quantities such as the adjoint process and the entropy production. To do so, we define a time reversed process as a "disorder reversed process" – we assume that, given a process $\{I, \mathbf{j}\}$ associated to one realization of disorder, there exists another realization of disorder which gives the adjoint process $I, -\mathbf{j}$.

5.2.1 Fundamental formula and boundary conditions

On the macroscopic scale L^d, the radiation is defined by an intensity $I(\mathbf{r})$ and a current $\mathbf{j}(\mathbf{r})$, satisfying

$$\begin{cases} \nabla \cdot \mathbf{j}(\mathbf{r}) & = 0 \\ \\ j_\alpha(\mathbf{r}) & = -D\nabla_\alpha I(\mathbf{r}) + \sigma_{\alpha\beta} E_\beta(\mathbf{r}) + \sqrt{\frac{\sigma_{\alpha\beta}}{L}}\eta_\beta(\mathbf{r}). \end{cases} \tag{5.37}$$

where $\boldsymbol{\eta}$ is a Gaussian white noise,

$$\langle \eta_\alpha(\mathbf{r})\eta_\beta(\mathbf{r}')\rangle = \delta_{\alpha\beta}\delta(\mathbf{r}-\mathbf{r}')\,. \tag{5.38}$$

Recall that, as discussed in chapter 3, the noise term $\sqrt{\frac{\sigma_{\alpha\beta}}{L}}\eta_\beta(\mathbf{r})$ represents here the perturbations induced by the coherent effects. It does not represent the distribution of the scatterers, but the occurrence of quantum crossings. To highlight the difference with thermal noise, we will refer to the noise in Eq.(5.37) as *mesoscopic noise*, resulting from *mesoscopic disorder* – the occurrence of the quantum crossings. We include in Eq.(5.37) the possibility of having an external field $\mathbf{E}(\mathbf{r})$. For light, an experimental way to apply such an external field would be, for example, to choose a material with a non homogeneous refractive index. Note also that the mobility σ is here written is tensor form. In the case where the illuminating light beam is not monochromatic, the mobility could in fact have a more complicated form as in the Langevin equation (3.1), derived for a monochromatic radiation.

For simplicity, we further on focus on the case where $\mathbf{E}(\mathbf{r}) = 0$ and σ is a scalar, but the generalization of our results to more complicated situations can be obtained by following the same methods.

Boundary conditions

As discussed in chapter 2, the mesoscopics boundary conditions for the diffusive intensity $I(\mathbf{r})$ are not trivial, and are derived from the boundary conditions on the current $\mathbf{j}(\mathbf{r})$. Since diffusion processes happen inside the disordered medium, the boundary conditions are that any incoming diffusive light current $\mathbf{j}$ must vanish at every point of the interface:

$$\mathbf{j_{in}}(\mathbf{r}) \cdot \widehat{\mathbf{n}} = 0 \text{ for any } \mathbf{r} \in \text{the interface} \tag{5.39}$$

with $\widehat{\mathbf{n}}$ the normal vector of the interface and the average being done over vectors $\widehat{\mathbf{s}}$ directed inwards. More precisely, if we take into account internal reflexions on the inside wall of the interface, the boundary condition becomes:

$$\mathbf{j_{D,in}}(\mathbf{r}) \cdot \widehat{\mathbf{n}} = R\, \mathbf{j_{D,out}}(\mathbf{r}) \cdot \widehat{\mathbf{n}} \tag{5.40}$$

with R the reflexion coefficient.
This leads to the following boundary conditions for $I(\mathbf{r})$:

$$\frac{1}{2}(1-R) I_D(\mathbf{r}) = \frac{l}{3}(1+R)\widehat{\mathbf{s}} \cdot \nabla I_D(\mathbf{r}) + (1-R)\gamma(\mathbf{r})\,. \tag{5.41}$$

In the slab geometry Fig.5.2, we can replace the mixed boundary condition (5.41) by a Dirichlet condition at a distance $\frac{2l}{3}$ from the border, outside of the medium. For absorbing edges ($R = 0$), the boundary conditions thus become

$$\begin{cases} I(\mathbf{r}) = 0 \text{ for } \mathbf{r} = \left(-\frac{2l}{3}, y, z\right) \text{ or } \mathbf{r} = \left(L + \frac{2l}{3}, y, z\right) \\ \\ \mathbf{j_{in}}(\mathbf{r}) \cdot \widehat{\mathbf{n}} = 0 \text{ for } \mathbf{r} \in \partial V \end{cases} \tag{5.42}$$

Fundamental formula

Using the Martin-Siggia-Rose procedure, we obtain the fundamental formula – the probability to observe a profile $\{I, \mathbf{j}\}$

$$\mathcal{P}[\{I, \mathbf{j}\}] \sim \exp\left(-\frac{1}{2} L^d \int_{\tilde{V}} d\mathbf{x}\, (j_\alpha + D_{\alpha\beta}\nabla_\beta I)\sigma^{-1}_{\alpha\gamma}(j_\gamma + D_{\gamma\delta}\nabla_\delta I) \right). \tag{5.43}$$

5.2.2 Adjoint process

We now introduce the notion of adjoint process for coherent light. Remind that the adjoint process is usually defined as the time reverse of a given process. In the present context of coherent light, time reversal means reversed realizations of disorder. We note θ the "reverse disorder realization" operator. By analogy with time reversal, we write explicitly the dependence of I and $\mathbf{j}$ on the disorder ξ, and we note ξ^* the reversed disorder realization,

$$\begin{cases} \theta(I(\mathbf{r}, \xi^*)) = I(\mathbf{r}, \xi) \\ \\ \theta\mathbf{j}(\mathbf{r}, \xi^*) = -\mathbf{j}(\mathbf{r}, \xi) \end{cases} \tag{5.44}$$

By definition, the disorder reversed probability $\mathcal{P}^*$ associated to the adjoint process $\{\theta I, \theta\mathbf{j}\}$ satisfies

$$\frac{\mathcal{P}[\{I, \mathbf{j}\}]}{\mathcal{P}^*[\{\theta I, \theta\mathbf{j}\}]} = 1\,. \tag{5.45}$$

If we are interested only in the probability of observing a profile I, it is given by

$$\mathcal{P}[I] \quad = \int \mathcal{D}\mathbf{j}\, \delta(\boldsymbol{\nabla} \cdot \mathbf{j}) \exp\left[-\tfrac{L^d}{2} \int_{\tilde{V}} d\mathbf{x}\, \tfrac{(\mathbf{j}(\mathbf{x}) + D\boldsymbol{\nabla} I(\mathbf{x}))^2}{\sigma} \right] \tag{5.46}$$

where the integral in the exponent is taken over the renormalized volume $\tilde{V} = [0,1]^d$, a d dimensional hypercube. Using the same technique as in 5.1.3, we introduce the Lagrange multiplier p and we re-write $\mathcal{P}[I]$ as

$$\mathcal{P}[I] = \int \mathcal{D}\mathbf{j}\mathcal{D}p \exp\left[-L^d \int d\mathbf{r}\; p\boldsymbol{\nabla}\cdot\mathbf{j} + \frac{\left(\mathbf{j}(\mathbf{r}) + D\boldsymbol{\nabla}I(\mathbf{r})\right)^2}{2\sigma}\right] \tag{5.47}$$

Integrating $p\boldsymbol{\nabla}\cdot\mathbf{j}$ by parts, and then forming a Gaussian square in $\mathbf{j}$ and integrating over $\mathbf{j}$, we obtain

$$\mathcal{P}[I] = \int \mathcal{D}p\; \exp\left[-L^d \int_{\tilde{V}} d\mathbf{r}\left(D\boldsymbol{\nabla}I\cdot\boldsymbol{\nabla}p - \sigma(\boldsymbol{\nabla}p)^2/2\right)\right]. \tag{5.48}$$

This equation defines the action or cost functional,

$$\mathcal{S}[I,p] = L^d \int_{\tilde{V}} d\mathbf{r}\left(D\boldsymbol{\nabla}I\cdot\boldsymbol{\nabla}p - \sigma(\boldsymbol{\nabla}p)^2/2\right). \tag{5.49}$$

We can obtain the disorder reversed behavior of p, using the fact that Eq.(5.48) is dominated by the saddle point solution. Derivating according to p leads to

$$\nabla\cdot(D\boldsymbol{\nabla}I - \sigma\boldsymbol{\nabla}p) = 0\,. \tag{5.50}$$

We recognize a continuity equation, which allows us to identify the expression in the parenthesis with $\mathbf{j}$. The current $\mathbf{j}$ then writes, in terms of p,

$$\mathbf{j}(p) = -D\boldsymbol{\nabla}I + \sigma\boldsymbol{\nabla}p \tag{5.51}$$

Hence, θp must be such that $\theta\mathbf{j}(\mathbf{r},\xi^*) = -\mathbf{j}(\mathbf{r},\xi)$, which leads to

$$\boldsymbol{\nabla}(\theta p) = \frac{2D\boldsymbol{\nabla}I}{\sigma} - \boldsymbol{\nabla}p\,. \tag{5.52}$$

Note that the Legendre multiplier p has a physical signification. It is the conjugate of the mesoscopic noise, and represents the realizations of the mesoscopic disorder.

5.2.3 Correlation function

Let's now derive the correlation function of the fluctuating intensity. Following the macroscopic fluctuation theory, we use the stochastic formalism to derive a generating function for the correlators. We provide first a general derivation, for any coefficients D and σ, and then we focus on the case of a constant D and quadratic σ to recover the expected results for coherent light in first order in $1/g$ (see chapter 3). Remind that, for coherent light, the long ranged intensity correlation function is, to the first order in $1/g$,

$$\langle\delta I(\mathbf{r})\delta I(\mathbf{r}')\rangle = \int_V d\mathbf{R}\,\frac{\sigma''(I_D)}{2}|\nabla I_D(\mathbf{R})|^2 P_D(\mathbf{r},\mathbf{R})P_D(\mathbf{R},\mathbf{r}')\,. \tag{5.53}$$

General expression

From Eq.(5.48), the probability to observe the intensity profile I is

$$\mathcal{P}[I] \sim \int \mathcal{D}p\; \exp\left(-L^d\mathcal{S}[I]\right) \tag{5.54}$$

where $\mathcal{S}[I]$ is given by Eq.(5.49).

We introduce the so called pressure functional [40], a generating functional for the correlation functions,

$$\mathcal{G}[h] = \log\langle e^{L^d \int d\mathbf{x}\, h(\mathbf{x}) I(\mathbf{x})}\rangle_{\mathcal{P}[I]}, \tag{5.55}$$

where $\langle ...\rangle_{\mathcal{P}[I]}$ denotes the average with respect to $\mathcal{P}[I]$. The saddle point principle implies that

$$\mathcal{G}[h] \simeq \max_{I,p} \int dx\, h(x) I(x) - \mathcal{S}[I,p]\,, \tag{5.56}$$

from which we deduce

$$\langle I(x_1)...I(x_n)\rangle = \left.\frac{\delta \mathcal{G}(x)}{\delta h(x_1)...h(x_n)}\right|_{h=0} \tag{5.57}$$

The pressure functional $\mathcal{G}$ is therefore a generating function for the correlation functions of the intensity.

Finding either $\mathcal{S}$ or $\mathcal{G}$ explicitly is extremelly difficult in general (although analytical results have been obtained for some processes such as the simple symmetric exclusion process [73]). However, a full analytical expression of these functionals is not necessary to derive the correlation functions, since, as expressed in Eq.(5.57), the correlation functions depend only on the variations of $\mathcal{G}$ around $h = 0$. To obtain these fluctuations, we perform a perturbation development of I and p,

$$\begin{cases} I(x) = I_D + \epsilon I_1 + \epsilon^2 I_2 + ... \\ \\ p = \epsilon p_1 + ... \end{cases} \tag{5.58}$$

and we consider h to be of order ϵ, since it is small and assumed analytic. Then, $\mathcal{G}$ can be expressed perturbatively

$$\mathcal{G}[h] \simeq \int d\mathbf{x}\, I_D\, h(\mathbf{x}) + \frac{1}{2}\int d\mathbf{x} d\mathbf{y}\, C(\mathbf{x},\mathbf{y}) h(\mathbf{x}) h(\mathbf{y}) + ... \tag{5.59}$$

We can solve Eqs.(5.58) by orders of ϵ using the saddle point solutions of Eq.(5.56),

$$\begin{aligned} \nabla\cdot(D\boldsymbol{\nabla} I - \sigma \boldsymbol{\nabla} p) &= 0 \\ D\Delta p + \tfrac{1}{2}\sigma'(\boldsymbol{\nabla} p)^2 &= -h\,. \end{aligned} \tag{5.60}$$

To zeroth order, Eqs.(5.60) give $p = 0$, and I_D satisfies $\nabla\cdot(D\nabla I) = 0$. This is the optimal density profile. To first order in ϵ, we find

$$\begin{aligned} \boldsymbol{\nabla}\cdot(D_0'\boldsymbol{\nabla} I_D I_1 + D_0 \boldsymbol{\nabla} I_1 - \sigma_0 \boldsymbol{\nabla} p_1) &= 0 \\ D_0 \Delta p_1 &= -h, \end{aligned} \tag{5.61}$$

where we have defined $X_0 \equiv X(I_D)$. Using Green's functions, we obtain

$$\begin{aligned} I_1(\mathbf{x}) &= \int d\mathbf{y}\, \boldsymbol{\nabla}_{\mathbf{y}} \omega(\mathbf{x},\mathbf{y}) \cdot (\sigma_0(\mathbf{y}) \boldsymbol{\nabla}_{\mathbf{y}} p_1(\mathbf{y})) \\ p_1(\mathbf{x}) &= -\int d\mathbf{y}\, \kappa(\mathbf{x},\mathbf{y}) \frac{h(\mathbf{y})}{D_0(\mathbf{y})}, \end{aligned} \tag{5.62}$$

where the functions g, ω are the Green's functions solutions to

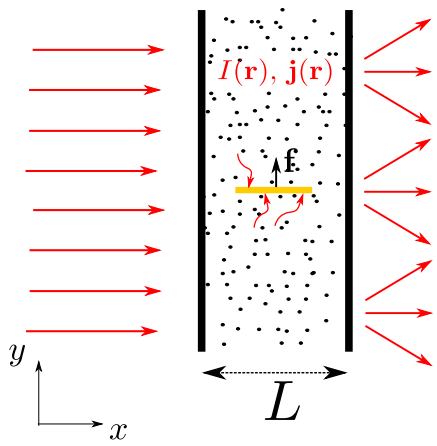

FIGURE 5.2: A scattering medium, contained in a slab of length L and surface $S_\perp$, is illuminated by a light beam. The fluctuating current exerts a force $\mathbf{f} = \langle \mathbf{f} \rangle + f$ on a thin plate or membrane (yellow) of surface S is suspended inside the medium.

$$\begin{aligned} &\nabla_x^2 \kappa(\mathbf{x},\mathbf{y}) = \delta(\mathbf{x}-\mathbf{y}) \\ &\nabla_x \cdot (D_0'(\mathbf{x}) \boldsymbol{\nabla}_\mathbf{x} I_D(\mathbf{x}) \omega(\mathbf{x},\mathbf{y}) + D_0(\mathbf{x}) \boldsymbol{\nabla}_\mathbf{x} \omega(\mathbf{x},\mathbf{y})) = \delta(\mathbf{x}-\mathbf{y}). \end{aligned} \tag{5.63}$$

Using Eq.(5.56), Eqs.(5.63) and comparing with Eq.(5.59), we obtain the two points correlation function,

$$C(\mathbf{x},\mathbf{y}) = \int d\mathbf{z} \, \frac{2\sigma_0(\mathbf{z})}{D_0(\mathbf{y})} \boldsymbol{\nabla}_\mathbf{z} \omega(\mathbf{x},\mathbf{z}) \boldsymbol{\nabla}_\mathbf{z} \kappa(\mathbf{z},\mathbf{y}) - \frac{\sigma_0(\mathbf{z})}{D_0(\mathbf{x}) D_0(\mathbf{y})} \boldsymbol{\nabla}_\mathbf{z} \kappa(\mathbf{z},\mathbf{y}) \boldsymbol{\nabla}_\mathbf{z} \kappa(\mathbf{z},\mathbf{x}). \tag{5.64}$$

Note that higher moments of the light intensity fluctuations, C_n, can readily be obtained by repeating the same method, using terms of higher order in ϵ in Eq.(5.58). This stochastic approach provides a simple and systematic method, easy to implement numerically, to obtain the correlation functions C_n, otherwise cumbersome to derive in mesoscopics.

The case of a constant D and quadratic σ

In the specific case of coherent light, D is constant and $\sigma(I_D) = c_0 I_D^2$ is a quadratic function of I_D, which leads to

$$C(x,y) = \frac{1}{D^2} \int d\mathbf{z} \, \sigma_0(\mathbf{z}) \boldsymbol{\nabla}_\mathbf{z} \kappa(\mathbf{z},\mathbf{x}) \cdot \boldsymbol{\nabla}_\mathbf{z} \kappa(\mathbf{z},\mathbf{y}) \, . \tag{5.65}$$

This expression corresponds exactly to the correlation function obtained from the Langevin equation and the diagrammatic calculation, Eq.(5.53).

5.2.4 Entropy production rate and Gallavotti-Cohen relation

We have established, in 5.2.2, that we could adapt the notion of adjoint process for the time independent problem of coherent light, by substituting the notion of time reversal by that of "disorder reversal". It is therefore natural to try to obtain a Gallavotti-Cohen relation, as well as the notion of entropy production rate.

Consider a slab geometry, where the scattering medium is contained in a slab of width L , section $S_\perp$ and total volume $V = S_\perp L$. The medium is illuminated by an external light beam, Fig.5.2. Consider a profile $\{I, \mathbf{j}\}$, and its disorder reversed counterpart $\{I, -\mathbf{j}\}$. From Eq.(5.43), we obtain the ratio of the probabilities to observe $\{I, \mathbf{j}\}$ versus $\{I, -\mathbf{j}\}$,

$$\log \frac{\mathcal{P}[\{I, \mathbf{j}\}]}{\mathcal{P}[\{I, -\mathbf{j}\}]} = -\int_V d\mathbf{r} \sum_\alpha j_\alpha \frac{D}{\sigma} \partial_\alpha I. \tag{5.66}$$

Let us note

$$\Sigma[I, \mathbf{j}] = \log \frac{\mathcal{P}[\{I, \mathbf{j}\}]}{\mathcal{P}[\{I, -\mathbf{j}\}]}\,.$$

The quantity $\Sigma[I, \mathbf{j}]$ represents the dissipation, or the energy loss, associated to the transfer between $\{I, \mathbf{j}\}$ and $\{I, -\mathbf{j}\}$. This interpretation can be intuited if we consider the average of Σ. By definition, it is given by

$$\langle \Sigma \rangle_\mathcal{P} = \int \mathcal{D}I\, \mathcal{D}\mathbf{j}\, \mathcal{P}[I, \mathbf{j}] \Sigma[I, \mathbf{j}]\,,$$

which is dominated by the stationary solutions I_D, $\mathbf{j_D}$. Using Fick's law 2.30, we obtain

$$\langle \Sigma \rangle_\mathcal{P} \simeq \int_V d\mathbf{r}\, \frac{|\mathbf{j_D}(\mathbf{r})|^2}{\sigma(I_D)} \tag{5.67}$$

If we consider the case of a single particle, driven by an external field $\mathbf{E}$, then dynamics are described by $\mathbf{j}(\mathbf{r}) = \sigma(\mathbf{r})\mathbf{E}(\mathbf{r})$ and the dissipation is defined by $\mathbf{j} \cdot \mathbf{E} = |\mathbf{j}|^2/\sigma$, as in Eq.(5.67).

The average dissipation Eq.(5.67) corresponds to the entropy production rate for mesoscopics [72], formulated in the macroscopic fluctuation theory language. Within the Boltzmann-Einstein theory of equilibrium thermodynamics [74], the probability to observe a fluctuation from equilibrium in a macroscopic system of volume V is proportional to $\exp[V\Delta\mathcal{S}/k_B]$, where $\mathcal{S}$ is the entropy and k_B the Boltzmann constant. The macroscopic fluctuation theory extends this notion to far from equilibrium systems [26]. In fact, the entropy production rate Eq.(5.67) provides a quantitative measure of "how far from equilibrium" the system is. For a system in equilibrium, there is no dissipation which implies that all processes are reversible. Here, the entropy production rate Eq.(5.67) depends on $|\mathbf{j_D}|^2$, which implies that $\langle \Sigma \rangle_\mathcal{P} = 0$ iff $\mathbf{j_D} = 0$. In other words, the diffusive currents drive the system out of equilibrium.

Interestingly, it is straightforward to show that the entropy production rate Eq.(5.67) it is proportional to the dimensionless conductance (see details in the appendix C),

$$\langle \Sigma \rangle_\mathcal{P} = g_\mathcal{L}\, \omega \tag{5.68}$$

where ω is a geometric factor, and where we remind that $g_\mathcal{L} = \frac{k^2 l \mathcal{L}}{3\pi}$, with $\mathcal{L}$ a characteristic size of the system. Since $g_\mathcal{L}$ is easilly tunable, its relationship with the entropy should prove useful in experiments.

The expression Eq.(5.66) also holds for energy transfer. More precisely, consider the setup Fig.5.2, where the light current applies a radiative force on the membrane of surface S and normal vector $\hat{\mathbf{y}}$, suspended inside the medium. Using Eq.(4.2), we

find that the work δQ necessary to move the membrane vertically over the distance δy is,

$$\delta Q = \frac{1}{v^2} \int_{\delta V} d\mathbf{r}\, \mathbf{j}(\mathbf{r}) \cdot \widehat{\mathbf{y}}$$

where $\delta V = S\delta y$ is the volume covered during this process. We restrict ourselves to this small volume, and replace V with δV in Eq.(5.43). Then, the probability $P[Q]$ to observe the energy transfer Q is

$$P[Q] = \int \mathcal{D}I\, \mathcal{D}\mathbf{j}\, \delta \left(Q - \frac{1}{v^2} \int_{\delta V} d\mathbf{r}\, \mathbf{j}(\mathbf{r}) \widehat{\mathbf{y}} \right) \mathcal{P}[I, \mathbf{j}]\,. \tag{5.69}$$

The probability Eq.(5.69) is dominated by a saddle point solution, which implies that one trajectory $\{I, \mathbf{j}\}$ dominates. Exploiting the saddle point solution, we can also show [75] that the optimal profile corresponding the the reversed energy transfer, $P[-Q]$, is $\{I, -\mathbf{j}\}$. Therefore,

$$\log \frac{P[\delta Q]}{P[-\delta Q]} = \log \frac{\mathcal{P}[I, \mathbf{j}]}{\mathcal{P}[I, -\mathbf{j}]} = -\int_{\delta V} d\mathbf{r} \sum_\alpha j_\alpha \frac{D}{\sigma} \partial_\alpha I. \tag{5.70}$$

The reasoning also holds for a macroscopic energy transfer to the system, $Q = \int_V d\mathbf{r}\, \mathbf{j}(\mathbf{r}) \cdot \widehat{\mathbf{n}}$, where $\widehat{\mathbf{n}}$ is some unit vector. In the macroscopic fluctuation theory, Q is understood as the energy transfered by the reservoirs; here, it is interpreted as the work of the radiative forces. We obtain the relation

$$\log \frac{P[Q]}{P[-Q]} = -\int_{\delta V} d\mathbf{r} \sum_\alpha j_\alpha \frac{D}{\sigma} \partial_\alpha I. \tag{5.71}$$

The equation (5.71) equivalent to Eq.(5.34). Obtaining a Gallavotti-Cohen relation similar to Eq.(5.35) requires to have the mobility σ being a function of I, and not I_D, as we so far assumed. Indeed, recall that, in 5.1.5, we used the Einstein relation $D/\sigma(\rho) = f_0''(\rho)$ to pass from Eq.(5.34) to the final result Eq.(5.35). For coherent light, we checked that the Einstein relation holds on average, $D/\sigma(I_D) = 1/\chi(I_D)$, but determining whether it is valid in general is still an open question. Note however that the results derived in this chapter using the assumption that $\sigma \propto I_D^2$, namely the derivation of the light intensity correlation function Eq.(5.65) and the entropy production Eq.(5.67), remain valid even if we had assumed that $\sigma \propto I^2$. Indeed, Eq.(5.67) is an average quantity. To obtain Eq.(5.65), we used a development to first order in the fluctuations; taking $\sigma \propto I^2$ instead would have added corrections of order two, which would have been neglected and hence changing $\sigma \propto I_D^2$ to $\sigma \propto I^2$ yields the same result Eq.(5.65).

To summarize this chapter, we found that the time independent, mesoscopic problem of coherent light can be efficiently described in the macroscopic fluctuation theory. A few adjustments are required, such as translating time reversal in a mesoscopic language by introducing the notion of disorder reversal. We find that the stochastic approach allows to recover known results from mesoscopics – the intensity correlation function. However, the question of whether the mobility σ is, in general, a function of the fluctuating intensity I or of its average value I_D, is still to be answered. Solving this question would give interesting insight in the study of mesoscopics. Indeed, the stochastic formalism provides a systematic method for derivating intensity correlation functions at any order, which is otherwise very difficult in a diagrammatic approach. Moreover, the correspondance between mesoscopics and far from equilibrium hydrodynamics sheds a new light on mesoscopics, introducing the notion of entropy production, and its relation with the easily tunable conductance g, which could be useful for optimizing energy loss in experiments. It would also be interesting to apply these methods to other systems in mesoscopics, such as the cases mentioned in 5.2 of an applied field in an optics, or to other situations in nanoelectronics and superconductivity [44]. From a statistical mechanics viewpoint, our findings should motivate the study of a new class of diffusive time independent systems, accessible experimentally.

Chapter 6

Conclusion

In conclusion, the work presented here shows that fluctuations of light, due to coherent effects, induce mechanical forces, which could be measured and used experimentally. Indeed, mechanical forces due to coherent light has never been envisaged, and offer a new perspective in the field. As mentioned in the introduction, these forces could provide a new type of tool to probe matter at submicronic scale, which could be useful in soft condensed matter, biophysics [24], nanoelectromechanical (NEMS) and quantum technologies [59, 60]. Moreover, since these forces depend on the strength of disorder by means of the conductance g, they can be used as a new effective probe to study the Anderson localization transition [77, 78] for light [79, 80], using a non transport quantity – as opposed to electronic transport, which is the preferred candidate for the study of the Anderson localization.

Moreover, we have shown that these coherent effects are efficiently described with an effective Langevin equation, and we have established a mapping between mesoscopics and far from equilibrium systems. A clear asset of this type of approach is that it allows to characterize complex mesoscopic phenomena by means of two parameters only, the diffusion coefficient D and the mobility σ. This approach should therefore be a candidate for efficient numerical simulations and machine learning algorithms. Furthermore, this mapping is easily generalizable to a large class of quantum or classical mesoscopic effects

For future perspectives, the connection between coherent effects in mesoscopics and non equilibrium stochastic processes, well described in the macroscopic fluctuation theory, should be of interest for both the mesoscopics and statistical mechanics communities. For the former, the mapping to non equilibrium hydrodynamics provides a new insight to mesoscopic physics as well as useful tools to study quantities otherwise difficult to access, such as higher orders intensity correlation functions. For the latter, this work should motivate further study of time independent processes inspired from mesoscopics.

Appendix A

Derivation of the Green's function Eq.(4.33) – Image method

We provide here some details on the derivation of Eq.(4.33). Consider the geometry on Fig.(A.1). We seek the Green's function s.t. :

$$-D\Delta_{\mathbf{r}'}P_D(\mathbf{r},\mathbf{r}') = \delta(\mathbf{r}-\mathbf{r}') \text{ for all } \mathbf{r},\mathbf{r}' \text{ between the plates } P_1,\, P_2$$

and

$$P_D(\mathbf{r},\mathbf{r}') = 0 \text{ for all } \mathbf{r}' \in P_1 \cup P_2$$

The planes P_1, P_2 are located at $y = -\frac{l}{2}$ and $y = \frac{l}{2}$ respectively. Let us check that the following function is a solution :

$$P_D(\mathbf{r},\mathbf{r}') = \frac{1}{4\pi D}\left(\frac{1}{|\mathbf{r}-\mathbf{r}'|} + \sum_{m\in\mathbb{Z}^*}\frac{(-1)^m}{|\mathbf{r}-\mathbf{r}'_\mathbf{m}|}\right)$$

with $\mathbf{r}'_\mathbf{m}$ the image of $\mathbf{r}'$ w.r.t. the plane $y = sign(m)\frac{l}{2}(2m+1)$ (see fig.).

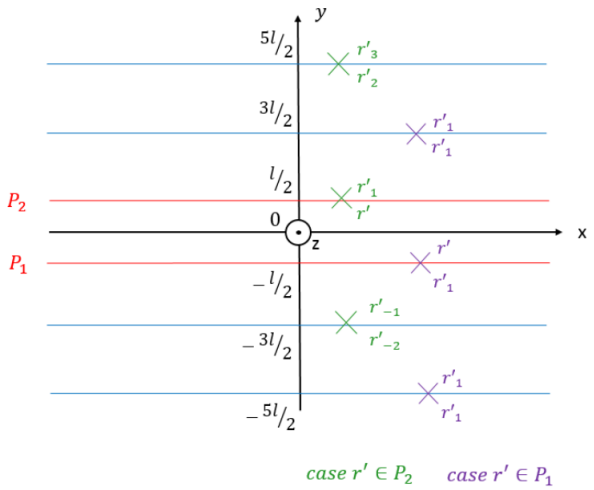

FIGURE A.1: Schematic representation of the image method. In order to derive the Green's function whose boundary conditions are fixed at the planes P_1 and P_2, we make the system periodic by artificially adding boundary conditions on the fictitious blue planes, obtained by translating P_1 and P_2.

Explicitly: $\mathbf{r}' = (x', y'_m, z')$ with $y'_m = ml + (-1)^{|m|}y'$.
It is straightforward that: $-D\Delta_{\mathbf{r}'}P_D(\mathbf{r},\mathbf{r}') = \delta(\mathbf{r}-\mathbf{r}')$ for all $\mathbf{r},\mathbf{r}'$ between the plates.
Let's check the boundary conditions.

For $\mathbf{r}' \in P_2$ (green on the figure), then $\mathbf{r}' = \mathbf{r'_1}$ and $\mathbf{r'_{2m}} = \mathbf{r'_{2m+1}}$ for $m \neq 0$. Thus:

$$P_D(\mathbf{r},\mathbf{r}') = \frac{1}{4\pi D}\left(\underbrace{\frac{1}{|\mathbf{r}-\mathbf{r}'|} - \frac{1}{|\mathbf{r}-\mathbf{r'_1}|}}_{=0} + \sum_{m\geq 1}\underbrace{\frac{1}{|\mathbf{r}-\mathbf{r'_{2m}}|} - \frac{1}{|\mathbf{r}-\mathbf{r'_{2m+1}}|}}_{=0} + \sum_{m\leq -1}\underbrace{-\frac{1}{|\mathbf{r}-\mathbf{r'_{2m-1}}|} + \frac{1}{|\mathbf{r}-\mathbf{r'_{2m+2}}|}}_{=0}\right) \quad \text{(A.1)}$$

The same reasoning applies for $\mathbf{r}' \in P_1$.

Finally, let us check the convergence of the series $\sum_{m\in\mathbb{Z}} \frac{(-1)^m}{|\mathbf{r}-\mathbf{r'_m}|}$. It is an alternating series, of terms whose absolute value decrease to zero: $\frac{1}{|\mathbf{r}-\mathbf{r'_m}|} \to_{|m|\to 0} 0$. Abel's theorem thus ensures the convergence of the series.

Appendix B

Details on light fluctuation induced forces

In this section, we provide analytical expressions and orders of magnitude of the light fluctuation induced forces for different boundary conditions, for the cases discussed in the main text of a point source and a plane wave. We also discuss the case where the illuminating light beam is Gaussian.

B.1 Orders of magnitude

We consider fluctuations of the interaction force between the membranes, $\sqrt{f_{\mathbf{12}}^2}$, discussed in 4.4.6; see Fig.(4.8). Experimentally, these fluctuations could be measured by means of the tension of a spring connecting the two membranes. We remind that

$$f_{\mathbf{12}}^2 = f_{p_+}^2 + f_{p_-}^2 \underbrace{-\frac{1}{c^4}\int_{p_1} d\mathbf{r}\int_{p_2} d\mathbf{r}' D^2 \partial_y \partial_{y'} \langle \delta I_1(\mathbf{r}) \delta I_1(\mathbf{r}')\rangle + \langle \nu_{y,1}(\mathbf{r}) \nu_{y,1}(\mathbf{r}')\rangle}_{f_c^2}$$

where we note: $f_c^2 = -\frac{1}{c^4}\int_{p_1} d\mathbf{r}\int_{p_2} d\mathbf{r}' D^2 \partial_y \partial_{y'} \langle \delta I_1(\mathbf{r}) \delta I_1(\mathbf{r}')\rangle + \langle \nu_{y,1}(\mathbf{r}) \nu_{y,1}(\mathbf{r}')\rangle$ the cross term.

We also impose $L_1 = 2_2$, in order to cancel out the average forces, $\langle \mathbf{f}_{p_\pm} \rangle = 0$. The results are summarized in the Table B.1, followed by comments for each case.

Let's introduce a few parameters: those related to the light source (I_0 for a plane wave and P_0 for a point source, k, the coherence length L_ϕ), and related to the medium: l. We then look for the optimal choice of lengths $L, L_\perp, L_1$, which maximize $\sqrt{f_{\mathbf{12}}^2}$. Note that the expressions given here for the force fluctuations may differ from those in the summary table: this is because we present the optimized expressions, and in some cases this imposes relations between the lengths, e.g. $L = L_\perp$. We will see that the optimal values for the length can be related to the parameters l, L_ϕ, which makes it easier to predict the order if magnitude of the Casimir forces for other values of l, L_ϕ.

We consider for now:

$$l = 10^{-6}m, k = \frac{2\pi}{\lambda} \sim \frac{6}{6\cdot 10^{-7}} m^{-1} \sim 10^7 m^{-1}\,,\, \frac{k^2 l}{3\pi} \sim 10^7 m^{-1}\,,\, I_0 = 10^6 W.m^{-2}\,,\, P_0 = 1W$$

Point source, $g_{\mathcal{L}} = \frac{k^2 l}{3\pi} L L_1 L_\perp \left(\frac{1}{L^2} + \frac{1}{L_1^2} + \frac{1}{L_\perp^2}\right)$			
	B.C. (D or N)	Expr. f_{12}^2	O.M. of $\sqrt{f_{12}^2}$
(*i*)	D. dir. x D. dir. z N. on membranes	$2\beta'' \frac{P_0^2}{v^2} \frac{3\pi}{k^2 l} \frac{L^2}{4L_1^3}$, $\beta'' \approx 0.11$ Main contribution: K_0	$[2 \cdot 10^{-8} N, 2 \cdot 10^{-7} N]$
(*ii*)	D. dir. x D. dir. z D. on membranes	$3\alpha'' \frac{P_0^2}{v^2} \frac{3\pi}{k^2 l} \frac{1}{3^3 L}$ $\alpha'' = 0.05 \frac{2^{17}}{9\pi^{10}} \approx 0.008$ Main contribution: C_2	$10^{-11} N$
Plane wave, $g_{\mathcal{L}} = \frac{k^2 l V}{3\pi \max(L^2, L_1^2, L_\perp^2)}$			
	B.C. (D or N)	Expr. f_{12}^2	O.M. of $\sqrt{f_{12}^2}$
(*iii*)	N. dir. x D. dir. z N. on membranes	$4\beta \frac{I_0^2}{v^2} \frac{3\pi}{k^2 l} \frac{L_\perp^5}{L_1 L}$, $\beta \approx 0.13$ Main contribution: K_0	$[4 \cdot 10^{-9} N, 10^{-6} N]$
(*iv*)	N. dir. x D. dir. z D. on membranes	$5 \frac{\alpha}{4} \frac{I_0^2}{v^2} \frac{3\pi}{k^2 l} L L_1^2 \left[\frac{1}{\left(\frac{2}{L_1^2} + \frac{1}{L^2}\right)^2} + \frac{L_1^2}{2L^2} \right]$ $\alpha = \frac{3 \cdot 2^{13} \cdot 1{,}15}{\pi^{10}} \approx 0.302$ Main contribution: C_2	$[2 \cdot 10^{-10} N, 2 \cdot 10^{-8} N]$
(*v*)	D. dir. x D. dir. z N. on membranes	$4\beta' \frac{I_0^2}{v^2} \frac{l}{k^2} \frac{L_\perp^2}{L_1}$, $\beta' \approx 1.78$ (K_0)	$[4 \cdot 10^{-13} N, 4 \cdot 10^{-12} N]$
(*vi*)	D. dir. x D. dir. z D. on membranes	$5\alpha' \frac{I_0^2}{v^2} \frac{l}{k^2} \frac{L_\perp}{L_1^3 L^3} \frac{1}{\left(\frac{1}{L^2} + \frac{1}{L_1^2} + \frac{1}{L_\perp^2}\right)^3}$, $\alpha' \approx 5$ Main contribution: C_2	$10^{-14} N$

TABLE B.1: Analytical expressions of f_{12}^2, after simplifications, for different choices of boundary conditions (BC), either Dirichlet (D) or Neumann (N). Two types of light sources are considered, a point source placed between the membranes, and an external plane wave parallel to the membranes. For the orders of magnitude, we choose the most relevant values for $L, L_\perp, L_1$, as detailed in the text under "detailed comments".

General comments:

- The dimensionless numbers α, α', α'', β, β', β'' contain both the numerical fit factors which stem from several approximations (keeping only the lowest terms in the sums and integrating over cos and sin functions), and normalization factors of the eigenfucntions of the diffusion equations.
- The lengths $L, L_\perp, L_1$ cannot be smaller than a few l nor larger than L_ϕ. Whenever we need to minimize one of those parameters, we will write it in the form al, with $a \in [5, 10]$; when we need to maximize it, we write it in the form bL_ϕ, $b < 1$.
- With reflective membranes, the K_0 gives the main contribution. However since K_0 is short ranged, it does not contribute to f_c^2.
- With absorbing membranes, the C_2 gives the main contribution. Since C_2 is long ranged, it contributes to f_c^2.

Detailed comments:

(*i*) In the case of a point source, we assume that the source is placed between the

membranes only (no light above the higher membrane or underneath the lower membrane). With $L_1 = L_2 = L_3$, the fluctuations on each membrane are equal: $f^2_{p_+} = f^2_{p_-}$. This explains the factor 2 in the expression of $f^2_{\mathbf{12}}$. In the full expression for $f^2_{\mathbf{12}}$,

$$f^2_{\mathbf{12}} = \frac{2^5}{3^2\pi^4}\frac{P_0^2}{c^2}\frac{3\pi}{k^2 l_e}\frac{1}{L_1^3 L L_\perp} f\left(\frac{L_1}{L}, \frac{L_\perp}{L}\right),$$

with $\frac{2^5}{3^2\pi^4} \sim 0.037$ and

$$f\left(\frac{L_1}{L}, \frac{L_\perp}{L}\right) = \sum_{n_1,n_3>0,n_2,n_2'\geq 0} (-1)^{n_2+n_2'} \frac{\sin^2\left(\frac{n_1\pi(x_1+x_0)}{L'}\right)\cos\left(\frac{n_2\pi y_1}{L_1}\right)\cos\left(\frac{n_2'\pi y_1}{L_1}\right)\sin^2\left(\frac{n_3\pi(z_1+z_0)}{L'_\perp}\right)}{(n_1^2/L^2 + n_2^2/L_1^2 + n_3^2/L_\perp^2)(n_1^2/L^2 + n_2'^2/L_1^2 + n_3^2/L_\perp^2)}$$

L and $L_\perp$ play symmetric roles. We thus choose $L = L_\perp$. With this choice,

$$\begin{cases} f^2_{\mathbf{12}} \to_{L_1\to 0} \infty \\ f^2_{\mathbf{12}} \to_{L_1\to\infty} 0 \end{cases}, \quad \begin{cases} f^2_{\mathbf{12}} \to_{L\to 0} 0 \\ f^2_{\mathbf{12}} \to_{L\to\infty} \infty \end{cases}$$

the force fluctuations are higher for L_1 small and L high. We write $L_1 = al$, $L = bL_\phi$: $f^2_{\mathbf{12}} = \frac{\beta''}{2}\frac{P_0^2}{v^2}\frac{3\pi}{k^2 l}\frac{b^2 L_\phi^2}{a^3 l^3}$. With $a \sim 5$ and b ranging from 10^{-2} to 10^{-3}, we obtain the numerical values summarized in the table.

(*ii*) With absorbing membranes, the C_2 gives the main contribution and it contributes to f_c^2. With $L_1 = L_2 = L_3$, the fluctuations on each membrane are equal: $f^2_{p_+} = f^2_{p_-}$. This explains the factor 5 in the expression of $f^2_{\mathbf{12}}$. In the general expression for $f^2_{\mathbf{12}}$,

$$f^2_{\mathbf{12}} = a\frac{P_0^2}{c^2}\frac{1}{k^2 l_e}\underbrace{\frac{2^{17}}{3\cdot\pi^9}}_{\approx 1.5}\frac{1}{L L_\perp L_1^5}\frac{1}{\left(\frac{1}{L^2}+\frac{1}{L_1^2}+\frac{1}{L_\perp^2}\right)^3}, \tag{B.1}$$

with $a \sim 0.05$ a numerical fit factor, we have

$$\begin{cases} f^2_{\mathbf{12}} \to_{L_1\to 0} 0 \\ f^2_{\mathbf{12}} \to_{L_1\to\infty} 0 \end{cases}, \quad \begin{cases} f^2_{\mathbf{12}} \to_{L\to 0} 0 \\ f^2_{\mathbf{12}} \to_{L\to\infty} 0 \end{cases}, \quad \begin{cases} f^2_{\mathbf{12}} \to_{L_\perp\to 0} 0 \\ f^2_{\mathbf{12}} \to_{L_\perp\to\infty} 0 \end{cases}$$

There is an optimal, intermediate value for the parameters which maximize the force fluctuations. However it is very difficult to derive it analytically. We assume $L \approx L_\perp \approx L_1$. Replacing $L_1 = L_\perp = L$ in (B.1), we obtain the expression in the table above. The force fluctuations are then higher for L small; we write $L = al$, and take $a = 5$ in Table B.1.

(*iii*) Here, K_0 gives the main contribution. With $L_1 = L_2 = L_3$, the fluctuations on each membrane are equal: $f^2_{p_+} = f^2_{p_-}$. This explains the factor 4 in the expression of $f^2_{\mathbf{12}}$. In the general expression for $f^2_{\mathbf{12}}$,

$$f^2_{\mathbf{12}} = \frac{I_0}{c}\sqrt{\frac{2^7}{\pi^6}\frac{3\pi}{k^2 l_e}}\sqrt{\frac{L_\perp^5}{L}\left(\frac{1}{L_1}+\frac{1}{L_2}\right)},$$

we have:

$$\left\{ \begin{array}{l} f_{12}^2 \to_{L_1 \to 0} \infty \\ \\ f_{12}^2 \to_{L_1 \to \infty} 0 \end{array} \right. , \left\{ \begin{array}{l} f_{12}^2 \to_{L \to 0} \infty \\ \\ f_{12}^2 \to_{L \to \infty} 0 \end{array} \right. , \left\{ \begin{array}{l} f_{12}^2 \to_{L_\perp \to 0} 0 \\ \\ f_{12}^2 \to_{L_\perp \to \infty} \infty \end{array} \right.$$

The force fluctuations are then higher for L_1 and L small, and for $L_\perp$ large. We write $L = L_1 = al$, $L_\perp = bL_\phi$. The values in the table correspond to $a = 5$, $10^{-3} \leq b \leq 10^{-2}$. We do not choose higher values for b, since it seems difficult experimentally to produce a strong light beam ($I_0 \sim 10^6 W \cdot m^{-2}$) of a width larger than a few centimeters.

(*iv*) Here, C_2 gives the main contribution. With $L_1 = L_2 = L_3$, the fluctuations on each membrane are equal: $f_{p_+}^2 = f_{p_-}^2$. This gives the factor 5 in the expression of f_{12}^2. In the general expression for f_{12}^2,

$$f_{12}^2 = \frac{I_0^2}{c^2} \frac{3 \cdot 2^{13} \cdot 1.15}{\pi^{10}} \frac{3\pi}{k^2 l_e} \sum_{j=1,2} \tilde{f}_{ap}\left(\frac{L_j}{L}, \frac{L_\perp}{L}\right)$$

with

$$\tilde{f}_{ap}\left(\frac{L_j}{L}, \frac{L_\perp}{L}\right) = \frac{L_j L_\perp^5 / L^3}{\left(\frac{L_j^2}{L^2} + \frac{L_\perp^2}{L^2}\right)^2} \left[\frac{1}{\left(1 + \frac{L^2}{L_j^2} + \frac{L^2}{L_\perp^2}\right)^2} + \frac{1}{\frac{L^2}{L_j^2} + \frac{L^2}{L_\perp^2}} \right]$$

we have:

$$\left\{ \begin{array}{l} f_{12}^2 \to_{L_1 \to 0} 0 \\ \\ f_{12}^2 \to_{L_1 \to \infty} 0 \end{array} \right. , \left\{ \begin{array}{l} f_{12}^2 \to_{L \to 0} \infty \\ \\ f_{12}^2 \to_{L \to \infty} 0 \end{array} \right. , \left\{ \begin{array}{l} f_{12}^2 \to_{L_\perp \to 0} 0 \\ \\ f_{12}^2 \to_{L_\perp \to \infty} \infty \end{array} \right.$$

The force fluctuations are then higher for L small and for $L_\perp$ large, as in the case (*iii*); this was expected since the boundary conditions in the x and z directions are the same. There exists an optimal value for L_1 which maximizes the force fluctuations. Analytically, this value is a root of a polynomial of degree 8, for which we cannot derive a general analytical expression... Numerically, we found that the optimal value for L_1 is such that $L_1 \approx L_\perp$. We therefore choose $L_1 = L_\perp$ and obtain the expression in Table B.1. We write $L = al$, $L_1 = bL_\phi$. The values in the table correspond to $a = 5$, $10^{-3} \leq b \leq 10^{-2}$. We do not choose higher values for b for the same reason as explained in (*iii*).
We conjecture a physical interpretation of the existence of an optimal value for L_1. It can be interpreted as the competition between the probability $\frac{1}{g} \propto \frac{1}{L_1}$ to have a diffuson crossing, and the value of I_D, P_D in the bulk. Indeed, the y dependance of I_D, P_D is mainly due to the $n_2 = 1$ mode of the solution of the diffusion equation: $\frac{\sin(y/L_1)}{1/L_1^2} \approx L_1^2$. Increasing the value of L_1 results in increasing the value of $|\nabla I_D(\mathbf{r})|^2$ and $P_D(\mathbf{r}, \mathbf{r}')$ in the bulk. The factor $\frac{1}{g}$ is related to the Hikami box in the term C_2, and is also present in f_2^2.
Mathematically, it can be simply verified. In f_2^2, the derivatives ∂_y in f_2^2 give a term $\frac{1}{L_1^2}$. This term is related to the average radiative force, so we do not take it into

account (it can be renormalized). Schematically, the integrals in f_2^2 scale in the following way:

$$\iint\limits_{p\times p} d\mathbf{r}'d\mathbf{r}'\partial_y\partial_{y'}\int\limits_V d\mathbf{R}|\nabla I_D(\mathbf{R})|^2 P_D(\mathbf{r},\mathbf{R})P_D(\mathbf{r}',\mathbf{R}) \equiv$$

$$\underbrace{S_\parallel^2\frac{1}{L_1^2}}_{\to\overline{f}}\underbrace{LL_1L_\perp}_{\int_V}\underbrace{\left(\frac{1/L^4}{\left(\frac{1}{L^2}+\frac{1}{L_1^2}+\frac{1}{L_\perp^2}\right)^2}+\frac{1/L^2L_1^2}{\left(\frac{1}{L_1^2}+\frac{1}{L_\perp^2}\right)^2}+\frac{1/L^2L_\perp^2}{\left(\frac{1}{L_1^2}+\frac{1}{L_\perp^2}\right)^2}\right)}_{|\nabla I_D|^2}\underbrace{\frac{1}{L^2L_1^2L_\perp^2}\frac{1}{\left(\frac{1}{L_1^2}+\frac{1}{L_\perp^2}\right)^2}}_{P_DP_D}$$

The term

$$LL_1L_\perp\left(\frac{1/L^4}{\left(\frac{1}{L^2}+\frac{1}{L_1^2}+\frac{1}{L_\perp^2}\right)^2}+\frac{1/L^2L_1^2}{\left(\frac{1}{L_1^2}+\frac{1}{L_\perp^2}\right)^2}+\frac{1/L^2L_\perp^2}{\left(\frac{1}{L_1^2}+\frac{1}{L_\perp^2}\right)^2}\right)\frac{1}{L^2L_1^2L_\perp^2}\frac{1}{\left(\frac{1}{L_1^2}+\frac{1}{L_\perp^2}\right)^2}$$

can be written in the form:

$$\frac{L}{L_1L_\perp}\left(\frac{1/L^4}{\left(\frac{1}{L^2}+\frac{1}{L_1^2}+\frac{1}{L_\perp^2}\right)^2}+\frac{1/L^2L_1^2}{\left(\frac{1}{L_1^2}+\frac{1}{L_\perp^2}\right)^2}+\frac{1/L^2L_\perp^2}{\left(\frac{1}{L_1^2}+\frac{1}{L_\perp^2}\right)^2}\right)\frac{1}{L^2}\frac{1}{\left(\frac{1}{L_1^2}+\frac{1}{L_\perp^2}\right)^2}$$

where the term $\frac{L}{L_1L_\perp}$ is proportionnal to $\frac{1}{g}$ and the term in parenthesis tends to zero when $L_1\to 0$, and tends to a finite value when $L_1\to\infty$.

(*v*) K_0 gives the main contribution; with $L_1=L_2=L_3$, the fluctuations on each membrane are equal: $f_{p_+}^2=f_{p_-}^2$, which the factor 4 in the expression of $f_{\mathbf{12}}^2$. In the general expression for $f_{\mathbf{12}}^2$,

$$f_{\mathbf{12}}^2\sim\frac{I_0^2}{c^2}\frac{l_e}{k^2}\frac{2^9}{3\pi^3}\frac{L_\perp}{L^3L_1}\frac{1}{\left(\frac{1}{L^2}+\frac{1}{L_\perp^2}\right)^2} \tag{B.2}$$

we have

$$\left\{\begin{array}{l} f_{\mathbf{12}}^2\to_{L_1\to 0}\infty \\ f_{\mathbf{12}}^2\to_{L_1\to\infty}0\end{array}\right.,\quad\left\{\begin{array}{l} f_{\mathbf{12}}^2\to_{L\to 0}0 \\ f_{\mathbf{12}}^2\to_{L\to\infty}0\end{array}\right.,\quad\left\{\begin{array}{l} f_{\mathbf{12}}^2\to_{L_\perp\to 0}0 \\ f_{\mathbf{12}}^2\to_{L_\perp\to\infty}\infty\end{array}\right.$$

The force fluctuations are then higher for L_1 small and $L_\perp$ large. There is an optimal value of L which maximizes the force fluctuations. And standard calculations gives this optimal value: $L=\frac{L_\perp}{\sqrt{3}}$. Replacing in Eq.(B.2), we obtain the expression in the table above. Then, we write $L_1=al$, $L_\perp=bL_\phi$. The values in the table correspond to $a=5$, $10^{-3}\leq b\leq 10^{-2}$. We do not choose higher values for b, since it seems difficult experimentally to produce a strong light beam ($I_0\sim 10^6 W\cdot m^{-2}$) of a width larger than a few centimeters.

(*vi*) C_2 gives the main contribution; with $L_1=L_2=L_3$, the fluctuations on each membrane are equal: $f_{p_+}^2=f_{p_-}^2$, which explains the factor 5 in the expression of $f_{\mathbf{12}}^2$. The general expression for $f_{\mathbf{12}}^2$ is

$$f_{\mathbf{12}}^2 = a\frac{I_0^2}{c^2}\frac{l_e}{k^2}\frac{3\cdot 2^{21}}{\pi^9}\sum_{j=1,2}\frac{L_\perp}{L_j^3 L^3}\frac{1}{\left(\frac{1}{L^2}+\frac{1}{L_j^2}+\frac{1}{L_\perp^2}\right)^3}, \tag{B.3}$$

with $a \sim 0.05$ and $\frac{3\cdot 2^{21}}{\pi^9} \sim 100$. Therefore,

$$\left\{\begin{array}{l} f_{\mathbf{12}}^2 \to_{L_1\to 0} 0 \\ f_{\mathbf{12}}^2 \to_{L_1\to\infty} 0 \end{array}\right., \left\{\begin{array}{l} f_{\mathbf{12}}^2 \to_{L\to 0} 0 \\ f_{\mathbf{12}}^2 \to_{L\to\infty} 0 \end{array}\right., \left\{\begin{array}{l} f_{\mathbf{12}}^2 \to_{L_\perp\to 0} 0 \\ f_{\mathbf{12}}^2 \to_{L_\perp\to\infty} \infty \end{array}\right.$$

The force fluctuations are then higher for $L_\perp$ large, as in (v). There is an optimal value of L_1, L which maximizes the force fluctuations. Analytically, it is difficult to derive an expression for these optimal values, but since there are strong similarities with the case (v), we make the assumption $L \approx L_1 \approx L_\perp$, which is consistent with the numerics. Replacing in Eq.(B.3), we obtain the expression in the table above. Then, we write $L = bL_\phi$. The values in the table correspond $10^{-3} \leq b \leq 10^{-2}$.

B.2 Gaussian beam

In this section, we consider the case where the random medium is illuminated with a collimated beam (gaussian), of width w. The scattering medium is contained in a rectangular box $L_\perp \times L_\perp \times L$; two membranes are placed inside the medium, separated by a distance L_1, see Fig.(4.8). We note L_2 the distance between the upper membrane and the upper edge of the box. We impose Dirichlet boundary conditions on the edges of the box parallel to the incident beam, and Neumann boundary conditions on the edges perpendicular to the beam. We will study both the cases of absorbing (Dirichlet) and reflecting (Neumann) boundary conditions on the membranes.

In this geometry, the dimensionless conductance between the membranes is $g = \frac{k^2 l S_\perp}{3\pi L}$, with $S_\perp = L_1 L_\perp$ the illuminated surface between the membranes.

B.2.1 Reflecting membranes

• Derivation of $P_D(\mathbf{r},\mathbf{r}')$ and $I_D(\mathbf{r})$

We first derive the expressions of P_D and I_D. We will proceed in a similar way as in the previous sections, using the Laplace transform method. We note $x_0 = y_0 = \frac{2l}{3}$, $L' = L + 2x_0$ and $L_1' = L_1 + 2y_0$.

$P_D(\mathbf{r},\mathbf{r}')$ is solution of the problem:

$$\begin{array}{l} -D\Delta_{\mathbf{r}} P_D(\mathbf{r},\mathbf{r}') = \delta(\mathbf{r}-\mathbf{r}') \\ \partial_x P_D(\mathbf{r},\mathbf{r}') = 0 \text{ for } \mathbf{r}||\mathbf{r}' \in \{(0,y,z), y,z\in\mathbb{R}\} \cup \{(L,y,z), y,z\in\mathbb{R}\} \\ \partial_y P_D(\mathbf{r},\mathbf{r}') = 0 \text{ for } \mathbf{r}||\mathbf{r}' \in \{(x,0,z), x,z\in\mathbb{R}\} \cup \{(x,L_1,z), x,z\in\mathbb{R}\} \\ P_D(\mathbf{r},\mathbf{r}') = 0 \text{ for } \mathbf{r}||\mathbf{r}' \\ \cup\{(x,y,L_\perp+z_0), x,y\in\mathbb{R}\} \cup \{(x,y,-z_0), x,y\in\mathbb{R}\} \end{array} \tag{B.4}$$

Using the Laplace transform method, we find:

$$\begin{aligned} P_D(\mathbf{r},\mathbf{r}') &= \frac{2^3}{LL_\perp L_1 D\pi^2} \sum_{n_1,n_2\geq 0,n_3>0} \frac{1}{n_1^2/L^2+n_2^2/L_1^2+n_3^2/L_\perp^2} \\ &\times \cos\left(\frac{n_1\pi x}{L'}\right)\cos\left(\frac{n_1\pi x'}{L'}\right)\cos\left(\frac{n_2\pi y}{L_1}\right)\cos\left(\frac{n_2\pi y'}{L_1}\right) \\ &\times \sin\left(\frac{n_3\pi(z+z_0)}{L'_\perp}\right)\sin\left(\frac{n_3\pi(z'+z_0)}{L'_\perp}\right) \end{aligned} \tag{B.5}$$

We deduce $I_D(\mathbf{r})$ using the Green's formula:

$$\begin{aligned} I_D(\mathbf{r}) &= \frac{3DI_0}{l^2}\int_V e^{-(y'^2+z'^2)/w^2}e^{-x'/l}P_D(\mathbf{r},\mathbf{r}')d\mathbf{r}' \\ &\sim \frac{3\cdot 2^3 I_0}{LL_1L_\perp\pi^2 l}L_1L_\perp \sum_{n_1,n_2\geq 0,n_3>0} y_{n_2}z_{n_3}\frac{\cos\left(\frac{n_1\pi x}{L}\right)\cos\left(\frac{n_2\pi y}{L_1}\right)\sin\left(\frac{n_3\pi(z+z_0)}{L'_\perp}\right)}{\frac{n_1^2}{L^2}+\frac{n_2^2}{L_1^2}+\frac{n_3^2}{L_\perp^2}} \\ &= \frac{3\cdot 2^3 I_0}{L\pi^2 l}\sum_{n_1,n_2\geq 0,n_3>0} y_{n_2}z_{n_3}\frac{\cos\left(\frac{n_1\pi x}{L}\right)\cos\left(\frac{n_2\pi y}{L_1}\right)\sin\left(\frac{n_3\pi(z+z_0)}{L'_\perp}\right)}{\frac{n_1^2}{L^2}+\frac{n_2^2}{L_1^2}+\frac{n_3^2}{L_\perp^2}} \end{aligned} \tag{B.6}$$

with

$$\begin{cases} y_{n_2} = \int_0^1 d\tilde{y}e^{-L_1^2\tilde{y}^2/w^2}\cos(n_2\pi\tilde{y}) \\ z_{n_3} = \int_0^1 d\tilde{z}e^{-L_\perp^2\tilde{z}^2/w^2}\sin(n_3\pi\tilde{z}) \end{cases}$$

Note that, when $w\to\infty$, we recover the coefficients of the plane wave case:

$$y_{n_2}\to\begin{cases} 1\,,\, n_2=0 \\ 0\,,\, n_2\neq 0 \end{cases}, z_{n_3}\to\begin{cases} \frac{2}{\pi n_3}\,,\, n_3 \text{ odd} \\ 0\,,\, n_3 \text{ even} \end{cases}$$

• Average force

Since $\partial_y I_D = 0$ on the membranes, $\langle\mathbf{f}\rangle = 0$.

•Force fluctuations

Since $\partial_y I_D$ and $\partial_y P_D$ are equal to zero on the membranes, $\boldsymbol{f_1^2} = \boldsymbol{f_2^2} = 0$.
Let's calculate the K_0 contribution.

$$\begin{aligned} \boldsymbol{f_{\nu,0}^2} &= \frac{2\pi l v^2}{3k^2}\frac{1}{c^4 L_1}\int_p I_D(\mathbf{r})^2 d\mathbf{r} \\ &= \frac{2\pi l v^2}{3k^2}\frac{1}{c^4 L_1}\frac{3^2 I_0^2 2^6}{l^2L^2\pi^4}\int dxdy\left(\sum_{n_1,n_2\geq 0,n_3>0} y_{n_2}z_{n_3}\frac{\cos\left(\frac{n_1\pi x}{L}\right)\cos\left(\frac{n_2\pi y}{L_1}\right)\sin\left(\frac{n_3\pi(z+z_0)}{L'_\perp}\right)}{\frac{n_1^2}{L^2}+\frac{n_2^2}{L_1^2}+\frac{n_3^2}{L_\perp^2}}\right)^2 \\ &= \frac{I_0^2}{v^2}\frac{1}{k^2 l}\frac{2^5\cdot 3}{\pi^3}\frac{L_\perp}{L_1 L}\sum_{n_1,n_2,n_2'\geq 0,n_3>0} y_{n_2}y_{n_2'}z_{n_3}^2\frac{(-1)^{n_2+n_2'}}{\left(\frac{n_1^2}{L^2}+\frac{n_2^2}{L_1^2}+\frac{n_3^2}{L_\perp^2}\right)\left(\frac{n_1^2}{L^2}+\frac{n_2'^2}{L_1^2}+\frac{n_3^2}{L_\perp^2}\right)} \end{aligned} \tag{B.7}$$

This expression is well approximated by keeping only the lowest term; we find:

$$\begin{aligned} f^2_{\nu,\mathbf{0}} &\sim \frac{I_0^2}{v^2}\frac{3\pi L}{k^2 l L_1 L_\perp}\frac{2^5}{\pi^4}\frac{S_\parallel^2 L_\perp^4}{L^4} y_0^2 z_1^2 \\ &= T_{K_0,pw}\frac{\pi^2}{4} y_0^2 z_1^2 \end{aligned} \tag{B.8}$$

with $T_{K_0,pw} = \frac{I_0^2}{v^2}\frac{3\pi L}{k^2 l L_1 L_\perp}\frac{2^7}{\pi^6}\frac{S_\parallel^2 L_\perp^4}{L^4}$ the K_0 contribution for a plane wave, and

$$y_0 = \int_0^1 e^{-L_1^2\tilde{y}/w^2} d\tilde{y} = \frac{\sqrt{\pi}}{2}\frac{w}{L_1} Erf\left(\frac{L_1}{w}\right)$$

$$z_1 = \frac{w}{L_\perp}\int_0^{L_\perp/w} e^{-u^2}\sin\left(\pi\frac{wu}{L_\perp}\right) du$$

and $Erf(z) = \frac{2}{\sqrt{\pi}}\int_0^z dt e^{-t^2}$ is the error function.

Since, when $w \to \infty$, we have $y_0 \to 1$ and $z_1 \to \frac{2}{\pi}$, we recover the plane wave limit.

Replacing y_0, z_1 by their values, we can rewrite $f^2_{\nu,\mathbf{0}}$ in the form:

$$\begin{aligned} f^2_{\nu,\mathbf{0}} &= T_{K_0,pw}\frac{\pi^2}{4}\frac{\pi}{4}\frac{w^4}{L_1^2 L_\perp^2} Erf\left(\tfrac{L_1}{w}\right)^2 \left(\int_0^{L_\perp/w} du e^{-u^2}\sin\left(\pi\tfrac{wu}{L_\perp}\right)\right)^2 \\ &= \frac{I_0^2}{v^2}\frac{1}{g_1}\frac{2^3}{\pi^3}\frac{S_\parallel^2 L_\perp^4}{L^4}\frac{w^4}{L_1^2 L_\perp^2} Erf\left(\tfrac{L_1}{w}\right)^2 \left(\int_0^{L_\perp/w} du e^{-u^2}\sin\left(\pi\tfrac{wu}{L_\perp}\right)\right)^2 \\ &= \frac{I_0^2}{v^2}\frac{1}{k^2 l}\frac{3\cdot 2^3}{\pi^2}\frac{L_\perp^3 w^4}{L_1^3 L} Erf\left(\tfrac{L_1}{w}\right)^2 \left(\int_0^{L_\perp/w} du e^{-u^2}\sin\left(\pi\tfrac{wu}{L_\perp}\right)\right)^2 \end{aligned} \tag{B.9}$$

• Conclusion

The K_0 term alone contributes to the fluctuations, and the final expression can be approximated by:

$$\sqrt{f^2} = \frac{I_0}{c}\frac{1}{\sqrt{g_1}}\frac{S_\parallel L_\perp^2}{L^2}\frac{w^2}{L_1 L_\perp}\sqrt{\frac{2^5}{\pi^4}}\int_0^{L_1/w} du e^{-u^2}\left|\int_0^{L_\perp/w} du e^{-u^2}\sin\left(\pi\frac{wu}{L_\perp}\right)\right| \tag{B.10}$$

B.2.2 Absorbing membranes

• Derivation of $P_D(\mathbf{r},\mathbf{r}')$ and $I_D(\mathbf{r})$

We first derive the expressions of P_D and I_D. We will proceed in a similar way as in the previous sections, using the Laplace transform method. We note $y_0 = z_0 = \frac{2l}{3}$, $L'_\perp = L_\perp + 2x_0$ and $L'_1 = L_1 + 2y_0$.

$P_D(\mathbf{r},\mathbf{r}')$ is solution of the problem:

$$\begin{aligned} &-D\Delta_{\mathbf{r}} P_D(\mathbf{r},\mathbf{r}') = \delta(\mathbf{r}-\mathbf{r}') \\ &\partial_x P_D(\mathbf{r},\mathbf{r}') = 0 \text{ for } \mathbf{r}||\mathbf{r}' \in \{(0,y,z), y,z\in\mathbb{R}\}\cup\{(L,y,z), y,z\in\mathbb{R}\} \\ &P_D(\mathbf{r},\mathbf{r}') = 0 \text{ for } \mathbf{r}||\mathbf{r}' \in \{(x,-y_0,z), x,z\in\mathbb{R}\}\cup\{(x,L_1+y_0,z), x,z\in\mathbb{R}\} \\ &\cup\{(x,y,L_\perp+z_0), x,y\in\mathbb{R}\}\cup\{(x,y,-z_0), x,y\in\mathbb{R}\} \end{aligned} \tag{B.11}$$

Using the Laplace transform method, we find:

$$\begin{aligned} P_D(\mathbf{r},\mathbf{r}') &= \tfrac{2^3}{LL_\perp L_1 D\pi^2} \sum_{n_1\geq 0,n_2,n_3>0} \tfrac{1}{n_1^2/L^2+n_2^2/L_1^2+n_3^2/L_\perp^2} \\ &\times \cos\left(\tfrac{n_1\pi x}{L'}\right)\cos\left(\tfrac{n_1\pi x'}{L'}\right)\sin\left(\tfrac{n_2\pi(y+y_0)}{L_1'}\right)\sin\left(\tfrac{n_2\pi(y'+y_0)}{L_1'}\right) \\ &\times \sin\left(\tfrac{n_3\pi(z+z_0)}{L_\perp'}\right)\sin\left(\tfrac{n_3\pi(z'+z_0)}{L_\perp'}\right) \end{aligned} \tag{B.12}$$

We deduce $I_D(\mathbf{r})$ using the Green's formula:

$$\begin{aligned} I_D(\mathbf{r}) &= \tfrac{3DI_0}{l^2}\int_V e^{-(y'^2+z'^2)/w^2}e^{-x'/l}P_D(\mathbf{r},\mathbf{r}')d\mathbf{r}' \\ &\sim \tfrac{3\cdot 2^3 I_0}{LL_1L_\perp\pi^2 l}L_1L_\perp \sum_{n_1\geq 0,n_2,n_3>0} y_{n_2}z_{n_3}\frac{\cos\left(\frac{n_1\pi x}{L}\right)\sin\left(\frac{n_2\pi(y+y_0)}{L_1'}\right)\sin\left(\frac{n_3\pi(z+z_0)}{L_\perp'}\right)}{\frac{n_1^2}{L^2}+\frac{n_2^2}{L_1^2}+\frac{n_3^2}{L_\perp^2}} \\ &= \tfrac{3\cdot 2^3 I_0}{L\pi^2 l}\sum_{n_1\geq 0,n_2,n_3>0} y_{n_2}z_{n_3}\frac{\cos\left(\frac{n_1\pi x}{L}\right)\sin\left(\frac{n_2\pi(y+y_0)}{L_1'}\right)\sin\left(\frac{n_3\pi(z+z_0)}{L_\perp'}\right)}{\frac{n_1^2}{L^2}+\frac{n_2^2}{L_1^2}+\frac{n_3^2}{L_\perp^2}} \end{aligned} \tag{B.13}$$

with

$$\begin{cases} y_{n_2} = \int_0^1 d\tilde{y}e^{-L_1^2\tilde{y}^2/w^2}\sin(n_2\pi\tilde{y}) \\ z_{n_3} = \int_0^1 d\tilde{z}e^{-L_\perp^2\tilde{z}^2/w^2}\sin(n_3\pi\tilde{z}) \end{cases}$$

Note that, when $w\to\infty$, we recover the coefficients of the plane wave case:

$$y_{n_2}\to\begin{cases}\frac{2}{\pi n_2}\text{ , }n_2\text{ odd}\\ 0\text{ , }n_2\text{ even}\end{cases}\text{, }z_{n_3}\to\begin{cases}\frac{2}{\pi n_3}\text{ , }n_3\text{ odd}\\ 0\text{ , }n_3\text{ even}\end{cases}$$

• Force fluctuations

As in the plane wave case, the term that contributes the most is the C_2 term. We can make the same simplifications as in the plane wave case: replace the volume integral by the maximum of the integrand times a numerical factor ~ 0.05, and keep the lowest terms in the sums times a numerical factor ~ 1.15.

$$\begin{aligned} f_2^2 &= \tfrac{2\pi l v^2}{3k^2}\tfrac{D^2}{c^4}\int_{p\times p} d\mathbf{r}d\mathbf{r}'\partial_y\partial_{y'}\int_V d\mathbf{R}|\nabla I_D(\mathbf{R})|^2 P_D(\mathbf{R},\mathbf{r})P_D(\mathbf{R},\mathbf{r}') \\ &= a\tfrac{I_0^2}{v^2}\tfrac{1}{k^2 l}\tfrac{2^{15}}{\pi^5}y_1^2z_1^2\frac{L_\perp^5 L_1/L^3}{\left(\frac{L_1^2}{L^2}+\frac{L_\perp^2}{L^2}\right)^2}\left(\frac{1}{\left(1+\frac{L_1^2}{L_1^2}+\frac{L_\perp^2}{L_\perp^2}\right)^2}+\frac{1}{\frac{L_1^2}{L_1^2}+\frac{L_\perp^2}{L_\perp^2}}\right) \\ &= y_1^2z_1^2\tfrac{\pi^4}{2^4}T_{C_2,\uparrow,pw} \end{aligned} \tag{B.14}$$

with $a\sim 0.0521$ a numerical fit factor, and

$$T_{C_2,\uparrow,pw} = a\frac{I_0^2}{v^2}\frac{1}{k^2 l}\frac{2^{19}}{\pi^9}\frac{L_\perp^5 L_1/L^3}{\left(\frac{L_1^2}{L^2}+\frac{L_\perp^2}{L^2}\right)^2}\left(\frac{1}{\left(1+\frac{L^2}{L_1^2}+\frac{L^2}{L_\perp^2}\right)^2}+\frac{1}{\frac{L^2}{L_1^2}+\frac{L^2}{L_\perp^2}}\right)$$

the C_2 contribution to f^2 in the case of a plane wave, with the same boundary conditions. Since $y_1, z_1 \to \frac{2}{\pi}$ when $w \to \infty$, we recover the plane wave limit.

• Conclusion

The force fluctuations are mostly due to the C_2 term, and can be approximated by the following expression:

$$f^2 = y_1 z_1 \frac{I_0}{c}\sqrt{a\frac{2^{15}}{\pi^5}\frac{L_\perp^5 L_1/L^3}{\left(\frac{L_1^2}{L^2}+\frac{L_\perp^2}{L^2}\right)^2}\left(\frac{1}{\left(1+\frac{L^2}{L_1^2}+\frac{L^2}{L_\perp^2}\right)^2}+\frac{1}{\frac{L^2}{L_1^2}+\frac{L^2}{L_\perp^2}}\right)} \tag{B.15}$$

with $a \sim 0.0521$ and

$$\begin{cases} y_1 = \int_0^1 d\tilde{y} e^{-L_1^2\tilde{y}^2/w^2}\sin(\pi\tilde{y}) \\ z_1 = \int_0^1 d\tilde{z} e^{-L_\perp^2\tilde{z}^2/w^2}\sin(\pi\tilde{z}) \end{cases}$$

Appendix C

Derivation of Eq.(5.68)

In this section, we provide a proof of Eq.(5.68),

$$\langle \Sigma \rangle_{\mathcal{P}} = g_{\mathcal{L}} \omega \,. \tag{C.1}$$

Let's rewrite σ in terms of $g_{\mathcal{L}}$. First note that

$$\sigma = \frac{2\pi l v^2}{3k^2} I_D^2 = \frac{2\mathcal{L}}{g_{\mathcal{L}}} D^2 I_D^2 \,. \tag{C.2}$$

Using Fick's law, $\langle \mathbf{j} \rangle = -D \boldsymbol{\nabla} I_D$, we find

$$\begin{aligned} \langle \Sigma \rangle_{\mathcal{P}} &= D^2 \int_V d\mathbf{r} \, \tfrac{|\nabla I_D|^2}{\sigma} \\ &= \tfrac{g_{\mathcal{L}}}{2\mathcal{L}} \int_V d\mathbf{r} \, \tfrac{|\nabla I_D|^2}{I_D^2} \,. \end{aligned} \tag{C.3}$$

We switch to dimensionless variables $\mathbf{u} = \mathbf{r}/\mathcal{L}$, and we obtain

$$\langle \Sigma \rangle_{\mathcal{P}} = \tfrac{g_{\mathcal{L}}}{2} \int_{\tilde{V}} d\mathbf{u} \, \tfrac{|\nabla I_D(\mathbf{u})|^2}{I_D(\mathbf{u})^2} \,, \tag{C.4}$$

where $\tilde{V}$ is the rescaled volume. Hence,

$$\langle \Sigma \rangle_{\mathcal{P}} = g_{\mathcal{L}} \, \omega \,, \tag{C.5}$$

where $\omega = \frac{1}{2} \int_{\tilde{V}} d\mathbf{u} \, \frac{|\nabla I_D(\mathbf{u})|^2}{I_D(\mathbf{u})^2}$ is a dimensionless number, which depends on the boundary conditions and on the shape of the system, but not on the volume nor on the disorder.

Appendix D

Résumé en français

La propagation des ondes dans des milieux aléatoires, électroniques ou électromagnétiques, donne lieu à à de nombreux phénomènes riches en physique mésoscopique et ont été largement étudiés au cours des dernières décennies, à la fois théoriquement et expérimentalement [13]. Ces systèmes où les ondes se dispersent dans des milieux complètement aléatoires et désordonnés, sont fascinants en ce que des effets significatifs émergent de ce chaos apparent. Un exemple frappant sont les fluctuations de l'intensité lumineuse – d'amplitude comparable à l'intensité moyennée sur le désordre – qui sont se propagent sur de grandes distances. Le mot clé pour comprendre ces effets surprenants est la *cohérence*. Dans cette thèse, nous étudions les effets cohérents associés à la propagation des ondes dans les milieux, en particulier les ondes électromagnétiques. Dans les milieux faiblement désordonnés, l'intensité lumineuse fluctue spatialement, donnant des figures de diffractions caractéristiques, composées de taches sombres et lumineuses - les figures de speckle [14, 13, 15, 16, 17, 18, 19]. Ces fluctuations lumineuses se propagent sur de grandes distances, en raison d'effets cohérents mésoscopiques sous jacents, qui se produisent à une échelle microscopique. Nous montrons que ces fluctuations de lumière cohérente induisent des forces mécaniques, de nature radiative. Les forces mécaniques induites par la lumière ont été largement étudiées [20, 21, 22] - en particulier depuis l'introduction de lasers - et exploitées pour produire des capteurs en physique de la matière molle et biophysique [23, 24]. Ici, nous montrons l'existence de forces mécaniques d'un nouveau genre, induites uniquement par des effets cohérents mésoscopiques. Nous trouvons que l'amplitude de ces forces fluctuantes est déterminée par un paramètre unique et facilement réglable, la conductance adimensionnée g, qui dépend à la fois de la géométrie et des propriétés de diffusion du milieu. Nos résultats devraient donc avoir des applications intéressantes, telles que l'introduction de nouvelles sondes dans la matière condensée molle ou la biophysique. Du point de vue méthodologique, inspiré de [25], nous utilisons une approche hydrodynamique à la Langevin pour décrire les fluctuations lumineuses, où le bruit rend compte des effets cohérents mésoscopiques. Nous montrons comment systématiquement inclure les corrections cohérentes dans le terme de bruit afin de reproduire les fluctuations d'intensité lumineuse, de façon plus générale que dans le document original de A. Yu. Zyuzin et B. Z. Spivak. Cette description permet de comprendre les fluctuations de la lumière comme résultant d'un flux lumineux, placé hors équilibre par des effets cohérents. Le flux de lumière est caractérisé par deux paramètres seulement, le coefficient de diffusion et la mobilité, par ailleurs reliés par une relation d'Einstein. L'un des atouts évidents de cette méthode est sa dépendance à deux paramètres seulement, qui fournissent une description compacte mais précise des riches effets cohérents sous-jacents. De plus, cette approche de Langevin établit une correspondance entre le problème mésoscopique de la lumière cohérente et une classe de systèmes stochastiques hors équilibre, bien décrits dans le cadre

de la théorie des fluctuations macroscopiques [26, 27, 28]. Cette correspondance jette un nouvel éclairage sur notre compréhension de lumière cohérente, et devrait motiver la poursuite des recherches sur les systèmes mésoscopiques en utilisant le cadre théorique des fluctuation macroscopiques. En effet, la correspondance que nous présentons entre la lumière cohérente et l'hydrodynamique hors d'équilibre est facilement généralisable à une grande classe de problèmes d'onde quantiques ou classiques.

Le premier chapitre porte sur les propriétés de la lumière monochromatique se propageant à travers un milieu diélectrique aléatoire. Le rayonnement à l'intérieur du milieu est la solution d'une équation de Helmoltz,

$$\Delta E(\mathbf{r}) + k^2 \left(1 + \mu(\mathbf{r})\right) E(\mathbf{r}) = s_0(\mathbf{r}) \tag{D.1}$$

avec une constante diélectrique aléatoire, ce qui est extrêmement difficile à résoudre analytiquement. Les propriétés du rayonnement sont caractérisées par deux échelles de longueur, la longueur d'onde $\lambda = 2\pi/k$, où k est le nombre d'onde et le libre parcours moyen élastique l entre deux événements de diffusion. Bien que les solutions analytiques exactes soient difficiles à obtenir, on peut en dire beaucoup sur les quantités moyennes de désordre. Dans la limite de faible désordre $kl \gg 1$, l'intensité lumineuse se comporte de manière diffuse; sa propagation à travers le milieu peut être représentée par des trajectoires de type brownien. Pour une réalisation de désordre, l'intensité de la lumière fluctue spatialement autour de la valeur moyenne I_D, laquelle statisfait une équation de diffusion,

$$-D\Delta I_D(\mathbf{r}) = s(\mathbf{r}) \tag{D.2}$$

où D est le coefficient de diffusion, et s une distribution de sources lumineuses. L'intensité est reliée au flux lumineux moyen $\mathbf{j_D}$ par une loi de Fick,

$$\mathbf{j_D}(\mathbf{r}) = -D\boldsymbol{\nabla} I_D(\mathbf{r}) \tag{D.3}$$

Les fluctuations autour de I_D conduisent aux figures de speckle. Il est important de noter qu'un motif de speckle n'est pas un motif de diffraction, dans lequel chaque faisceau de lumière ne se diffuserait qu'une seule fois sur un diffuseur et sortirait du système. Les figures de speckle sont construites à partir de plusieurs trajectoires lumineuses en diffusion multiple, qui interfèrent de manière constructive malgré le caractère aléatoire du milieu. Quantitativement, les fluctuations d'intensité peuvent être décrites à l'aide de leur fonction de corrélation. Ce dernier est la somme d'un terme à courte portée et d'un terme à longue portée. Le terme à courte portée est le plus fort en amplitude et donne les taches lumineuses des speckles, tandis que le terme à longue portée découle d'effets cohérents sous-jacents connus sous le nom de *croisements quantiques*. Ces fluctuations à longue portée ont une amplitude plus faible – proportionnelle à $1/g$, qui est un petit nombre dans le régime de faible désordre – et sont donc plus difficiles à observer, mais elles conduisent de manière primordiale à des forces mesurables, qui sont décrites au chapitre 3.

Dans le second chapitre, nous montrons que les fluctuations lumineuses peuvent être décrites de manière différente mais équivalente en notant que les croisements quantiques se produisent à des longueurs d'ordre $(lk^{-2})^{1/3}$, plus petites que l'élastique chemin libre moyen l. Cela permet de séparer la physique diffusive incohérente à grande échelle ($\gg l$) des croisements quantiques à petite échelle, cohérents et préservant la phase. Cette partition d'échelle est décrite efficacement au moyen d'une équation de Langevin, obtenue en généralisant la loi de Fick (D.3),

$$\mathbf{j}(\mathbf{r}) = -D\boldsymbol{\nabla} I(\mathbf{r}) + \boldsymbol{\nu}(\boldsymbol{r}) \tag{D.4}$$

où les effets cohérents sont incorporés dans le terme de bruit par une méthode systématique inspirée de [25]. Le procédé peut être généralisé à d'autres systèmes diffusifs, par exemple le transport électronique dans les métaux aléatoires.

Dans le troisième chapitre, nous montrons que les fluctuations lumineuses à longue portée induisent des forces de nature radiative. En effet, le caractère longue portée de ces fluctuations soulève la question de savoir si les "confiner" induirait des forces analogues à celles de Casimir. La physique de Casimir recouvre une multitude de phénomènes où les forces entre les objets macroscopiques sont induites par des fluctuations à longue portée [4] d'origine classique ou quantique. L'exemple le plus célèbre est ce que l'on appelle l'effet Casimir électrodynamique quantique (QED) [1], mais de telles forces induites par des fluctuations apparaissent dans un large éventail de systèmes [5, 6, 47, 7, 8, 48, 11, 10]. Dans ce chapitre, nous montrons que les fluctuations lumineuses à longue portée induisent des forces mesurables, qui dépendent de la conductance sans dimension g - un paramètre facilement ajustable - qui permet de concevoir des expériences dans lesquelles ces forces fluctuantes dominent les autres forces connues en jeu [2, 3, 54]. Ces forces, notées $\boldsymbol{f}$, sont nulles en moyenne sur le désordre, mais sont significatives pour u ne réalisation donnée du désordre; l'amplitude des variations de $\boldsymbol{f}$ autour de la moyenne s'exprime simplement par

$$\langle \boldsymbol{f}^2 \rangle = \frac{1}{g_{\mathcal{L}}} \frac{\mathcal{P}^2}{v^2} \left(\mathcal{Q}_2 + \mathcal{Q}_\nu \right) . \tag{D.5}$$

où $\mathcal{Q}_2$, $\mathcal{Q}_\nu$ sont des facteurs géométriques, où $\mathcal{P}$ est la puissance lumineuse de la source, et v la vitesse de groupe.

Enfin, dans le dernier chapitre, nous explorons le lien entre le problème mésoscopique (indépendant du temps) de la lumière cohérente et la théorie des fluctuations macroscopiques. Quelques ajustements sont nécessaires, tels que traduire la notion de temps dans un langage mésoscopique, en la substituant par celle des réalisations du désordre. Nous trouvons que l'approche stochastique permet de récupérer des résultats connus en mésoscopie, telle la fonction de corrélation d'intensité. Cependant, cette correspondance entre la mésoscopie et la physique des systèmes stochastiques hors équilibre va au-delà d'une description redondante de phénomènes connus. En effet, le formalisme stochastique fournit une méthode systématique pour calculer des fonctions de corrélation d'intensité à n'importe quel ordre, ce qui est par ailleurs très difficile dans une approche diagrammatique. De plus, ce lien apporte un nouvel éclairage sur la mésoscopie, en introduisant la notion de production d'entropie, ce qui pourrait être utile pour optimiser la perte d'énergie dans les expériences. Il serait également intéressant d'appliquer ces méthodes à d'autres systèmes de mésoscopie, dans des systèmes nanoélectronique ou supraconducteurs [44, 45]. Du point de vue de la mécanique statistique, nos résultats devraient motiver l'étude d'une nouvelle classe de systèmes indépendants du temps de diffusion, accessibles expérimentalement.

En conclusion, les principaux résultats de ce travail sont, premièrement, de démontrer le potentiel que représente la lumière cohérente pour une utilisation expérimentale, et deuxièmement, de montrer l'intérêt de la mise en correspondance de la mésoscopie et d'un formalisme stochastique.

En effet, les forces mécaniques dus à la lumière cohérente n'ont jamais été envisagées et offrent une nouvelle perspective dans le domaine. Comme indiqué dans l'introduction, ces forces pourraient fournir de nouveaux types de capteurs à l'échelle submicronique, utiles dans la matière condensée molle, la biophysique [24], les nanoélectromécaniques (NEMS) et les technologies quantiques [59, 60]. De plus, comme ces forces dépendent de la force du désordre grâce à la conductance g, elles peuvent être utilisées comme nouvelle sonde efficace pour étudier la transition de localisation d'Anderson [77].

Sur le plan méthodologique, la connection présentée ici entre la lumière cohérente et l'hydrodynamique hors d'équilibre est facilement généralisable à une large classe d'effets mésoscopiques quantiques ou classiques. Un avantage évident de ce type d'approche réside dans sa dépendance à deux paramètres seulement, ce qui devrait en faire un candidat à des algorithmes d'apprentissage efficaces.

Pour les perspectives futures, le lien entre les effets cohérents en mésoscopique et les processus stochastiques hors équilibre, bien décrit dans la théorie des fluctuations macroscopique, devrait présenter un intérêt tant pour la communauté de physique mésoscopique que pour celle de mécanique statistique. Pour les premiers, la mise en correspondance avec l'hydrodynamique hors équilibre fournit des outils utiles pour étudier des quantités jusqu'ici difficiles d'accès. Pour ces derniers, ce travail devrait motiver davantage l'étude des processus indépendants du temps inspirés de la mésoscopie.

Bibliography

[1] H. B. G. Casimir. On the attraction between two perfectly conducting plates. *Proc. Kon. Ned. Akad. Wet.*, B51:793–795, 1948.

[2] S. K. Lamoreaux. Demonstration of the Casimir Force in the 0.6 to 6 μm Range. *Phys. Rev. Lett.*, 78:, 1997.

[3] A. Lambrecht, S. Reynaud. Casimir force between metallic mirrors. *Eur. Phys. J. B*, 8:309, 2000.

[4] M. Kardar, R. Golestanian. The Friction of Vacuum, and other Fluctuation-Induced Forces. *Rev. Mod. Phys.*, 71:, 1999.

[5] M. E. Fisher, P.-G. de Gennes. Phénomènes aux parois dans un mélange binaire critique. *C. R. Acad. Sci. Paris*, 287:, 1978.

[6] A. Aminov, Y. Kafri, M. Kardar. Fluctuation-Induced Forces in Nonequilibrium Diffusive Dynamics. *Phys. Rev. Lett.*, 114:230602, 2015.

[7] T. R. Kirkpatrick, J. M. Ortiz de Zárate, J. V. Sengers. Giant Casimir Effect in Fluids in Nonequilibrium Steady States. *Phys. Rev. Lett.*, 110:235902, 2013.

[8] T. R. Kirkpatrick, J. M. Ortiz de Zárate, J. V. Sengers. Fluctuation-induced pressures in fluids in thermal nonequilibrium steady states. *Phys. Rev. E*, 89:022145, 2014.

[9] S. Marcelja. Electrostatics of membrane adhesion. *Biophys. J.*, 61:1117–1121, 1992.

[10] L. Palova, P. Chandra, P. Coleman. The Casimir effect from a condensed matter perspective. *Am. J. Phys.*, 77:, 2009.

[11] R. Messina, D. A. R. Dalvit, P. A. Maia Neto, A. Lambrecht and S. Reynaud. Dispersive interactions between atoms and nonplanar surfaces. *Phys. Rev. A*, 80:022119, 2009.

[12] . 60 years of the Casimir effect, 23–27 June 2008, International Center for Condensed Matter Physics, Brasilia, DF, Brazil. *Journal of Physics: Conference Series*, 161, 2009.

[13] E. Akkermans, G. Montambaux. *Mesoscopic physics of electrons and photons*. Cambridge University Press, 2007.

[14] J. W. Goodman. *Statistical Optics*. Wiley Classics Library Edition, 2000.

[15] M. Kaveh, M. Rosenbluh, I. Freund. Speckle patterns permit direct observation of phase breaking. *Nature*, 326:778–780, 1987.

[16] F. Scheffold, G. Maret. Universal Conductance Fluctuations of Light. *Phys. Rev. Lett.*, 81:5800, 1998.

[17] F. Scheffold, W. Hartl, G. Maret, E. Matijevic. Observation of long-range correlations in temporal intensity fluctuations of light. *Phys. Rev. B*, 56:10942, 1997.

[18] J. F. de Boer, M. P. van Albada, A. Lagendijk. Transmission and intensity correlations in wave propagation through random media. *Phys. Rev. B*, 45:658, 1992.

[19] M. J. Stephen, G. Cwilich. Intensity correlation functions and fluctuations in light scattered from a random medium. *Phys. Rev. Lett.*, 59:285, 1987.

[20] A. Ashkin. Acceleration and Trapping of Particles by Radiation Pressure. *Phys. Rev. Letters*, 24:156, 1970.

[21] S. Gigan et. al. Self-cooling of a micromirror by radiation pressure. *Nature*, 444:67–70, 2006.

[22] A. Dogariu, S. Sukhov, J. Saenz. Optically induced 'negative forces'. *Nature Photonics*, 7:24–27, 2013.

[23] A light touch. *Nature Photonics*, 5:315, 2011.

[24] K. Bradonjić, J. D. Swain, A. Widom, Y. N. Srivastava. The Casimir Effect in Biology: The Role of Molecular Quantum Electrodynamics in Linear Aggregations of Red Blood Cells. *J. Phys.: Conf. Ser*, 161:, 2009.

[25] B. Z. Spivak, A. Yu. Zjuzin. Langevin description of mesoscopic fluctuations in random medium. *Sov. Phys. JETP*, 93:994–1006, 1987.

[26] L. Bertini, A. De Sole, D. Gabrielli, G. Jona-Lasinio, C. Landim. Macroscopic Fluctuation Theory for Stationary Non-Equilibrium States. *J. Stat. Phys.*, 107:, 2002.

[27] L. Bertini, D. Gabrielli, J. L. Lebowitz. Large Deviations for a Stochastic Model of Heat Flow. *J. Stat. Phys.*, 121:, 2005.

[28] B. Derrida. Non-equilibrium steady states: fluctuations and large deviations of the density and of the current. *J. Stat. Mech.*, page , 2007.

[29] A. Ishimaru. *Wave propagation and scattering in random media*. Academic Press, 1978.

[30] M. J. Stephen. *"Interference, Fluctuations and Correlations in the Diffusive Scattering of Light from a Disordered Medium" In "Mesoscopic Phenomena in Solids"*, volume 30. Ed. B. Altshuler, P. Lee, R. Webb, Modern Problems in Condensed Matter Sciences, 1991.

[31] P. A. Lee, T. V. Ramakrishnan. Disordered electronic systems. *Rev. Mod. Phys.*, 57:287, 1985.

[32] S. Hikami. Anderson localization in a nonlinear-σ-model representation. *Phys. Rev. B*, 24:2671, 1981.

[33] L.P. Gorkov, A. I. Larkin, D.E. Khmelnitskii. Particle conductivity in a two-dimensional random potential. *JETP Lett.*, 30, 1979.

[34] J. T. Edwards, D. J. Thouless. Numerical studies of localization in disordered systems. *J. Phys. C*, 5:, 1972.

[35] G. Montambaux A. Altland, Y. Gefen. What is the Thouless Energy for Ballistic Systems? . *Phys. Rev. Lett.*, 76(1130), 1996.

[36] A. Douglas Stone P. A. Lee. Universal Conductance Fluctuations in Metals. *Phys. Rev. Lett.*, 55:, 1985.

[37] O.L. Al'tshuler, B.I. Shklovskii. Repulsion of energy levels and conductivity of small metal samples . *Sov. Phys. JETP*, 64, 1986.

[38] S. Washburn. Fluctuations in the extrinsic conductivity of disordered metal. *IBM J. Res. Develop*, 32 (3):335, 1988.

[39] C. Kipnis, C. Marchioro, E. Presutti. Heat Flow in an Exactly Solvable Model. *J. Stat. Phys.*, 27:65, 1982.

[40] L. Bertini, A. De Sole, D. Gabrielli et al. Macroscopic fluctuation theory. *Rev. Mod. Phys.*, 87:593, 2015.

[41] H. Spohn. *Large Scale Dynamics of Interacting Particles*. Springer, Berlin, 1991.

[42] G. Gallavotti, E.G.D. Cohen. Dynamical ensembles in stationary states. *J Stat Phys*, 80:931–970, 1995.

[43] B. Z. Spivak, A. Yu. Zyuzin. *"Mesoscopic Fluctuations of Current Density in Disordered Conductors" In "Mesoscopic Phenomena in Solids"*, volume 30. Ed. B. Altshuler, P. Lee, R. Webb, Modern Problems in Condensed Matter Sciences, 1991.

[44] L. Henriet, A. N. Jordan and K. Le Hur. Electrical current from quantum vacuum fluctuations in nanoengines. *Phys. Rev. B*, 92:125306, 2015.

[45] C. H. L. Quay, D. Chevallier, C. Bena, M. Aprili. Spin imbalance and spin-charge separation in a mesoscopic superconductor. *Nat. Phys.*, 9:84–88, 2013.

[46] C. H. L. Quay, M. Aprili. Out-of-equilibrium spin transport in mesoscopic superconductors. *Philos. Trans. A*, 376, 2018.

[47] T. R. Kirkpatrick, E. G. D. Cohen. Fluctuations in a nonequilibrium steady state: Basic equations. *Phys. Rev. A*, 26:2, 1982.

[48] D. S. Dean, B.-S. Lu, A. C. Maggs, R. Podgornik. Nonequilibrium Tuning of the Thermal Casimir Effect. *Phys. Rev. Lett.*, 116:, 2016.

[49] J. Rodríguez, D. L. Andrews. Inter-particle interaction induced by broadband radiation. *Optics Communications*, 282:2267–2269, 2009.

[50] J. M. Auñón, M. Nieto-Vesperinas. Optical forces on small particles from partially coherent light. *J. Opt. Soc. Am. A*, 29:1389–1398, 2012.

[51] S. Sukhov, K. M. Douglass, A. Dogariu. Dipole–dipole interaction in random electromagnetic fields. *Optics Letters*, 38, 2013.

[52] G. Brügger, L. S. Froufe-Pérez, F. Scheffold, J. J. Sáenz. Controlling dispersion forces between small particles with artificially created random light fields. *Nat. Comm.*, 6:7460:, 2015.

[53] P. Haslinger et. al. Attractive force on atoms due to blackbody radiation. *Nat. Phys.*, 14:257–260, 2018.

[54] J. N. Munday, F. Capasso, V. A. Parsegian. Measured long-range repulsive Casimir-Lifshitz forces. *Nat. Letters.*, 457:170–173, 2009.

[55] G. F. Roach. *Green's functions*. Cambridge University Press, 1982.

[56] D. Yan R. Castillo-Garza, C.-C. Chang and U. Mohideen. Customized silicon cantilevers for Casimir force experiments using focused ion beam milling. *J. Phys. Conf. Ser.*, 161(1):012005, 2009.

[57] R. L. Jaffe. Casimir effect and the quantum vacuum. *Phys. Rev. D*, 72, 2005.

[58] S. M. Popoff, G. Lerosey, R. Carminati, M. Fink, A.C. Boccara, S. Gigan. Measuring the Transmission Matrix in Optics: An Approach to the Study and Control of Light Propagation in Disordered Media. *Phys. Rev. Lett.*, 104, 2010.

[59] T. J. Kippenberg and K. J. Vahala. Cavity Opto-Mechanics. *Opt. Express*, 15:17172, 2007.

[60] O. Arcizet, P.-F. Cohadon, T. Briant, M. Pinard, A. Heidmann. Radiation-pressure cooling and optomechanical instability of a micromirror. *Nature*, 444:71, 2006.

[61] L. Onsager. Reciprocal Relations in Irreversible Processes. I,II. *Phys. Rev.*, 37,38, 1931.

[62] L. Onsager, S. Machlup. Fluctuations and Irreversible Processes. *Phys. Rev.*, 91, 1953.

[63] C. Arita, P. L. Krapivsky, K. Mallick. Generalized exclusion processes: Transport coefficients. *Phys. Rev. E*, 90, 2014.

[64] L. Peliti. *Statistical Mechanics in a Nutshell*. Princeton University Press, 2011.

[65] L. Bertini, A. De Sole, D. Gabrielli, G. Jona-Lasinio, C. Landim. Towards a Nonequilibrium Thermodynamics: A Self-Contained Macroscopic Description of Driven Diffusive Systems. *J. Stat. Mech. Theory Exp*, 135:0857, 2009.

[66] P. C. Martin, E. D. Siggia, H. A. Rose. Statistical Dynamics of Classical Systems. *Phys. Rev. A*, 8:423, 1973.

[67] A. N. Jordan, E. V. Sukhorukov, S. Pilgram r. Fluctuation statistics in networks: A stochastic path integral approach. *J. Math. Phys.*, 45(11), 2004.

[68] E. M. Lifshitz L. D. Landau. *Mechanics*. Pergamon Press, 2nd Ed., 1969.

[69] C. Appert-Rolland, B. Derrida, V. Lecomte, F. van Wijland. Universal cumulants of the current in diffusive systems on a ring. *Phys. Rev. E*, 78:, 2008.

[70] L. Bertini, A. De Sole, D. Gabrielli, G. Jona-Lasinio, C. Landim. Non Equilibrium Current Fluctuations in Stochastic Lattice Gases. *J. Stat. Phys.*, 123:, 2006.

[71] T. Bodineau, B. Derrida. Distribution of current in nonequilibrium diffusive systems and phase transitions . *Phys. Rev. E*, 72:, 2005.

[72] U. Seifert. Entropy Production along a Stochastic Trajectory and an Integral Fluctuation Theorem. *Phys. Rev. Lett.*, 95, 2005.

[73] B. Derrida, J. L. Lebowitz, E. R. Speer. Large Deviation of the Density Profile in the Steady State of the Open Symmetric Simple Exclusion Process. *J. Stat. Phys.*, 107:599–634, 2002.

[74] E. M. Lifshitz L. D. Landau. *Statistical Physics*, volume 5. Pergamon Press, 1968.

[75] O. Shpielberg. Private communication.

[76] J. Tobiska, Yu. V. Nazarov. Inelastic interaction corrections and universal relations for full counting statistics in a quantum contact. *Phys. Rev. B*, 72, 2005.

[77] P. W. Anderson. Absence of Diffusion in Certain Random Lattices. *Phys. Rev.*, 109:1492, 1957.

[78] A. Lagendijk, B. van Tiggelen, D. S. Wiersma. Fifty years of Anderson localization. *Phys. Today*, 62 (8):24, 2009.

[79] K. Arya, Z. B. Su, J. L. Birman. Anderson Localization of Electromagnetic Waves in a Dielectric Medium of Randomly Distributed Metal Particles. *Phys. Rev. Lett.*, 57:, 1986.

[80] C. Aegerter, M. Störzer, S. Fiebig, W. Bührer, G. Maret. Scaling Behavior of the Anderson Localization Transition of Light. 06 2007.

université PARIS-SACLAY
ÉCOLE DOCTORALE
Physique en Île-de-France (EDPIF)

Titre: Forces induites par effets cohérents

Mots clés: Mésoscopie, cohérence, méthodes stochastiques, approche à la Langevin

Résumé: Dans cette thèse, nous étudions les effets cohérents associés à la propagation d'ondes dans les milieux diffusants, en particulier les ondes électromagnétiques. En milieux faiblement désordonnés, l'intensité lumineuse fluctue spatialement sur de grandes distances. Ce phénomène est le résultat d'effets cohérents mésoscopiques complexes, qui se produisent à une échelle microscopique. Nous montrons que ces fluctuations mésoscopiques cohérentes de la lumière induisent des forces de rayonnement d'un nouveau genre. L'amplitude de ces forces fluctuantes est déterminée par un paramètre unique et facilement réglable, la conductance adimensionnée, qui dépend à la fois de la géométrie et des propriétés de diffusion du milieu. Notre découverte devrait donc avoir des applications intéressantes, telles que de nouveaux capteurs pour la matière molle ou la biophysique. Du point de vue méthodologique, nous utilisons une approche à la Langevin pour décrire les fluctuations lumineuses cohérentes, où un bruit précisément calculé rend compte des effets cohérents mésoscopiques. Nous montrons comment inclure systématiquement les corrections cohérentes dans le terme de bruit, afin de reproduire les fluctuations d'intensité. Cette description permet de comprendre les fluctuations cohérentes comme résultant d'un flux lumineux hors équilibre, caractérisé par deux paramètres seulement, le coefficient de diffusion et la mobilité, qui sont par ailleurs liés par une relation d'Einstein. Un avantage évident de cette méthode est sa dépendance à deux paramètres seulement, ce qui fournit une description à la fois compacte et précise des riches effets cohérents sous-jacents. De plus, la correspondance que nous présentons entre la lumière cohérente et l'hydrodynamique hors d'équilibre est facilement généralisable à une large classe de problèmes d'ondes quantiques ou classiques. Pour les perspectives futures, cette connection entre les effets cohérents mésoscopiques et les processus stochastiques hors équilibre devraient intéresser les communautés de la mésoscopie et de la mécanique statistique. Pour les premiers, le lien avec l'hydrodynamique hors équilibre fournit un nouvel éclairage sur la physique mésoscopique, ainsi que des outils utiles pour étudier les quantités jusqu'ici difficiles d'accès, telles que les fonctions de corrélation d'intensité d'ordres supérieurs. Pour les seconds, ces travaux devraient motiver une étude plus approfondie des processus indépendants du temps inspirés de la mésoscopie.

Title: Forces induced by coherent effects

Keywords: Mesoscopics, coherence, stochastic methods, Langevin approach.

Abstract: In this work, we study coherent effects associated to wave propagation in scattering media, in particular electromagnetic waves. In weakly disordered media, light intensity fluctuates spatially over large distances. This phenomenon is the result of complex mesoscopic coherent effects, which occur at a microscopic scale. We show that these mesoscopic coherent fluctuations of light induce radiation forces of a new kind. The strength of these fluctuating forces is determined by a single and easily tunable parameter, the dimensionless conductance, which depends on both the geometry and the scattering properties of the medium. Our findings should therefore have interesting applications such as new sensors in soft condensed matter or biophysics. On the methodological viewpoint, we use a hydrodynamic Langevin approach to describe the coherent light fluctuations, where a properly tailored noise accounts for mesoscopic coherent effects. We show how to systematically include the coherent corrections in the noise term, in order to reproduce the intensity fluctuations. This description allows to understand coherent light fluctuations as resulting from a non equilibrium light flow, characterized by two parameters only, the diffusion coefficient and the mobility, otherwise related by an Einstein relation. A clear asset of this method is its dependence upon two parameters only, which provides a compact yet accurate description of the rich underlying coherent effects. Moreover, the mapping we present between coherent light and out of equilibrium hydrodynamics is easily generalizable to a large class of quantum or classical wave problems. For future perspectives, this connection between coherent effects in mesoscopics and non equilibrium stochastic processes should be of interest in both the mesoscopics and statistical mechanics communities. For the former, the mapping to non equilibrium hydrodynamics provides a new insight to mesoscopic physics as well as useful tools to study quantities so far difficult to access, such as higher orders intensity correlation functions. For the latter, this work should motivate further study of time independent processes inspired from mesoscopics.

Université Paris-Saclay
Espace Technologique / Immeuble Discovery
Route de l'Orme aux Merisiers RD 128 / 91190 Saint-Aubin, France